Master Thesis

Evaporative Cooling of a Bioreceptive Concrete Facade

Cas Verhoeven

TU Delft abt

Front page: Moss species Syntrichia ruralis by Oreshkin. (Retrieved from https://www.plantarium.ru/page/image/id/561698.html)

Designed by Marilse Nouws

For inquiries regarding this document please contact the author.

Evaporative cooling of a bioreceptive concrete facade

By

C.A.P. (Cas) Verhoeven

in partial fulfilment of the requirements for the degree of

Master of Science
in Civil Engineering

at the Delft University of Technology,
to be defended publicly on Thursday July 6, 2023 at 15:00 PM.

Student number: 4472683

Thesis committee:

Dr. ir. M. Ottelé, (chair)	TU Delft
Prof. dr.ir. H. M. Jonkers,	TU Delft
Dr. ir. H. R. Schipper,	TU Delft
Ir. M. I. A. Veeger,	TU Delft
Ir. M. S. Di Maggio,	ABT

TU Delft

abt

Contact information

Author

Name:	C. (Cas) A. P. Verhoeven
University:	Delft University of Technology
Master track:	Building engineering
Specialisation:	Buildings Physics & Technology
Student number:	4472683

Thesis committee

Name:	Dr. ir. M. (Marc) Ottelé (chair)
University:	Delft University of Technology
Section:	Materials, Mechanics, Management & Design (3Md) Materials and Environment

Name:	Prof. dr. ir. H. (Henk) M. Jonkers
University:	Delft University of Technology
Section:	Materials, Mechanics, Management & Design (3Md) Materials and Environment

Name:	Ir. M. (Max) I. A. Veeger
University:	Delft University of Technology
Section:	Materials, Mechanics, Management & Design (3Md) Materials and Environment

Name:	Dr. ir. H.R. (Roel) Schipper
University:	Delft University of Technology
Section:	Materials, Mechanics, Management & Design (3Md) Applied Mechanics

Name:	Ir. M.S. (Maria Sara) di Maggio
Company:	ABT
Profession:	Building Physics & Sustainability Engineer

Preface

This master thesis is the result of one year of hard work. I started my journey in Delft eight years ago at the Faculty of Architecture. Little did I know that after earning my Bachelor's degree, I would go on to graduate as a Building Engineer at the Faculty of Civil Engineering. The built environment interests me and luckily, I learned a lot about it during my time at the TU Delft. This all culminated in this final project that combined ecology, sustainability and engineering. The diversity of the project is something I really enjoyed. During these past months I have gathered moss plants in nature, made my own concrete, performed calculations, wrote code, devised research plans and modelled an energy balance which you can read all about in this report. It was a challenging journey from which I learned a lot.

However, I could not have done it without support. I would like to thank my supervisors from the TU Delft for their guidance throughout this project. Thank you to Max Veeger, Marc Ottelé, Henk Jonkers, Roel Schipper for your feedback, expertise and enthusiasm. Thank you to ABT, for allowing me to carry out my research at your company with a lot of expertise on building physics. And especially to Maria Sara di Maggio, for guiding me on a weekly basis and providing a different perspective from time to time. Also, a special mention to Willem van der Spoel, for helping me on a number of occasions with the modelling part of my research. Furthermore, I would like to express my gratitude to the people at The Green Village for helping me and thinking along with setting up my field research. And to Auke from Respyre in kindly providing samples for testing.

I would like to extend my appreciation to my family and friends, especially the ones that helped in any way, shape or form in the process of finishing this master thesis. Whether it was through studying alongside me, providing mental support, giving feedback or for just having faith in me. Thank you, you know who you are.

With great pleasure, I present this master thesis as a culmination of my academic journey. I hope that this work will not only contribute to the body of knowledge in this field but also inspire further research and innovation in pursuit of sustainable and impactful solutions.

Cas Verhoeven
Delft, June 2023

Executive summary

The urban heat island effect is a well-known and pressing problem in cities today related to urbanisation. It is the phenomenon of an increased ambient air temperature in cities compared to the surrounding rural areas. The use of nature-based solutions has been proposed as a way to help solve this problem. These interventions use nature and biodiversity to improve urban sustainability. By replacing materials that accumulate a lot of heat, the urban heat island effect is tackled. One way of doing this is by making use of so-called bioreceptive concrete on our facades, which allows for the biological growth of mosses to take place on the concrete substrate itself, without requiring any additional systems or maintenance.

This master thesis aimed to quantify the evaporative cooling effect of these moss-covered concrete facades on the urban environment. The research objective was to measure and model the amount of cooling resulting from the evapotranspiration of moss, by analysing water uptake and release, as well as the temperature decrease of a façade surface as a result of evaporation.

Laboratory experiments were conducted to examine the evaporation rates of various moss species under controlled ambient conditions. Bryum capillare displayed the highest water uptake, water retention, and drying time, with the ability to take up 32.4 g of water per 83 x 83 mm surface area. This is equivalent to 4703 g of water per square meter or 470 kg/m^3 volumetric weight. Pleurocarpous mosses showed a range of 27 to 27.4 g of water uptake, corresponding to 3919 to 3977 g of water per square meter or 392 to 398 kg/m^3. The concrete itself absorbed 21.1 g of water, which is equal to 3063 g of water per square meter or 204 kg/m^3 for the 15 mm thick sample that was tested.

Evaporation rates were found to be higher immediately after a watering event, with variability observed between different moss species. Highest variability was 5.56 g/h for Eurhynchium striatum versus 1.86 g/h for Syntrichia ruralis. However, after a certain time, most mosses exhibited similar evaporation rates. The exception was Bryum capillare, which consistently maintained a higher evaporation rate. This moss, growing in cushion form, demonstrated enhanced drought avoidance due to a reduced surface-to-volume ratio and additional capillary spaces for water retention. The highest levels of evaporation were observed in all moss species under conditions of high temperature (25°C) and low relative humidity (50% RH).

Field testing involved monitoring the temperature of two bioreceptive concrete façade panels, one covered in moss and the other left bare. On sunny days, when panel temperatures exceeded 15 to 20 °C, and the panels were dry, the moss panel temperature was 0 to 5 °C lower compared to the bare concrete panel. This temperature difference was attributed to the lower albedo of the moss (0.07 – 0.11) compared to the concrete (0.10 – 0.40). The moss absorbs more solar radiation and prevents it from reaching the surface beneath it. Infrared camera measurements confirmed that the dry moss surface temperature was about 2 to 3 °C warmer than the concrete panel surface due to lower albedo of the moss. On rainy or cloudy days minimal temperature differences were observed between the panels. Additionally, the moss acts as an insulation layer, trapping the air between its leaves, keeping the material behind it cooler. The potential implications of this additional insulation layer on top of the facade remain to be investigated. Based on its specific heat capacity and heat conductivity, it could help with heat gain in winter and cooling gain in summer. It is hypothesised that moss has a lower thermal mass than concrete, potentially facilitating quicker heat dissipation at night and contributing to reduced building surface temperatures.

Watering the panels significantly reduced surface temperatures, with the moss panel being 2 to 5 °C cooler than the concrete panel when wet. The moss exhibited higher water absorption and longer water retention compared to the porous concrete, enabling more evaporation resulting in lower façade temperatures. This cooling effect persisted for approximately two and a half hours after a 40 ml watering event, equivalent to a 1 mm rain event at low wind speeds. These findings indicate that applying moss on a concrete facade cools the surface temperature of a façade compared to a bare concrete façade.

A non-stationary model based on the energy balance of the facade system was calibrated using field testing data. This model provides accurate temperature profiles under different weather conditions. Evaporation modelling was calibrated using water events but could be improved by implementing a water balance. By computing the irrigation, precipitation, evaporation, throughflow and runoff in a dynamic balance, the evaporation and temperature profiles would become more accurate.

The model is used to simulate a heat wave and the thermal behaviour of the façade after rain events with different intensities. A 1 mm rain event decreases the surface temperature of the façade with a few degrees but the effect does not last for a very long time. A 10 mm rain event decreases concrete surface temperature up to 10 °C initially, and the effect lasts for a few hours. The length and intensity of cooling can be extended through the application of moss on a façade. Then, for a 10 mm rain event, the initial temperature reduction is equal to 15 °C. To increase this effect, the pore volume of the concrete could be increased. Also, a moss species should be cultivated on the concrete which grows in cushion form, is desiccation tolerant, and has natural protection against UV light.

The thesis concludes that applying bioreceptive concrete on facades has the potential to mitigate the urban heat island effect by maintaining cooler temperatures for an extended time following rain events depending on their severity. This approach replaces materials that accumulate and radiate excessive heat. To quantify the effect of bioreceptive concrete as a mitigation strategy more accurately, a computational fluid dynamics (CFD) model could be made to predict the ambient temperature decrease of the air in front of a bioreceptive facade.

By investigating and quantifying the evaporative cooling effect of moss-covered concrete facades, this thesis contributes to the understanding of nature-based solutions. The findings highlight the potential benefits of incorporating bioreceptive concrete in building facades to mitigate the urban heat island effect and improve thermal comfort in urban areas.

Table of contents

List of Figures

List of Tables

1

Introduction

Over the last 250 years, since the start of the industrial revolution, people have moved to the city in increasing numbers. Nowadays around 50 per cent of the world's population lives in urban areas. This number is expected to keep growing both in absolute numbers and relative to the world's population (The World Bank, 2023). This leads to more densely populated urban areas. Urban expansion and population growth have led to variability in land surface temperature causing a phenomenon called the urban heat island (UHI) effect (Yin et al., 2018). This is described as the atmospheric and surface temperatures in cities being detectably warmer than the temperature in rural areas (Amado, 2022). This increased heat stress can be bad for people's health. It can lead to heat-related mortality or respiratory problems (Kleerekoper et al., 2012; Sabrin et al., 2020).

So to increase the health of people living in cities it is important to mitigate the UHI effect. A possible mitigation strategy for the UHI effect is using nature-based solutions. Green areas in cities are inversely related to the UHI effect (Deilami et al., 2018). Implementing this can be done by using vegetation cover in the form of parks, street trees, private green gardens, and vegetation on roofs or facades.

One nature-based solution that might help is bioreceptive concrete facade panels. This concrete facilitates the growth of microorganisms on its surface, like mosses. This reduces maintenance and removes the need for an irrigation system compared to the application of a regular green wall. For the microorganisms to grow, the concrete has been modified in terms of its pH value, porosity, and water retention features (Kosanović et al., 2018).

Mosses growing on green roofs help with mitigating the UHI effect through evaporation and transpiration (evapotranspiration). The green surface absorbs a lot of heat and uses it for evaporation causing a small sensible heat flux (Takebayashi & Moriyama, 2007). Mosses growing on bioreceptive concrete might have the same effect. It is however not yet known how much water these mosses might retain and how much cooling is then achieved through the evaporation of water. So the goal of this work is to find out whether bioreceptive concrete might help in mitigating the heat stress caused by the UHI effect.

The relevance of this research at an academic level is to increase the body of knowledge on the benefits of bioreceptive materials and the integrated durability and sustainability of the built environment. Current research tries to link building materials to biology to increase their effectiveness or usefulness by increasing functionality. This in turn increases the relevance at the industry level because these materials increase the well-being of nature, and people and the development of sustainable buildings and cities. More knowledge is needed for companies to decide on large-scale usage of the product.

2

Research framework

2.1 Problem statement

Currently, a lot of building facades are covered in concrete which has a negative effect on the urban heat island effect. Concrete absorbs shortwave solar radiation causing the ambient temperature of the urban environment to heat up. The consequence of this heating of the urban environment is that the city can heat up to extreme heights during heat waves. The expectation is that heat waves will worsen in Europe due to climate change. Both the intensity and the frequency of heat waves are expected to increase (Fischer & Schär, 2010). When the environment heats up, this can harm the health of humans. Heat-related illnesses include skin eruptions, fatigue, exhaustion, heat cramps, heat syncope, and heat stroke (Koppe et al., 2004). But also less severe symptoms like a decrease in productivity at work is a known effect of hot days (Pogačar et al., 2018). In the worst case, heat stress leads to an increase in mortality. Especially vulnerable groups like the elderly and people with cardiovascular diseases are at risk. The number of heat-related deaths is also projected to increase under climate scenarios established in the fifth assessment report of the Intergovernmental Panel on Climate Change (IPCC) (D'Ippoliti et al., 2010; Gasparrini et al., 2017).

A current strategy to decrease the heating of the urban environment is to use Living Wall Systems (LWS). Vegetation has been proven to work against the heating of the urban environment by providing shade and evaporative cooling (Koch et al., 2020). But these living wall systems are expensive and require a lot of maintenance. In an ideal situation, bioreceptive concrete can help in mitigating the urban heat island effect through cooling when applied in a facade. A lot of facades in current building stock have a negative effect on urban heat because of the abundance of heat-absorbing materials being used in them. Bioreceptive concrete is easily applied over current facades. When enough moisture is present mosses evaporate water. This leads to the cooling of the air (Blok et al., 2011). The bioreceptive concrete itself is also more porous than regular concrete allowing for more absorption of water and therefore evaporative cooling. It is also proven that decreasing albedo can be an effective way of mitigating the urban heat island effect (Taha, 1997). Mosses are expected to have a lower albedo than concrete (Hamerlynck et al., 2000). The third mitigating effect of mosses is their insulating function. Concrete is capable of storing a lot of heat. This heat is given off during the night which means the city is not capable of cooling down. The temperature difference between cities and rural areas is, therefore, the biggest at night (Johnson et al., 1991). A high temperature at night time can keep indoor temperatures high resulting in more health problems (Heaviside et al., 2017). When moss is applied on a concrete façade, the concrete won't be exposed to solar radiation meaning the concrete will also not store as much heat. The moss is expected to have a lower heat capacity than concrete.

In conclusion, when mosses are grown on facades, the ambient temperature of the urban environment is expected to decrease because of the water evaporative cooling, decrease in albedo, and a decreased amount of heat storage. However, the amount of benefit the proposed solution yields is yet unknown. Therefore, this study proposes to quantify the cooling effect of mosses when applied on bioreceptive facades. And especially the cooling through the evaporation of water from the moss-covered concrete panel and its effect on the comfort of people. In this way, the study will provide insight into the effectiveness of moss-covered concrete facades in reducing heat stress in urban environments under different weather conditions. These findings can help urban planners and architects looking to incorporate this product as a means of reducing the heat island effect.

2.2 Research objective

This research aims to find out whether bioreceptive concrete can help to reduce the heat stress caused by the urban heat island effect in terms of evaporative cooling. This is done with the following objectives:

- Identifying the factors of heat increase leading to health problems which need to be mitigated
- Quantifying the amount of water retention and water release of mosses over time
- Quantifying the amount of water retention and water release of porous concrete over time
- Find a relation between the amount of temperature decrease and water evaporative cooling properties of bioreceptive concrete
- Create an understanding of the thermal behaviour (and correlating variables) of a (bioreceptive) concrete façade and make a model of it
- Find moss species that would be best suited to reduce ambient temperature based on biological characteristics

2.3 Research questions

To help solve the urban heat island effect through the use of biobased solutions, a way to quantify the amount of temperature change when bioreceptive concrete is applied, is needed. Therefore, the objective of this research is to quantify the amount of temperature change through the evapotranspiration of moss by measuring and modelling the amount of water uptake and release and the temperature decrease that it induces on the facade. Hence, the research question is: what is the evaporative cooling effect of moss-covered concrete facades on the urban environment?

The sub-questions being answered in this research are:

- What factors affect thermal comfort and how is it influenced by the urban environment?
- What is the dynamic water transport behaviour in porous concrete?
- How does moss take up, retain and release water?

- What is the relationship of moss and concrete to the evaporation of water under different ambient conditions?
- How is the relative temperature change of a bioreceptive concrete panel related to the weather conditions?

- How can the cooling behaviour of bioreceptive concrete panels be captured in a model?
- What are the ideal characteristics of a bioreceptive concrete façade panel for decreasing the temperature of the urban environment?

2.4 Research outline

The research outline, illustrated in Figure 2.1, describes how the research will be conducted. How an answer to the research questions will be found. The objective of this research is to find the properties of bioreceptive concrete which influence the cooling effect. These will be determined through experiments, after which simulations will be run to quantify their impact on thermal comfort. But first, a literature study is conducted to find the state of the art on what is already known.

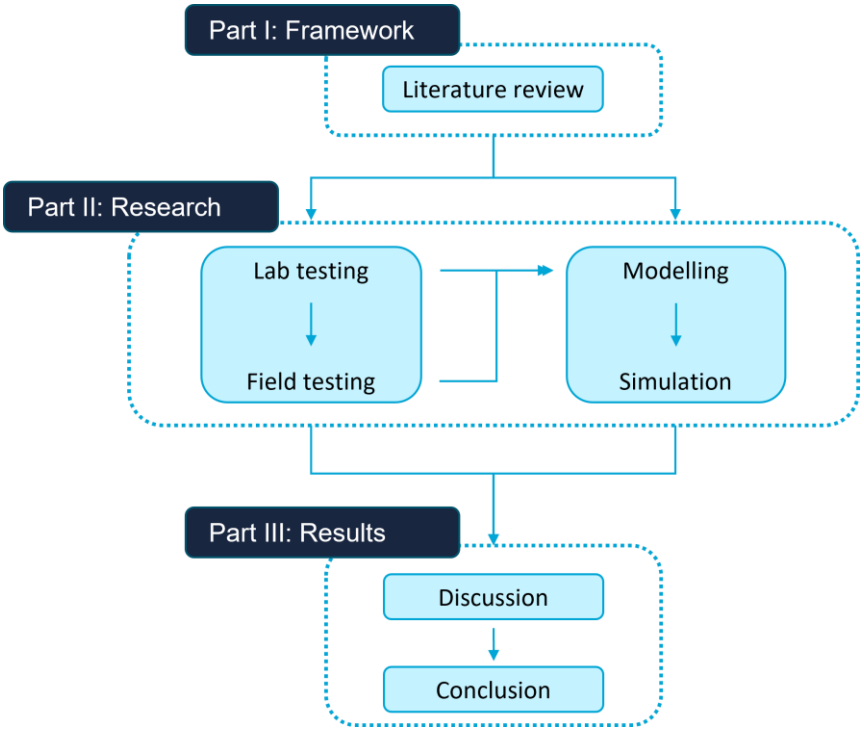

Figure 2.1: Schematic overview research outline

2.4.1 Literature study

Through a literature study, the following information was obtained. Broken down into three categories.

Urban heat island effect and thermal comfort (section 3.1)

This section reviews the current literature on the urban heat island effect, including the environmental factors that contribute to perceived heat, the health implications associated with high temperatures, and the demographics and predisposing factors that make certain populations more vulnerable to these effects. The chapter also explores the various mitigation strategies that have been proposed to reduce the urban heat island effect, including building material physics, energy balance, and the PET comfort index. The sub-research question answered in this section is: *What factors affect thermal comfort and how is it influenced by the urban environment?*

Moss growth on concrete facades (section 3.2)

This section provides an overview of the general concept of bioreceptive concrete, including the growth of moss on concrete façades. The chapter discusses the conditions for concrete to become bioreceptive. How moss attaches itself to and can grow on facades and the circumstances that are most suitable for moss cultivation like shading/lighting, moisture and orientation. Also, the water behaviour in porous concrete is debated. The sub-research question answered in this section is: *What is the dynamic water transport behaviour in porous concrete?*

Water retention and evaporation in mosses (section 3.3)

This section of the thesis provides a guide to understanding the key concepts related to moss water dynamics. It covers the topics of how mosses take up water, and how they retain it. But also, how water evaporates from moss plants and the biological differences between different types of moss. The sub-research question answered in this section is: *How does moss take up, retain and release water over time?*

2.4.2 Experiments

Experiments are conducted in Chapter 4 to find the building physics parameters of the bioreceptive concrete. An important factor is evaporative cooling. For different moss species and for the bioreceptive concrete an experiment is done to quantify the water content, evaporation rate, and cooling effect of this evaporation. This gives a notion of water uptake and water release in the moss and concrete over time at a certain temperature and relative humidity. The sub-research question answered in this section is: *What is the relationship of moss and concrete to the evaporation of water under different ambient conditions?*

Chapter 5 of the report provides an overview of the monitoring process used to investigate the cooling properties of moss on a panel compared to a panel without moss. It explains how weather conditions, such as air temperature, solar irradiance, wind speed, precipitation amount, and relative humidity, can impact the surface temperature difference between the two panels. In this way, the test results can be compared for characteristic weather days. The sub-research question answered in this section is: *How is the relative temperature change of a bioreceptive concrete panel related to the weather conditions?*

2.4.3 Modelling

A dynamic model is made in Excel to simulate the energy balance of a bioreceptive concrete façade panel. With different input variables, this model can then calculate the temperatures of the panels for different conditions. Data from a weather station is used as input. The model is validated using measured data from field testing under different weather conditions. Sections 6.1 and 6.2 discuss the model setup and validation respectively. The sub-research question answered in this section is: *How can the cooling behaviour of bioreceptive concrete panels be captured in a model?*

2.4.4 Simulations

In the model, all the measurement results come together. Simulations will be run to recreate heat wave conditions in the Netherlands to see how much cooling effect the bioreceptive concrete has with and without a moss layer. By playing around with parameters, the ideal characteristics for bioreceptive concrete can be determined. These simulations and the results are shown in section 6.3 and 6.4. The sub-research question answered in this section is: *What are the ideal characteristics of a bioreceptive concrete panel for decreasing the temperature of the urban environment?*

2.4.5 Results

Finally, all experiments and research are discussed in Chapter 7. Drawbacks and limitations are given of the different research methods and the reliability of results is debated. Chapter 8 concatenates all conclusions drawn in the different subsections to answer the main research question. Ultimately, recommendations for further research or work are given in Chapter 9. The sub-research question answered in this section is: *What is the evaporative cooling effect of moss-covered concrete facades on the urban environment?*

3

Literature review

3.1 Urban heat island effect and thermal comfort

3.1.1 Physiological aspect

The thermoregulatory system of the body tries to keep the body temperature at around 37 °C at rest. The body does this by balancing the heat gains with heat loss. Heat is gained internally as a result of metabolic activity and externally by for example the sun or other radiative forcing. The body can lose this heat through convection, conduction, respiration, radiation, and evaporation of sweat (Koppe et al., 2004; Kuijpers-Van Gaalen et al., 2006). Figure 3.1 shows the heat balance of the human body.

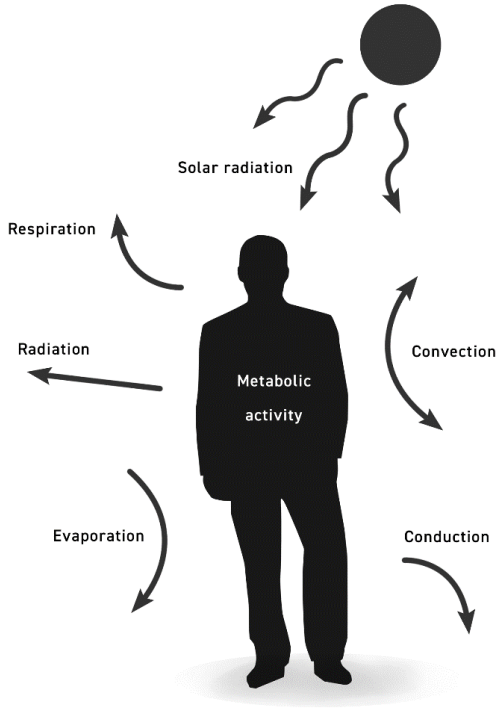

Figure 3.1: Human heat balance

Certain environmental factors influence the human heat balance. When the ambient air temperature is higher than that of the skin, heat is gained by the body. The radiant temperature exchange between the human body and its environment is another environmental factor. When materials around a person are hot, they radiate heat toward the person. The humidity of the air plays a role in the amount of moisture that can flow from the skin to the environment. Evaporation of sweat is an important way for the human

body to dissipate heat. High ambient vapour pressure does not allow the evaporation of sweat. The last environmental factor is wind speed. When wind speed is high, convection increases resulting in more heat loss (Kleerekoper et al., 2012; Koppe et al., 2004). So the worst situation for a person to be in is a hot, humid environment with no wind and materials surrounding it which take up a lot of heat and with high radiative emissivity.

When the body cannot keep the heat gains and heat losses in balance, heat-related illnesses may occur. Heat-related illnesses are skin eruptions, heat fatigue, heat cramps, heat syncope, heat exhaustion and heat stroke. Most heat-related illnesses are consequences of failure in the thermoregulatory system (Kleerekoper et al., 2012; Koppe et al., 2004). Predisposing factors for heat-related illness include age, lack of acclimatisation, dehydration, use of drugs or medication, pre-existing diseases, low fitness, obesity and fatigue (Koppe et al., 2004). Elderly people have reduced sweating capacity. They also use medication more often than younger people which affects the temperature regulation system. Therefore the elderly are more prone to suffering from health implications related to heat. And with an ageing population in most Western European countries, this puts an increasing amount of people at risk (Koppe et al., 2004; Santamouris, 2020). But although heat-related mortality is most pronounced among the elderly, children and people with chronic diseases are also at risk (Kovats & Hajat, 2008).

Another predisposing factor which plays a role in heat stress is socioeconomic status. The type of dwelling is considered one of the main factors which contribute to the risk of heat-related mortality (Heaviside et al., 2017). People of lower socioeconomic status often have poor-quality housing. These low-income households experience discomforting indoor conditions during hot periods, with indoor temperatures exceeding health protection thresholds. The cost of air conditioning is an extra burden for low-income populations, and many households cannot afford to satisfy their cooling needs. Additionally, people living in poorer areas within a city are more likely to have other risk factors for heat-related death. These neighbourhoods experience excess heat stress and high urban heat island intensity due to limited vegetation cover, and a higher density of buildings (Santamouris, 2020; Semenza et al., 1996; Smoyer et al., 2000).

3.1.2. Urban thermal comfort

A widely discussed problem related to urbanisation is the urban heat island effect. This phenomenon can be described as the increased ambient air temperature in cities compared to the surrounding rural areas. Its cause is the abundance of materials with low albedo, high admittance rates, anthropogenic heat and lack of vegetation in cities (Amado, 2022; Oke, 1982; Taha, 1997).

Heat stress as a result of the urban heat island effect is increased because of this rise in temperature of the environment. But also, the wind velocity in cities is generally lower. This results in a reduced rate of heat dissipation by convective cooling. However, complex airflow patterns and turbulence can exist in urban canyons which might increase wind speeds locally. The urban heat island effect in a city is related to population size, topographic and climatic position and distribution of urban structures. It is more pronounced during summer in middle latitudes (Koppe et al., 2004).

Epidemiological studies have been performed to find the connection between summer temperatures and changes in baseline mortality. By looking at changes in baseline mortality, results are more general for different age groups and countries. The results of these studies show that mortality rates were expected to increase by 3.74% for every additional day of summer heat. (G. B. Anderson & Bell, 2011) For every 1% increase in mean daily maximum temperature, mortality would increase by 0.43% (Medina-Ramón & Schwartz, 2007).

Because of climate change, the urban heat island is expected to increase even more in the coming years. Under the different scenarios of the IPCC, temperatures are expected to increase from 0,7 °C to 4,3 °C in Europe. In the worst scenario, excess mortality is expected to increase by 5 to 10% (Gasparrini et al., 2017; Koppe et al., 2004).

Shortwave radiation is absorbed in low-albedo materials. Increasing the albedo of surfaces can help to reduce the amount of solar radiation absorbed by facades and therefore the building material temperatures (Kleerekoper et al., 2012). By increasing the surface albedo from 0.25 to 0.40 in a mid-latitude warm climate, air temperatures on summer days can be lowered by as much as 4°C (Gago et al., 2013). Moss is a material which has an albedo of 0.07-0.11 which is quite low. (Stache et al., 2022) However, when considering the urban heat island effect, it is not only albedo that matters. Also, the ability of surfaces to convert absorbed energy into latent heat instead of convectional heat is important. Stache (2022) also states that for common building materials, the amount of total energy that is converted to convective heat is equal to 63 to 91% which means these heat up the air a lot. For concrete, this number is 83%. While for mosses this number is equal to 47% which is lower than common building materials but also lower than most other vegetation types (Stache et al., 2022).

The Physiological Equivalent Temperature (PET) is a thermal comfort index for people on the street that is commonly used in the Netherlands. It is based on a human body energy balance model for a standardised male of 35 years old, 1.75 m tall, 75 kg, clothing factor 0.9 (measure for thermal insulation of clothing) and metabolic rate of walking (Koopmans et al., 2020). So this person is not representative of the groups of people with increased risk as discussed in Chapter 3.1.1.

Next to the energy balance of the human body, the PET index is based on the 2 m air temperature (Ta), solar irradiance (Qs), wind speed at 1.2 m height (u1.2), wet bulb temperature (Tw), Stefan Boltzmann constant (σ), solar elevation angle (ϕ), Bowen ratio (Bb), the sky view factor (Svf) and the diffuse irradiation (Qd). And it makes a distinction between sunlit and shaded or night conditions. The two formulas to calculate PET are as follows (Koopmans et al., 2020):

Sunlit PET equation:

$$PET_{sun} = -13.26 + 1.25T_a + 0.011Q_s - 3.37\ln(u_{1.2}) + 0.078T_w + 0.0055Q_s\ln(u_{1.2}) + 5.56\sin(\varphi) - 0.0103Q_s\ln(u_{1.2})\sin(\varphi) + 0.0546B_b + 1.94S_{vf} \quad (3.1)$$

Shadow and night PET equation:

$$PET_{shade,night} = -12.14 + 1.25T_a - 1.47\ln(u_{1.2}) + 0.060T_w + 0.015S_{vf}Q_d + 0.0060\left(1 - S_{vf}\right)\sigma\,(T_a + 273.15)^4 \quad (3.2)$$

When PET increases or decreases by 6 °C, the grade of physiological stress changes. For example when the PET index increases from 30 °C to 36 °C, heat stress on human beings, increases from moderate heat stress to strong heat stress (Matzarakis et al., 1999). The full range of thermal perceptions and accompanying physiological stresses can be seen in Table 3.1.

Table 3.1: Thermal perception for different PET temperatures and accompanying physiological stress (Matzarakis et al., 1999)

PET	Thermal perception	Physiological stress
4 °C	Very cold	Extreme cold stress
8 °C	Cold	Strong cold stress
13 °C	Cool	Moderate cold stress
18 °C	Slightly cool	Slight cold stress
23 °C	Comfortable	No thermal stress
29 °C	Slightly warm	Slight heat stress
35 °C	Warm	Moderate heat stress
41 °C	Hot	Strong heat stress
	Very hot	Extreme heat stress

3.1.3 Mitigation strategies

Different measures, including health advice and weather-based warnings, are being used to prevent deaths from heatwaves. However, there is no clear evidence on the most effective interventions at a community level, particularly for the most vulnerable (Kovats & Hajat, 2008). Using heat stress indicators and monitoring weather forecasts, heat-related effects on human health are predicted. When a certain threshold is expected to be exceeded, warning procedures are activated. These can differ from country to country or even city to city but often consist of warning the general population through mass media and more custom-made solutions to protect the vulnerable. For example by increasing hospital emergency staff or providing extra shelter for the homeless (Koppe et al., 2004).

Instead of warning people about the problem, another way to tackle the problem is to make sure the urban environment does not heat up so much. By applying reflective roofs, for example, more short-wave solar radiation is reflected back into the atmosphere. This means less solar heat is absorbed resulting in a lower surface temperature of the roof and a lower ambient temperature in the city. Cool roofs reduce the energy demand for cooling in buildings, increasing indoor comfort (Akbari & Matthews, 2012).

Another cooling measure is the use of misting equipment. This equipment sprays small water droplets into the air. This cools down the air and if it comes in contact with the human skin, convection and evaporation of the water droplets cool a person down (Lamke & Wedin, 1971; Nilsson, 1987). The extent of cooling depends on nozzle size, injection height, droplet size, spraying intensity, and the microclimatic context in which they are placed. (Ulpiani et al., 2019, 2020).

Through urban planning, urban heat accumulation can also be reduced. For example by providing shading through overhead structures in the form of arcades or canopies (Koppe et al., 2004; Santamouris et al., 2019). The configuration of urban canyons is also a design consideration. Wide canyons receive more sunlight because they are less shaded by other buildings. However, the hot air can escape easier at night compared to a narrow canyon. By creating narrow streets the solar radiation is prevented from reaching the street level. At night, these streets trap heat more easily (Norton et al., 2013). Streets with a north-south orientation will have more sun exposure during the middle of the day whereas east-west-orientated streets will receive direct sun throughout the majority of the day (Norton et al., 2013). Urban planning could also integrate the generation of wind flow in urban fabric reducing perceived temperature. Through modelling wind patterns, this effect can be incorporated into the design of a city. For example, by strategically placing a few high-rise towers, airflow within a canyon can be increased which leads to lower air temperature (Priyadarsini et al., 2008; Rajagopalan et al., 2014).

Nature-based solutions are another way of preventing the urban environment from heating up. These interventions on the urban scale use nature and biodiversity to improve urban sustainability. They can be green or blue infrastructures referring to vegetation or water ecosystems. By replacing the materials which accumulate a lot of heat, urban heat island is tackled (Amado, 2022). This can for example be done with vegetation. Vegetation can actively cool the urban environment through evapotranspiration and passively by covering surfaces that would otherwise absorb a lot of short-wave radiation. And through long-wave radiation, green fields allow heat to escape quickly during the night (Kleerekoper et al., 2012). The extent of cooling through vegetation in general is around 1 - 4.7 °C that can spread 100-1000m into an urban area. However, this effect is highly dependent on the amount of water available to the plant or tree (Schmidt, 2009). Vegetation-covered façades have a cooling effect on both the building and the urban environment. This is because the vegetation uses evapotranspiration to cool the area and prevents shortwave radiation absorption by shading low albedo materials. Additionally, the green layer has an insulating property that keeps heat outside in the summer and inside in the winter, reducing indoor temperature. Greening leads to an average temperature decrease of 0.2-1.2°C in near-ground temperatures and can result in a cooling energy saving of 4-40% (Kleerekoper et al., 2012).

Higher temperatures can also lead to an increase in the formation of ground-level ozone in urban areas and exacerbate cardio-respiratory diseases. A way to tackle this problem is to use plants. Plant leaves can filter dust and other harmful substances out of the air (Kleerekoper et al., 2012; Koppe et al., 2004).

Water can cool by evaporation, absorbing heat, or transporting heat out of an area. The cooling effect of water evaporation depends on the airflow and other weather conditions. Studies have shown that water bodies can reduce air temperature by 1-3°C up to a range of 35 m (Kleerekoper et al., 2012). The risk of heat-related mortality can be reduced by the presence of heat sinks like water bodies which can lower ambient temperature and improve thermal comfort (Santamouris, 2020).

3.2 Moss growth on concrete facades

3.2.1 Bioreceptive concrete

An example of a nature-based solution as explained in section 3.1.3, is the use of bioreceptive concrete. Bioreceptivity was first defined in 1995 by Guillitte as: 'the aptitude of a material to be colonised by one or several groups of living organisms without necessarily undergoing any biodeterioration.' Bioreceptive concrete is an alternative strategy for creating green facades. This is done by direct natural colonisation of the cementitious construction material by for example fungi, algae, lichens and mosses (Guillitte, 1995; Manso et al., 2014).

To make concrete bioreceptive, several requirements were found based on existing literature. A substrate with sufficient surface roughness, high water uptake and retention capacity, and the presence of nutrients, particularly phosphate (Kurth, 2008; Manso et al., 2014; Mustafa et al., 2021; Prieto & Silva, 2005). However, the addition of bone ash to the concrete mixture and using crushed expanded clay did increase bioreceptivity even more. (Veeger et al., 2021) Bulk density and open porosity are other governing factors in the ability of concrete to store and circulate water. Without water, the concrete would not be bioreceptive. Capillary water, which is related to the open porosity, determines the time that the concrete remains wet. In outside applications, capillary action is the main driver for the entrance of water into the concrete when only one face is exposed to the exterior. Statistical analysis by Prieto & Silva confirms the importance of this parameter for bioreceptivity, as it has the highest predictive value (Prieto & Silva, 2005). The behaviour of water in the concrete is discussed in more detail in section 3.2.3.

When mosses are grown on facades, other aspects become (more) important like the shading/lighting, orientation, moisture availability and wind. Based on a field survey, mosses seem to grow easier on vertical surfaces when they are roughened, when they face north, in a moist environment and when surrounded and shaded by greenery (Klein, 2020).

3.2.2 Moss growth on concrete

Westhoff (2020) breaks down how mosses can grow on concrete in three steps: weathering of the concrete, formation of the biofilm and growth of vegetation on the surface. Weathering of the concrete surface means that the surface alkalinity is lowered and the surface is roughened (George et al., 2013). Even a thin layer of weathered concrete will allow microorganisms to settle and grow in the pores of the concrete creating a biofilm (Albers et al., 2017; Sparrius, 2016). The growth of the biofilm is influenced by several factors and can be captured in three components: a hospitable concrete surface, the availability of energy sources, and initial colonization. A hospitable concrete surface is a boundary condition which is accomplished when the surface has a suitable concrete microstructure and enough surface roughness. Energy sources and essential elements are needed for the metabolic processes carried out by the microorganisms. These include the need for water, nutrients, and minerals. The presence of water is particularly essential in the fertilization and photosynthesis processes of Bryophytes. Higher relative humidity values help to maintain adequate moisture content in the air to promote moss growth (Manso et al., 2014). Initial colonization happens as a result of deposition by rainwater, wind, and runoff or due to contact of the concrete with soil, vegetation, animals, or animal faeces. This is how the transportation of spores, dust, and other nutrients to the growth site happens. The growth and reproduction of microorganisms can then happen. The then-formed biofilm can develop

into vegetation on concrete, such as moss. Mosses produce rhizoids which are rootlike structures mostly functioning as anchorage. They settle into the pores and cracks of the concrete structure for good adhesion to the surface. Mosses prefer humid, half-sheltered areas with high water retention (Westhoff, 2020). Cooler ambient temperature prevents drying out of the mosses, and the absence of direct sunlight reduces evaporative water loss. Moss growth happens mainly in wet seasons when moisture is readily available. In hot, sunny weather conditions, above a temperature of 25 °C, mosses do not photosynthesize. However, mosses can survive these periods of drought which will be discussed in section 3.3.2. They tolerate big fluctuations in temperature better in a dry than in a wet state (Glime, 2022; Mustafa et al., 2021).

3.2.3 Water behaviour in concrete

Because moisture is important in the colonisation of concrete by mosses, water behaviour in concrete is studied. Moisture is present either in liquid or gaseous form within a building material. In gaseous form, water vapour moves through diffusion. Vapour permeability is rather constant when the material is dry. Diffusion will diminish if the pore system is filled with moisture (Hagentoft, 2007). In general, the diffusive transport of vapour through a construction can be described using the following formula (de Wit, 2009; Mir, 2011):

$$g = \frac{\Delta p}{R_d} * 1000 \tag{3.3}$$

g: vapour transport [g/m^{2}s]

Δp: difference between inside and outside vapour pressure (p_i - p_e) [Pa]

R_d: vapour diffusion resistance [m/s]

When the moisture content of concrete is discussed in this thesis, evaporable water is referred to and not chemically bound water since this water is not capable of evaporating under 105 °C. Evaporable water can be present inside the pores of the concrete in the form of water vapour, absorbed water in the walls, liquid water on the pore walls or liquid water completely saturating the pores (Quincot et al., 2011).

Bioreceptive concrete is porous. Porosity is defined as the total volume of capillary voids in the concrete. Otherwise referring to the volume of its pores divided by the total volume (solid + air). When referring specifically to the volume fraction taken by the open pores, it is called the open porosity. Typically, high porosity is accompanied by low thermal conductivity and low density (de Wit, 2009). Permeability is the property that governs the flow rate of a fluid into a porous solid. It depends on the porosity and the connectivity of the pores in the concrete. Concrete can have a large porosity but if the pores are not connected, the permeability of moisture is still low. This is illustrated in Figure 3.2. The water retention capacity of concrete is defined as the capacity of concrete to absorb and hold water. Concrete with a high permeability and high porosity will have a higher water retention capacity (de Wit, 2009; Westhoff, 2020).

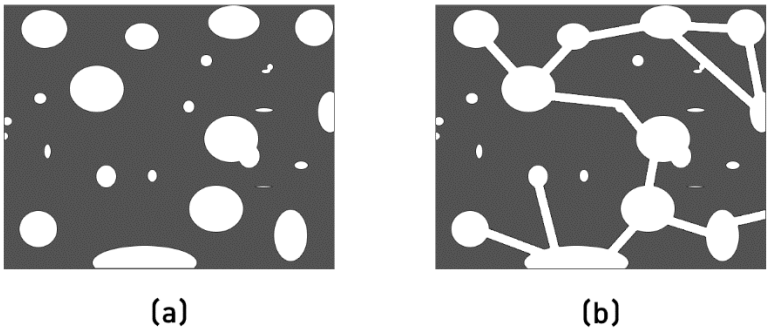

Figure 3.2: Pore structure of concrete with (a) closed pores and (b) open pores

In porous materials, moisture content and moisture transport are related to a phenomenon known as capillary attraction. The surface tension of a liquid within a capillary causes a force that points inward toward the liquid and is normal to the surface. If the surface is concave, water is drawn into the capillary due to adhesive forces, while a convex surface requires an external force to get water into the capillary. The pressure difference across the surface is known as the capillary suction, and it increases as the contact angle decreases and as the radius of the capillary decreases (de Wit, 2009).

The one-dimensional flow of evaporable water in concrete is defined as the sum of the flow velocities due to water diffusion, sorptivity and permeability. In the water diffusion process, a lower ambient temperature and water-cement ratio as well as a higher environmental relative humidity result in greater pore humidity, and thus higher water content in concrete. The relationship between the normalised water diffusion coefficient and pore humidity follows an S-shaped curve. Sorptivity is the amount of water taken up by concrete and can be measured by weighing the sample. There is a linear relationship between the water absorption amount and speed of absorption for concrete with different initial pore humidity and temperatures. Cumulative water absorption decreases with increasing initial pore humidity and decreasing ambient temperature. This can be explained by a greater pore water pressure that is available at a higher temperature to overcome the surface tension, which therefore increases the capillary flow (Wong et al., 2001).

The moisture content of concrete reaches an equilibrium moisture content with the external environment. This happens at the surface of the concrete and the rate at which moisture is transferred at the surface is called the moisture-vapour emission rate. This is unrelated to the slab thickness. However, if the concrete slab is thicker, it will take longer to reach an equilibrium moisture content. The drying time of concrete depends on the w/c ratio and the drying environment. Concrete with a lower w/c ratio shortens the drying time. But the drying rate of higher w/c ratio concretes is also higher since there is more initial water present in the concrete. This is true to the point that the concrete becomes too porous (Kanare, 2007). Porosity is related to the w/c ratio. The lower the w/c ratio, the lower the porosity and the lower the pore connectivity (Quincot et al., 2011). Lower relative humidity and higher temperature increase the drying rate of concrete. The drying time for a 100 mm thick concrete slab is about three months for concrete with a w/c ratio up to 0.5 when drying occurs on one side or surface only. This increases to six months for a 150 mm thick slab and twelve months for a 200 mm thick slab (Kanare, 2007).

3.3 Water retention and evaporation in mosses

First moss morphology is discussed to clarify how mosses can take up water. Then the water behaviour in moss plants is explained. Followed by a section about the evaporation of water from the moss plant.

3.3.1 Moss morphology

There is some discussion about the definition of bryophytes. Bryophytes in the broader sense of the word comprise three groups: liverworts, hornworts and mosses. In a stricter sense, bryophytes are only seen as mosses. The taxonomic group of mosses can be further defined into the following classes: Takakiopsida, Sphagnopsida (peat mosses), Andreaeopsida (granite mosses), Andreaebryopsida (lantern mosses), Polytrichopsida, Tetraphidopsida, Buxbaumiopsida and Bryopsida (Glime, 2022). The group that is focused on in this literature review are Bryopsida, the largest group of mosses.

Mosses differ from vascular plants in that they do not have meristematic tissue, lignin, tracheid and sieve cells. Meristematic tissue consists of cells that are capable of cell division. Mosses do not have this tissue. Therefore, their growth happens apical, lengthening at the tips of roots or shoots. Lignin is the biopolymer that provides strength and rigidity to plant cell walls. Because mosses lack lignin, they are restricted in how big they can become. Tracheid cells transport water and sieve cells are sugar-conducting. However, there are mosses which have hydroids and/or leptoids to replace the function of tracheid or sieve cells respectively. The water-conducting hydroid cells form the hydrome, of which the central strand of a moss plant is often composed (Scheirer, 1980; Zamski & Trachtenberg, 1976). Another difference between vascular plants and mosses is that they produce rhizoids. These are rootlike structures mostly functioning as an anchorage but in some mosses also as transportation for water and nutrients. Because they do not necessarily use the rhizoids for water uptake, their water transport system is different from plants. In fact, mosses can take up water over their entire surface. (Jones & Dolan, 2012). Moss leaves do not have stomata. The lack of stomata means that the moss plant can lose water unwillingly. Their hydration state is controlled by their environment. Therefore, they like living in moist places (Glime, 2022).

The Bryopsida are traditionally divided into two groups based on branching patterns and the position of the sexual organs. Acrocarpous mosses are generally erect mosses with terminal sporangia at the apex of the stem. They are usually unbranched or sparsely branched. Pleurocarpous mosses produce their sporangia on short, specialised lateral branches or buds and are typically prostrate, forming free-branching mats (Glime, 2022).

Mosses have developed water-conducting structures. They gain water either through internal transport through a central cylinder (endohydric) or externally along the surface (ectohydric) using capillary movement (Buch et al., 1938). Drought-tolerant mosses, which can be applied in a façade, are often ectohydric. Ectohydric bryophytes sustain a constant internal water content through the absorption of water from external capillary spaces like a sponge. These spaces are present amongst the leaves, in fine hairs on the stem of rhizoids, and in papilla systems on leaf surfaces. The papillae are a dense system of bumps on the leaves of mosses. The papillae consist of layers of cuticles, a waxy substance found on the

surface of leaves that aids in preventing water loss. These structures allow the leaves to retain water by increasing the surface area to which it can adhere. A smoother surface would allow water to run off or evaporate, whereas a rough surface has a lot of space for water to be trapped in its nooks (Glime, 2022; Proctor, 2000b).

3.3.2 Water behaviour in mosses

First water availability starts from contact of the tips of stems and leaves with fog, rain or dew and not necessarily from the soil. Mosses move water from one part to another in one of four ways: through hydroid cells, free spaces in cell walls, cell to cell, or externally. Tension forces facilitate the movement of water. Moisture moves up through the mosses between the leaves and stem and is taken in by younger cells with thin walls at the tips of the stem and branches. From there, it spreads out through the internal tissue (Glime, 2022).

When moss becomes hydrated, its capillarity changes due to the expansion and untwisting of its leaves. When they dry out, the opposite happens. This is illustrated in Figure 3.3. Mosses benefit from a large surface area in relation to their volume because of numerous leaves and other structures such as paraphyllia and tomentum. Paraphyllia are leaflike structures attached to the stem or branches of some moss plants. The tomentum is a dense hairy covering on the rhizoids. External movement of water happens faster than internal movement and mosses are capable of absorbing water over their entire surface. Most mosses that form tufts (acrocarpous) are (partially) endohydric, while most that form mats and carpets (pleurocarpous) are ectohydric. When fully hydrated, the water content of these organisms is typically very high. When dry, they are capable of surviving for months or even years (Glime, 2022).

Figure 3.3: Microscope photo of drying of moss leaves, Anomodon viticulosus

Another strategy of moss plants to gain and retain water is to form cushions. By forming clumps The surface-to-volume ratio is decreased which reduces transpiration and creates additional capillary spaces. The shape of the clump is important in this relationship, particularly in mitigating the effects of wind. However, for this strategy to work, the surface of the cushion must be as smooth as possible. Wind flow patterns over moss cushions matched the measured water loss from surfaces of varying roughness. Above a critical wind speed, moisture loss increases rapidly. Greater roughness, caused by protruding shoots, increases the turbulent airflow. This leads to higher evaporation. However, leaf hairs protruding above the cushion surface reduced boundary layer conductance by about 20-35% in, for example, Grimmia pulvinata, which is a commonly found moss species in the Netherlands. Another adaptation to reduce water loss (Glime, 2022).

One more advantage of the cushion growth form and its water retention is the slowing of the drying rate. Humidity within the cushion plays an important role in water retention. When the humidity of the air a few centimetres above the cushion is 50%, it can be as much as 90% within the clump (Proctor, 2000a). Larger volumes of moss have the capacity to hold more water, and volume increases more rapidly than surface area. Larger cushions have a greater volume of water per unit of surface area, which makes them lose less water to evaporation than small cushions. The larger the cushion, the more resistance it has to water loss. However, with increasing size, the water holding capacity per unit of dry mass does not change. The combination of these two factors contributes significantly to the hydration period length (Glime, 2022).

3.3.3 Evaporation and transpiration in mosses

Because the water in a moss plant is only held by capillary forces, it is much more prone to evaporation compared to plants with stomata that have to open before evaporation is possible (M. Anderson et al., 2010). This means that almost all the water available in a moss plant can evaporate because in most cases only the sexual organs have stomata. The evaporation from moss leaves in a situation where the relative humidity is lower than that of full saturation happens rather fast. This is unrelated to the moss species (Krupa, 1977).

Mosses have some measures to delay the evaporation of water, like the growth form as mentioned in section 3.3.2. But also other structural adaptations like branch and leaf arrangements, rhizoidal tomentum, mucilage, paraphyllia and cuticles may reduce loss by transpiration (Glime, 2022). The presence of vascular plants may also reduce water loss, mainly by reducing wind speed at the moss surface (Heijmans et al., 2001), and thereby also protect the mosses from desiccation (Nichols and Brown, 1980). Mixed moss species can also help each other, especially if one is good at moving water and one is good at retaining it (Glime, 2022).

The relative humidity of the air also influences the evaporation rate of the moss. The moss Physcomitrella patens is a model moss species for studies at cellular level. Physcomitrella patens samples were dried at different ambient relative humidity. The samples were used 4 to 6 weeks after subculture and the mosses comprised both protonemal filaments, thread-like structures that develop from spores, and gametophores, the stem-like structures that grow from the protonemal filaments. The moss colony was cut up into sections approximately 2 cm in diameter. The water content of mosses drying at relative humidity of 13%, came to equilibrium at about 18% water content after 24h. And the water content of mosses drying at 97% relative humidity reached equilibrium at around 35% after 150h. Mosses drying to water contents less than ca. 0.3 g g/dm did not survive. This makes this moss desiccation sensitive. The water content of the tested samples ranged between 11 to 23 g/g dm (Koster et al., 2010).

Mosses use evaporative cooling to keep their temperature lower than the ambient temperature in hot conditions. They do this to reach their optimum temperature for growth. Temperatures in the range of 42-51 °C are typically lethal for mosses when they are hydrated. If temperatures do reach levels that are too high to sustain water in the moss plants, they survive through a state of dormancy called desiccation. In this state, their temperature tolerance is much higher (Glime, 2022).

4

Lab testing

4.1 Methodology

To find the cooling effect through evaporation of a moss-covered façade, the extent of evaporation from a moss-covered concrete surface must be known. This can differ for different moss species and different ambient conditions. No measuring device can identify the amount of water present in a moss plant at a certain moment in time. Therefore, to quantify the amount of water that evaporates from a moss surface, certain key figures were established in the lab by drying the moss over time.

These key figures include the water uptake, evaporation rate and drying times of the concrete surface in combination with different moss species. As a baseline, the evaporation of the concrete surface without moss is also measured and the mosses are also tested separately. All samples were tested at different ambient temperatures and relative humidity.

4.1.1 Moss samples

Before experiments were carried out on the mosses in the lab, first these mosses had to be found in nature. The mosses had to be epilithic (growing on a rock-like surface) and were found somewhere in Delft or its surroundings. Appendix A shows an extended overview of the mosses that were sampled in nature and the procedure of sampling.

Of each species, three samples with a size of around 10 x 10 cm were gathered. The samples were taken back to the lab and with a microscope, the specific species were established. The mosses that were selected for the lab experiments were chosen to have variety in the material of the substrate layer and their growth form (acrocarpous or pleurocarpous). The chosen species are listed below.

Moss 1: *Rhynchostegium confertum (pleurocarpous)*

Location: *Jaffalaan*

Material of the substrate layer: *Natural stone*

Figure 4.1: Finding location of moss Rhynchostegium confertum with microscope photo of moss leaves

Moss 5: *Eurhynchium striatum (pleurocarpous)*

Location: *Bieslandse bos*

The material of the substrate layer: *Brick*

Figure 4.2: Finding location of moss Eurhynchium striatum with microscope photo of moss leaves

Moss 7: *Bryum capillare (acrocarpous)*

Location: *Kandelaarbrug*

The material of the substrate layer: *Concrete/asphalt*

Figure 4.3: Finding location of moss Bryum capillare with microscope photo of moss leaves

Moss 8: *Syntrichia ruralis (acrocarpous)*

Location: *Ackerdijkse plassen*

The material of the substrate layer: *Concrete*

Figure 4.4: Finding location of moss Syntrichia ruralis with a microscope photo of moss leaves

4.1.2 Concrete samples

As mentioned in section 3.2.1, bioreceptive concrete is different from regular concrete in that it should be able to take up more water. A different mixture is used to increase porosity. Also, the surface is roughened and different additives are used. Among other things, concrete samples were made using the ingredients described in Table 4.1. The amounts of the different constituents are classified since the concrete mixture is being used for research.

Table 4.1: Concrete mixture used for making concrete samples

Constituents
Cement (CEMIII/B)
Mineral admixture (bone ash)
Aggregate (Recycled concrete 0/4)
Water

The mixture was poured into plastic trays which were pre-processed with a surface retarder. As a result, when the concrete hardened and was taken out of the trays, the surface was rough. After production, they were kept at normal room conditions for 7 weeks before testing began. The sample blocks measure 83 x 83 x 15 mm.

4.1.3 Experiment description

To find the water uptake, evaporation rate and drying times of the concrete and mosses, the following experiment was conducted. First, samples were weighed before testing commenced. Then the samples were submerged in water to fully saturate them. Subsequently, they were placed in a climate chamber (Nüve TK120) under different ambient conditions, and their weight was monitored. In this way, the key parameters are found for the different moss and concrete samples. In this section, the execution of the experiment is discussed in more detail.

Four types of moss were tested: Rhynchostegium confertum, Eurhynchium striatum, Bryum Capillare and Syntrichia ruralis. Of each species, 3 samples were collected. In total, this means that there were 12 moss samples. These were labelled and each one was linked to a concrete sample. First, the evaporation from the moss and the evaporation from the concrete was determined separately during one week of measurements. Then, the evaporation from the moss and the concrete together was determined for the second week of measurements. This was done for the conditions shown in table 4.2, resulting in eight weeks of measurements.

Table 4.2: Ambient conditions of testing

	Temperature (°C)	Relative humidity (%)
High temperature High humidity	25	80
High temperature Low humidity	25	50
Low temperature High humidity	15	80
Low temperature Low humidity	15	50

Before the actual testing started, the moss samples were cleaned. Excess branches, sand and other clutter were taken out as much as possible. The mosses were submerged in water for 2 minutes each. When taking them out of the water again, the excess water was allowed to drain off. After which they were placed in a tinfoil tray and left in the climate chamber to dry. See Figure 4.5.

Figure 4.5: Moss species Bryum capillare in tinfoil tray after water uptake

The concrete samples were each submerged in water for 10 minutes. At the end of this time interval, no more air was seen leaving the concrete. Then, the sides and back of the concrete were wrapped in plastic foil. See Figure 4.6. This allowed moisture to evaporate from one surface only just like it would in a façade. This surface is the rough surface of the concrete.

Figure 4.6: Concrete sample wrapped in plastic foil

This procedure was repeated for the concrete + moss measurements. The difference is that the moss is placed on top of the concrete sample covering the surface from which evaporation takes place. See Figure 4.7.

Figure 4.7: Concrete sample with Rhynchostegium confertum

In all the experiments, all the samples were weighed at the start of the test and hourly after that during the day. In most cases, after the 50-hour mark, the samples showed sufficiently low evaporation so an interval of measuring every 2 hours was sufficient.

Samples were weighed every hour between 08.00 am and 17.00 pm. This resulted in 10 measurement points during one day. The samples were weighed again the next day to see if they completely dried out the day before or not. If this was not the case the measurements continued hourly. Missing data points overnight were found from the trend line when the data points were plotted against time. The experiment stopped when the weight did not change anymore in three consecutive data points or after 5 working days.

4.1.4 Result processing

The data of weight decrease for the samples was interpolated for missing data points overnight. This gives a function of weight decrease for each sample. Using cubic spline polynomials the found functions are smoothened. The derivatives of these functions show the amount of water in grams that evaporates over time in hours. This is the evaporation rate of the samples.

From the plotted functions .csv files were extracted to obtain the values for weight decrease or evaporation per hour. These files were used to read the drying time for example, or the evaporation rate at a specific moment in time. Statistical tests were performed on this data to find the averages and standard deviations for the different samples.

4.2 Results

Testing was done to find the evaporation rates of different moss species, the evaporation rate of bioreceptive concrete and see the effect mosses have on the evaporation of a concrete sample. For each moss and concrete sample, the amount of water uptake, evaporation rate and amount of time until completely dry were examined for the moss and concrete separately and combined. This was done for the four scenarios with different temperatures and relative humidity.

4.2.1 Water uptake

In an absolute sense, the moss species that takes up the most water on average is Bryum capillare. When looking at the water uptake relative to the dry weight of the moss, Eurhynchium striatum can absorb the most water. It is also interesting to note that all mosses, when wet, are constituent of water by 75% or more. Table 4.3 shows values on the water uptake of mosses. These are averages for the three samples per moss species and the eight times they were submerged in water. The percentage of dry weight is the weight of water taken up divided by the weight of the moss when dry. The percentage of wet weight is the weight of water taken up divided by the weight of the moss when completely saturated.

Table 4.3: Average water uptake of different moss species

	Water uptake (g)	% of dry weight	% of wet weight
Rhynchostegium confertum	27.4 (SD 4.96)	311	76
Eurhynchium striatum	27.0 (SD 5.24)	1173	92
Bryum capillare	32.4 (SD 6.48)	354	78
Syntrichia ruralis	25.3 (SD 5.37)	788	89

For concrete, all the samples take up almost the same amount of water. The average water uptake is 21.1 g (SD 1.05). Differences between samples can occur because of how dry the samples were when wetting them (the amount of moisture still present in the samples), the porosity of the samples and the exact amount of time they were submerged in water.

4.2.2 Evaporation rate mosses

Figure 4.8 shows the decrease in weight over time for the different moss species at 25°C and 80% RH. The figures of weight decrease for other conditions can be seen in Appendix C. From these figures, the drying times of the moss can be found for the different conditions.

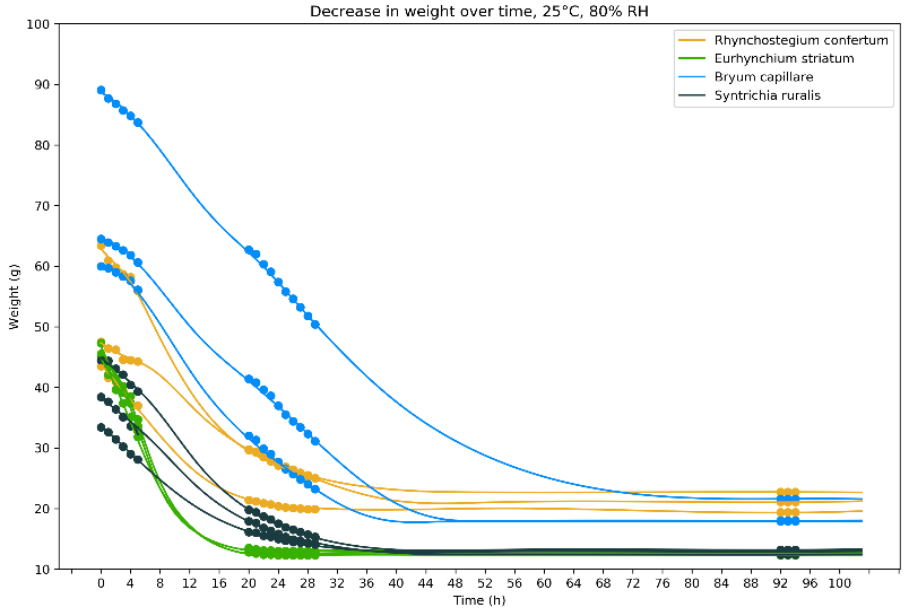

Figure 4.8: Decrease in weight (g) over time (h) for different moss species at 25°C, 80% RH

Table 4.4 shows the results for average drying time. These numbers are found by looking at the time which has passed when the derivative of the curve is equal to zero for two decimal points. Under almost all conditions, Bryum capillare is capable of holding moisture the longest. Eurhynchium striatum loses its water the quickest under high temperatures. For the driest condition of 25°C and 50% RH, drying times are the fastest for all moss species.

Table 4.4: Average drying time (h) for four moss species under different conditions

	25°C, 80% RH	25°C, 50% RH	15°C, 80% RH	15°C, 50% RH
Rhynchostegium confertum	50 h (SD 7.0)	39 h (SD 4.5)	73 h (SD 6.7)	46 h (SD 3.6)
Eurhynchium striatum	37 h (SD 0.6)	31 h (SD 1.0)	53 h (SD 2.0)	44 h (SD 2.1)
Bryum capillare	70 h (SD 14.5)	40 h (SD 1.5)	90 h (SD 12.2)	59 h (SD 10.0)
Syntrichia ruralis	51 h (SD 1.5)	28 h (SD 3.5)	44 h (SD 3.8)	43 h (SD 2.5)

The derivatives of the weight curves represent the evaporation rates of the moss species. These evaporation rates at 25 °C and 80% RH are plotted against time in Figure 4.9.

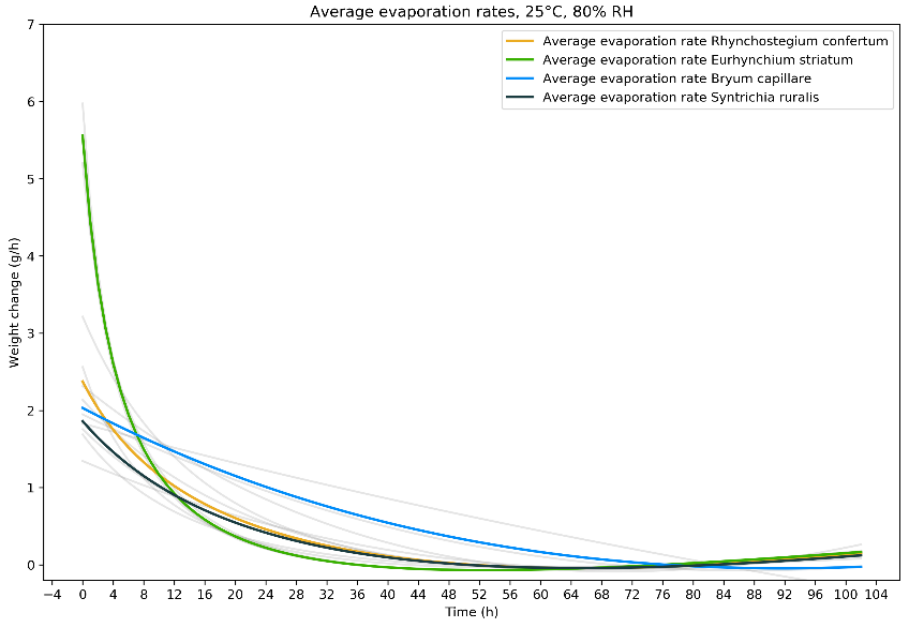

Figure 4.9: Average evaporation rate moss samples 25°C, 80% RH

The figures of evaporation rate for other conditions can be seen in Appendix C. From these figures, information was obtained about the evaporation rate of the different moss species under different conditions. Some general observations that are important to note are:

- Evaporation rates for all moss species are highest for the situation of 25°C and 50% RH.
- Evaporation rates at the beginning of the tests have a lot of difference between the moss species. After some time, most mosses evaporate water at roughly the same speed. Bryum capillare is the exception. It sustains a higher evaporation rate throughout the experiment.
- For the lower temperature of 15°C, there is less variability in the evaporation rates throughout the experiment.
- Eurhynchium striatum seems to be affected by an increase in temperature the most.

Table 4.5 shows the drying rates at the beginning of the tests for the different moss species.

Table 4.5: Average evaporation rates at the start of the test for different moss species under different conditions

	25°C, 80% RH	25°C, 50% RH	15°C, 80% RH	15°C, 50% RH
Rhynchostegium confertum	2.37 g/h (SD 0.9)	3.34 g/h (SD 0.9)	0.93 g/h (SD 0.2)	1.85 g/h (SD 0.4)
Eurhynchium striatum	5.56 g/h (SD 0.4)	6.05 g/h (SD 0.3)	1.36 g/h (SD 0.1)	2.23 g/h (SD 0.5)
Bryum capillare	2.03 g/h (SD 0.3)	2.97 g/h (SD 1.2)	0.88 g/h (SD 0.5)	1.68 g/h (SD 0.4)
Syntrichia ruralis	1.86 g/h (SD 0.2)	6.32 g/h (SD 1.5)	2.69 g/h (SD 0.6)	2.26 g/h (SD 0.5)

From these numbers, it can be seen that Eurhynchium striatum and Syntrichia ruralis have the highest variability in drying rates for different conditions. Therefore, they are most affected by different climatic conditions. The other mosses are more constant. Syntrichia ruralis is an acrocarpous moss growing in cushions so one would expect a higher ability of this moss to retain water. However, during the experiment, after drying, the individual branches were not able to stick together in a cushion which might lower its ability to retain water. Also, it is desiccation tolerant which means that it does not necessarily have to stay hydrated at all costs. Many moss species can tolerate desiccation, allowing them to live in environments with periodic dryness. Some species of mosses have high physiological desiccation tolerance, while others have developed adaptations to avoid dry periods (Glime, 2022; Vitt et al., 2014). This is illustrated in Figure 4.10.

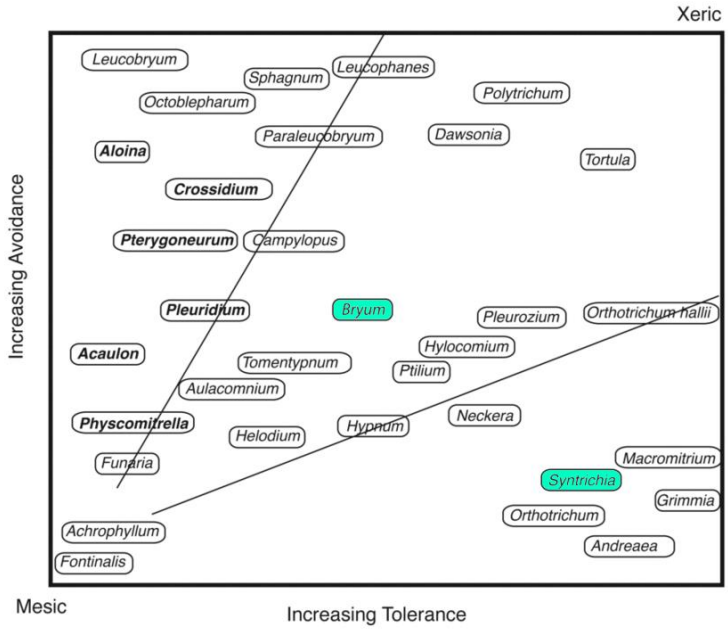

Figure 4.10: Distribution of some moss species along a dryness gradient (adapted from Vitt et al., 2014)

Bryum capillare has the lowest drying rate of the mosses under all conditions. This moss grows in cushion form. As explained in section 3.3.2, this growth form increases the drying time of the moss and reduces the evaporation rate (Glime, 2022).

4.2.3 Evaporation rate concrete

All the concrete samples have the same material parameters. Therefore only the weight differs between samples and the evaporation rate is not expected to differ much. Figure 4.11 shows the weight decrease of the concrete samples under 25 °C and 80% RH. The figures for weight decrease for other conditions can be seen in Appendix C. The results show that drying occurs rapidly at the beginning of the test. And that drying occurs faster for higher temperatures and lower relative humidity.

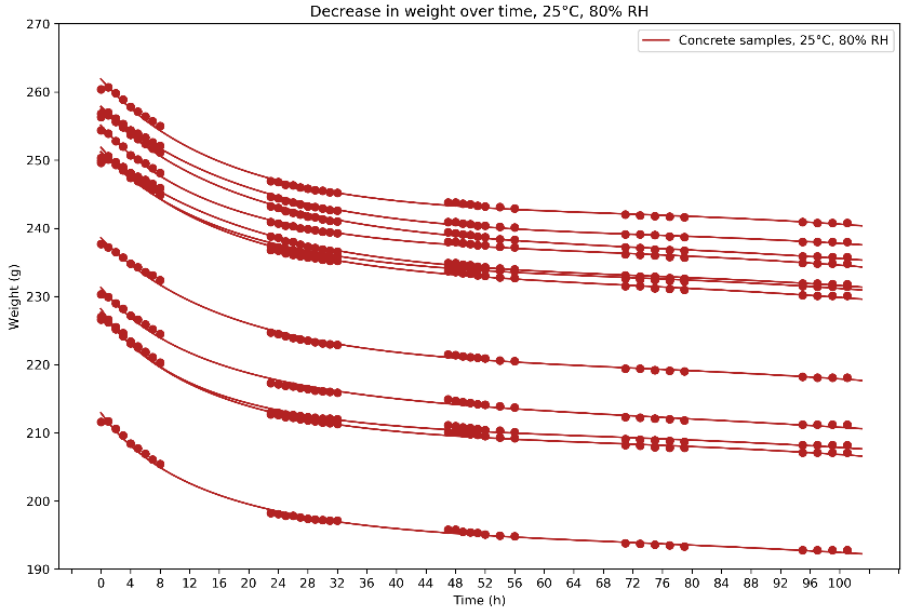

Figure 4.11: Decrease in weight (g) over time (h) for concrete samples 25°C, 80% RH

When all concrete samples are averaged for the different conditions, the drying times can be found. It was found that the concrete does not completely dry out during the time of the experiment. However, a tipping point can be found after which evaporation is almost constant. This is the point at the end of the elbow of the curve. The time it takes to reach this point can be seen in Table 4.6.

Table 4.6: Average drying time (h) for concrete samples under different conditions to reach the tipping point

	25°C, 80% RH	25°C, 50% RH	15°C, 80% RH	15°C, 50% RH
Concrete	46 h (SD 3.9)	38 h (SD 1.5)	52 h (SD 7.3)	44 h (SD 2.9)

The derivatives of the weight curves represent the evaporation rates of the concrete samples. These evaporation rates at 25 °C and 80% RH are plotted against time in Figure 4.12. The figures for the evaporation rate for other conditions can be seen in Appendix C.

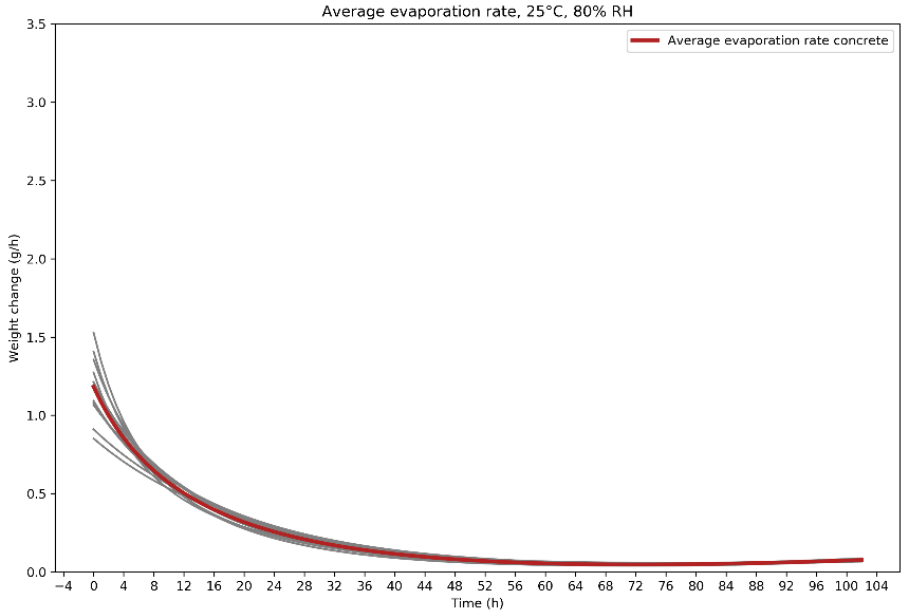

Figure 4.12: Average evaporation rate concrete samples 25°C, 80% RH

From these figures, it can be seen that the evaporation rate is highest for the condition of 25°C and 50% RH. (3.02 g/h) After the tipping point, evaporation happens at a rate of 0.07 g/h. Table 4.7 shows the drying rates at the beginning of the tests and the drying rates after the tipping point for the other conditions as well.

Table 4.7: Average drying rates start of the test and after the tipping point

	25°C, 80% RH	25°C, 50% RH	15°C, 80% RH	15°C, 50% RH
Drying rate start of the test	1.18 g/h (SD 0.2)	3.02 g/h (SD 0.2)	0.49 g/h (SD 0.2)	1.40 g/h (SD 0.3)
Drying rate after tipping point	0.10 g/h (SD 0.01)	0.07 g/h (SD 0.02)	0.05 g/h (SD 0.05)	0.06 g/h (SD 0.01)

4.2.4 Evaporation rate concrete + moss

Figure 4.13 shows the decrease in weight over time for different conditions for the different moss species in combination with the concrete samples under 25 °C and 80% RH. The figures of weight decrease for other conditions can be seen in Appendix C. From these figures, the drying times of the moss + concrete can be found for the different conditions.

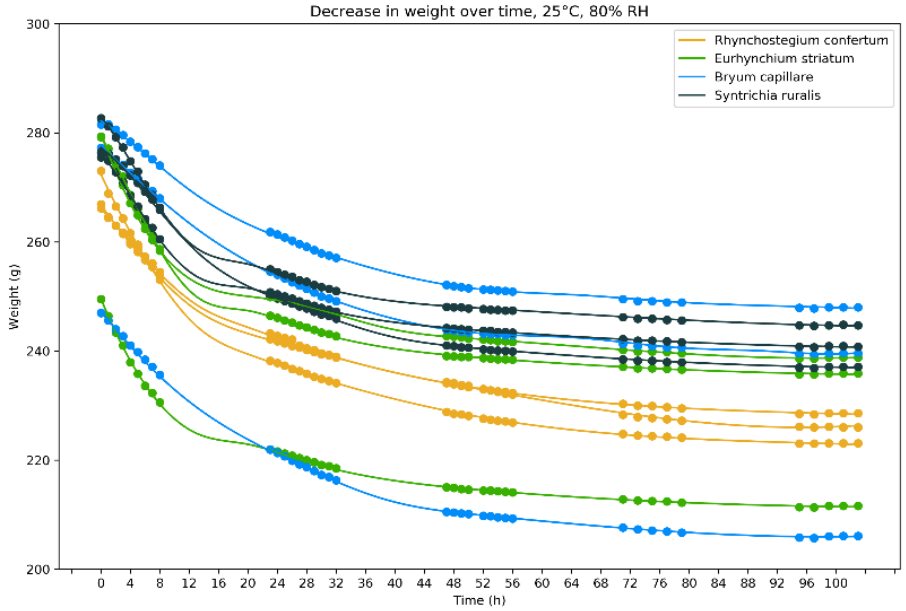

Figure 4.13: Decrease in weight (g) over time (h) for concrete with different moss species at 25°C, 80% RH

When all samples are averaged for the different conditions, the drying times can be found. It was found that the concrete with moss does not completely dry out during the time of the experiment. However, a tipping point can be found after which evaporation is almost constant. This is the point at the end of the elbow of the curve. The time it takes to reach this point can be seen in Table 4.8.

When comparing these numbers to the drying time of just the concrete, it can be seen that the drying times are not necessarily longer under any conditions for most mosses. Only the average drying time of Bryum capillare is significantly longer.

Table 4.8: Average drying time (h) for concrete + moss samples under different conditions to reach tipping points

	25°C, 80% RH	25°C, 50% RH	15°C, 80% RH	15°C, 50% RH
Rhynchostegium confertum	43 h (SD 3.1)	40 h (SD 1.2)	37 h (SD 9.5)	49 h (SD 5.5)
Eurhynchium striatum	40 h (SD 2.3)	37 h (SD 1.0)	40 h (SD 1.5)	42 h (SD 0.0)
Bryum capillare	56 h (SD 2.1)	46 h (SD 2.1)	63 h (SD 13.2)	59 h (SD 4.6)
Syntrichia ruralis	44 h (SD 6.6)	37 h (SD 3.0)	47 h (SD 4.2)	45 h (SD 2.5)

The derivatives of the weight curves represent the evaporation rates of the concrete + moss samples. These evaporation rates at 25 °C and 80% RH are plotted against time in Figure 4.14.

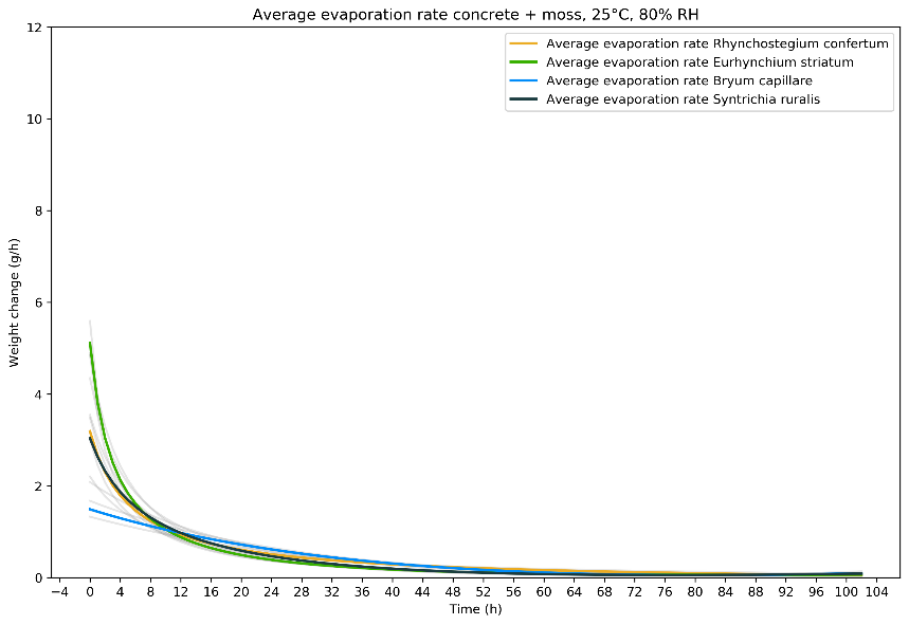

Figure 4.14: Average evaporation rate concrete + moss samples 25°C, 80% RH

The figures of evaporation rate for other conditions can be seen in Appendix C. From these figures, information can be obtained about the evaporation rate of the different moss species with concrete samples under different conditions. There are not a lot of differences between the evaporation profiles of the mosses separately. The evaporation rates are naturally higher because there is more moisture available in the system. Bryum capillare is still the most constant and evaporates the most water.

Table 4.9 shows the drying rates at the beginning of the tests for the different moss species. Table 4.10 shows the drying rates after the tipping point for the different moss species. The evaporation rates at this point were higher than that of just the concrete.

Table 4.9: Evaporation rate at the start of the test for different moss species with concrete under different conditions

Start of test	25°C, 80% RH	25°C, 50% RH	15°C, 80% RH	15°C, 50% RH
Rhynchostegium confertum	3.19 g/h (SD 1.1)	7.48 g/h (SD 3.6)	2.17 g/h (SD 1.1)	2.81 g/h (SD 1.6)
Eurhynchium striatum	5.11 g/h (SD 0.4)	10.79 g/h (SD 1.1)	3.16 g/h (SD 0.8)	4.98 g/h (SD 1.4)
Bryum capillare	1.49 g/h (SD 0.2)	3.49 g/h (SD 1.4)	1.12 g/h (SD 0.4)	2.88 g/h (SD 0.1)
Syntrichia ruralis	3.04 g/h (SD 0.8)	6.41 g/h (SD 0.7)	1.83 g/h (SD 0.3)	4.36 g/h (SD 0.2)

Table 4.10: Evaporation rate after the tipping point for different moss species with concrete under different conditions

After tipping point	25°C, 80% RH	25°C, 50% RH	15°C, 80% RH	15°C, 50% RH
Rhynchostegium confertum	0.27 g/h (SD 0.03)	0.10 g/h (SD 0.04)	0.29 g/h (SD 0.07)	0.17 g/h (SD 0.02)
Eurhynchium striatum	0.18 g/h (SD 0.02)	0.11 g/h (SD 0.02)	0.23 g/h (SD 0.02)	0.16 g/h (SD 0.04)
Bryum capillare	0.14 g/h (SD 0.01)	0.05 g/h (SD 0.03)	0.27 g/h (SD 0.16)	0.03 g/h (SD 0.04)
Syntrichia ruralis	0.16 g/h (SD 0.02)	0.10 g/h (SD 0.03)	0.24 g/h (SD 0.03)	0.07 g/h (SD 0.03)

4.3 Discussion

4.3.1 Lab experiments

Sand was part of the weight of the mosses but gradually fell off during the first week of the experiment. Calculating the water percentage of dry weight is therefore not accurate for the first measurement and not included in the calculation. In future research, it would be best to first dry the samples once, before starting the actual experiment to be able to brush off all the sand.

Samples were placed horizontally in the climate chamber and therefore data on evaporation is less accurate. Evaporation is more efficient on vertical surfaces, which results in higher total heat transfer rates and evaporation time is up to 10% shorter when moss is applied vertically in a façade (Qi et al., 2019). When evaporation happens, a temperature difference between surface and air is created. For horizontal evaporation, a stagnant cooler air layer appears above the sample surface. In vertical samples, the colder air would be able to circulate away allowing for more warmer air to aid in the evaporation process.

Another influence that was not accounted for in the climate chamber was air circulation. It is assumed that air circulation was quite low, but it might affect the evaporation of the samples. The position of samples in the climate chamber might influence results because the movement of air is not the same throughout the climate chamber. The position of the samples in the chamber was not changed during the experiment.

A drawback of using a biological material like moss is that it is not uniform. The weight or surface area can differ from sample to sample. Because it is alive, experiments might also influence its properties. Drying and rewetting for example might damage the cell structure of the moss. Especially if it happens quickly (Glime, 2022). This might influence the performance of taking up water or holding it. However, a decrease in the performance of the mosses was not seen over the course of the experiment. Water uptake was not very constant for all the moss species. The standard deviation of measurements was quite high compared to the water uptake by the concrete. This also has to do with loss of material, and plants falling apart. It is hard to keep the same amount of biomaterial during all the weeks of testing.

4.3.2 Result processing

The evaporation rates are an approximation based on data from the actual situation. This can for example be seen at the end of the evaporation graphs. They should be equal to zero because evaporation stopped. But because a cubic spline polynomial is used as an approximation, it is not equal to zero. This should be taken into account when studying the graphs. The accuracy of these approximations would increase for a higher number of samples.

Weighing samples sometimes was not done exactly on the hour resulting in minor measurement errors. And the use of the scale which was not always level also influenced the measurement of the weight. However, when approximating the interpolated data using cubic spline polynomials these measurement errors are compensated. This can result in an underfitting or overfitting of data. But, because multiple samples were averaged, the overall results are more reliable and standard deviations are given to indicate the range in which the values might fall.

4.4 Conclusion

The concluding remarks for this chapter are given in answer to the sub-research question:

What is the relationship of moss and concrete to the evaporation of water under different ambient conditions?

Four different moss species, Rhynchostegium confertum, Eurhynchium striatum, Bryum capillare and Syntrichia ruralis were tested on their water uptake, evaporation rate and drying time. They all took up water in the range of 25.3 and 32.4 g which is between 311 and 1173% of their dry weight and between 76 and 92% of their wet weight.

Under all conditions, Rhynchostegium confertum and Bryum capillare have the longest drying times. The drying times for all mosses ranged from 28 to 90 h under the different conditions.

When examining the drying rates of various moss species, it was found that under conditions of 25°C and 50% RH, all moss species demonstrated the highest levels of evaporation. At the beginning of the tests, there was a high degree of variability in the evaporation rates between the different species. However, after a certain amount of time had passed, most mosses seemed to evaporate water at approximately the same speed. The exception to this rule was Bryum capillare, which maintained a consistently higher evaporation rate throughout the experiment. At the lower temperature of 15°C, there was less variability in the evaporation rates throughout the experiment. It appears as though Eurhynchium striatum is the species most affected by an increase in temperature.

Eurhynchium striatum and Syntrichia ruralis have the highest variability in drying rates for different conditions. Although Eurhynchium striatum can take up a lot of water relative to its own weight, it loses water very quickly. In contrast, Syntrichia ruralis is an acrocarpous moss that grows in cushions, which would suggest that it has a higher ability to retain water. However, during the experiment, the individual branches were not able to stick together in a cushion which may have lowered its ability to retain water. Additionally, it is desiccation tolerant, which means that it does not necessarily have to remain hydrated at all times. It can survive for a longer time when dry. As a result, these mosses are the most affected by different climatic conditions. The other mosses are more consistent in their behaviour.

Bryum capillare was able to take up the most water, retain water for the longest time, and maintain a higher evaporation rate throughout the process. Among the mosses tested, Bryum capillare had the lowest drying rate under all conditions. This moss grows in cushion form, and by forming clumps, the surface-to-volume ratio is decreased, which reduces transpiration and creates additional capillary spaces. The larger the cushion, the more resistance it has to water loss. However, as the cushion grows in size, the water-holding capacity per unit of dry mass does not change. The combination of these two factors contributes significantly to the length of the hydration period.

Bioreceptive concrete samples of 83 x 83 x 15 mm took up 21.1 g of water on average. The concrete samples did not completely dry out during the tests. They did reach a point where evaporation rates dropped to a constant (0.05 to 0.10 g/h). It took them 38 to 52 h under the different conditions to reach this point.

When the concrete and moss were sampled together, the time to reach the point where evaporation rates dropped to a constant did not significantly increase. Except for Bryum, here the drying times were longer in combination with the concrete. The other moss samples dried out on top of the concrete and did not seem to be fuelled by the water from the concrete. This could be different when the mosses actually grow on the concrete and are applied vertically.

5

Field testing

5.1 Methodology

The goal of testing in the field is to see what the impact is of applying bioreceptive concrete facades in an actual outdoor environment. Through monitoring the temperature of a bioreceptive concrete façade panel with moss and a panel without moss, the difference in cooling properties will become clearer. The results are compared to the results from the tests in the lab. By monitoring the temperature over an extended period, the influence of characteristic weather conditions can be examined. At the Green Village of the TU Delft, a test site is available for conducting experiments on innovations.

5.1.1 Configuration of test equipment

To perform tests on bioreceptive concrete façade panels a frame was built in which two concrete panels were placed. The two bioreceptive concrete panels of 900 x 180 x 30 mm were mounted vertically on the frame. One of them was covered in moss, the other one was not. Both were kindly provided by Respyre, a company which is working hard on the development of this product. The mosses used on this panel are not known. Respyre uses a mixture of different moss species which are cultivated on the panels. It was however clear that all mosses on the panel were pleurocarpous.

On the backside of the frame, a Styrofoam board of 100 mm thickness, which is a reasonably good insulator, was applied to prevent cooling or heating on the backside of the panels by wind or sun for example. The frame was placed perpendicular to the true north so the façade panels were facing south and they were situated in front of a fairly open field. They were exposed to the sun nearly all day. Therefore, it was possible to investigate the effect of cooling under hot conditions. Figure 5.1 shows the setup of the panels.

Figure 5.1: Front and back view of the frame with mounted façade panels and measuring equipment

Each panel had three PRT thermocouple temperature sensors which measured the temperature of the panel. They had an accuracy of 0.5 °C. Holes were drilled in the back of the panels in which the sensors were mounted. They reached just under the surface of the panels. The configuration as can be seen in Figure 5.2 shows how the thermocouples were placed to get a good image of the temperature distribution on the panel. By using multiple measurement points, potential outliers can be picked out. For example when the moss was not evenly distributed or did not have enough coverage on the panel in each place.

As a double measurement, a FLIR Exx series thermal imaging camera was used. It provided thermal images of the moss-covered concrete panel and the adjacent control surface. This allowed for the calibration of the thermocouples and gave information about the temperature behaviour on the surface. The thermocouples logged data for an extended time. The IR camera was only available for a limited time and could not be left alone. So on a specific day, pictures were taken every few minutes during the daytime for one hour. The output of the IR camera helps to interpret the results of the thermocouples measurements.

An ATMOS 22 Ultrasonic anemometer was placed on top of the frame which measured wind speeds (m/s), wind gust speeds (m/s), wind direction (°) and air temperature (°C). Both the anemometer and the temperature sensors logged data every 5 minutes. The testing started on the 13th of March and ended on the 30th of April.

Figure 5.2 shows what the test setup ultimately looked like.

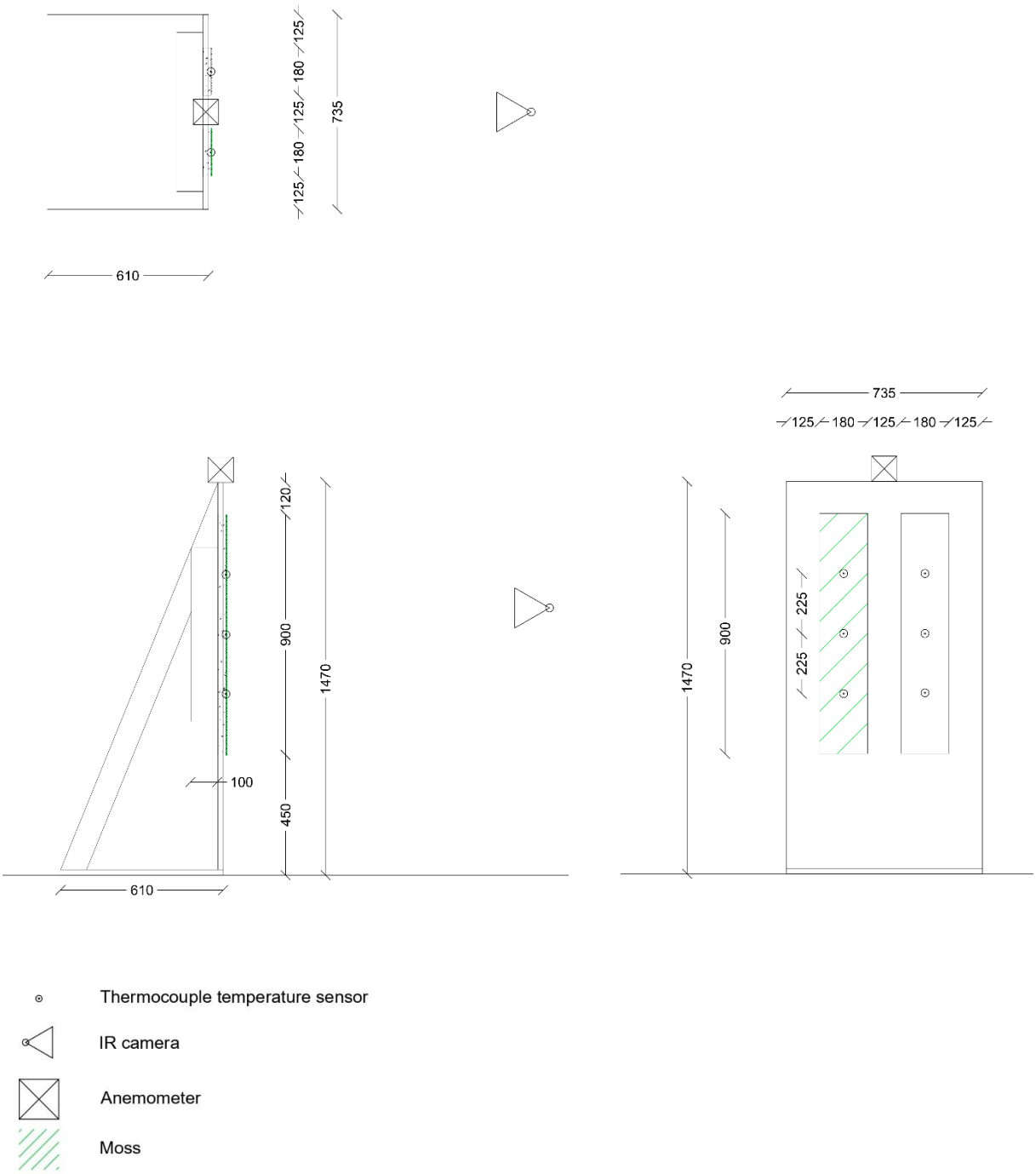

Figure 5.2: Plan, section, and front view of the test set-up configuration, sizes are given in mm

Since the panel was exposed to varying weather conditions, the objective was to identify characteristic weather days. A distinction is made between sunny, rainy and cloudy days. A sunny day has no precipitation, clear skies (12.5% or less cloud coverage) and low wind speeds (0 - 2.5 m/s). A rainy day has at least 3 mm of precipitation. And a cloudy day has no precipitation and mostly cloudy skies (62.5% or more cloud coverage). These days were found by utilizing the weather data from the Green Village weather station located on the roof of the office lab building, as shown in Figure 5.3. The weather station was located 30 m. as the crow flies from the panel location. The data files in .csv format included the following variables: solar radiation (W/m^2), relative humidity (%) and precipitation (mm). The data was retrieved from the Grafana data platform of the Green Village. The data interval was set to 5 minutes. Air temperature, wind speed and wind direction were already measured by the anemometer.

Figure 5.3: Test site Green Village with the location of the weather station (red circle) and concrete panels (red line) with an image of the actual situation as of 14-03-2023

The data gathered from both the lab and outdoor experiments was used to examine the release of water from the façade and the cooling that it induces. Trends may be found for different weather conditions and an indication is given of which parameters are most influential in the cooling effect of the bioreceptive concrete. It is expected that the concrete panel with moss growth will cool the air in front of it for a longer time than a panel without moss growth. The extent of cooling is expected to vary based on the weather conditions, i.e. for a hot sunny day after a period of hot days, the system is less likely to contribute to the cooling of the environment than for a hot day after a period of wet days.

5.1.2 Experiment description

Testing was done for a period of seven weeks. The six temperature sensors were connected to a Fluke 2638A Hydra Series III data logger. Data was retrieved from the datalogger every week on Monday. During this process, one or two data points were skipped because the data could not be retrieved when the test was running. The Styrofoam board was placed after two days of measurements on the 15th of March. This impacted the results of the measurements on that day since the temperature sensors had to be taken out.

On the 4th of April, a reference measurement of the temperature of the panels was done using an IR camera. This provided insight into the accuracy of the temperature sensors in the panels and showed the difference in surface temperature between the two panels. 40 ml of water was added to both panels using a plant sprayer. By taking thermal pictures subsequently every minute, the thermal behaviour of the surface of the panels is mapped quantitively in a visual representation.

Every day, the moss was watered to keep it alive. A log was kept on the status of the moss on the concrete panel. After a few weeks, the moss started to detach from the panel as shown in Figure 5.4. This could have happened because of a combination of weather conditions like frost, high wind speeds and high temperatures or another unknown reason like UV light damage or bad attachment of the moss in the lab. After four weeks, half of the panel was bare. Therefore, for the results of this experiment, mostly data is used from the first few weeks of testing.

Figure 5.4: Moss degradation per 2 weeks starting from the 13th of March

5.2 Results

Testing was done to find differences in the thermal behaviour of the two concrete panels. First temperature sensor data was compared for different weather conditions. Then, IR camera measurements were examined and compared to the temperature sensor measurements. Underlying trends were explained based on observations and weather data.

5.2.1 Temperature sensor measurements

The results of the field tests show a difference in temperature between the moss panel and the concrete panel. This temperature difference occurs when the temperature of the panels reaches 15° C to 20° C. On average, it ranges from 0° C difference to 5° C. See Figure 5.5.

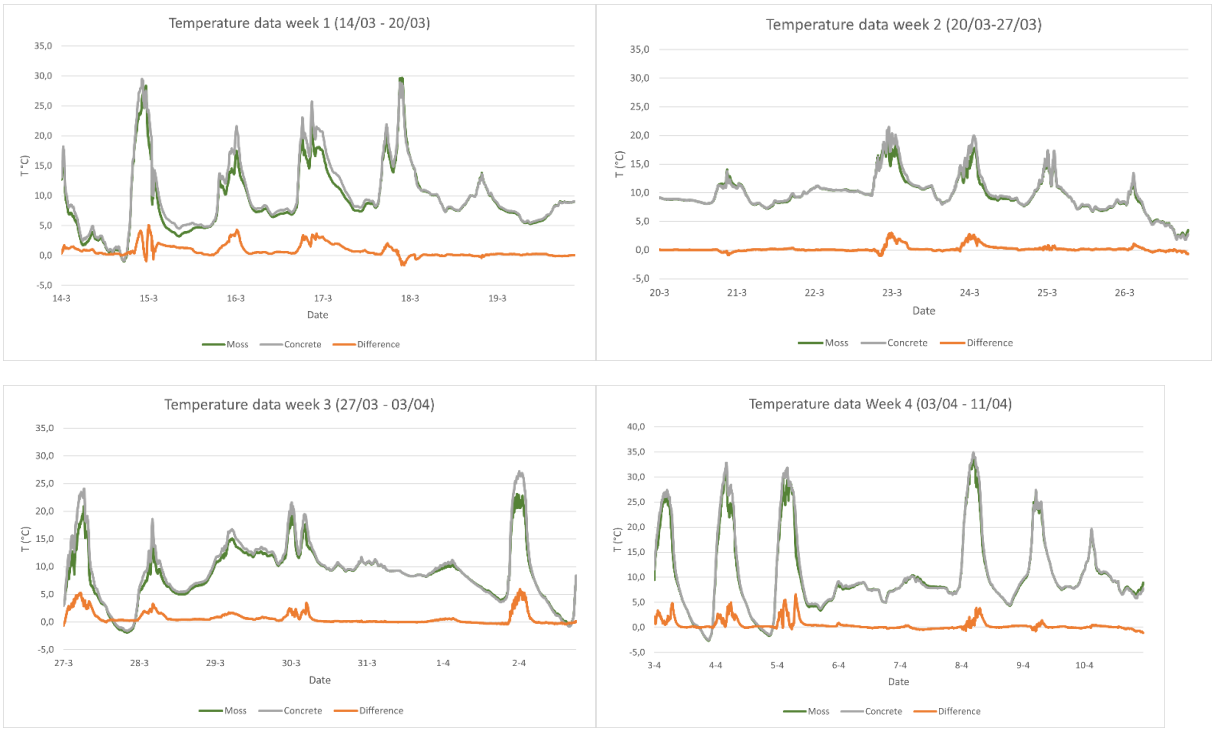

Figure 5.5: Temperature data moss and concrete panel per week with temperature difference between them

This difference especially occurs on sunny days. Therefore it is suggested that this temperature difference is partly caused by the difference in albedo between the two panels. The albedo of concrete is somewhere in the range of 0.10 - 0.40 whereas the albedo of moss is equal to 0.07 - 0.11 (Stache et al., 2022). This means that the moss reflects less incoming shortwave radiation and absorbs more of it. The temperature sensor situated behind the moss layer will therefore be cooler. The moss acts as a heat buffer.

When comparing two consecutive days, the 28th and 29th of March, this result is corroborated. On both days, the weather conditions were nearly the same. However, the 29th of March was a cloudy day. The temperature difference between the panels is a lot smaller for this day. It can also be seen when comparing the graphs of the temperature difference between the panels and the graphs of the solar radiation on both days. See figure 5.6.

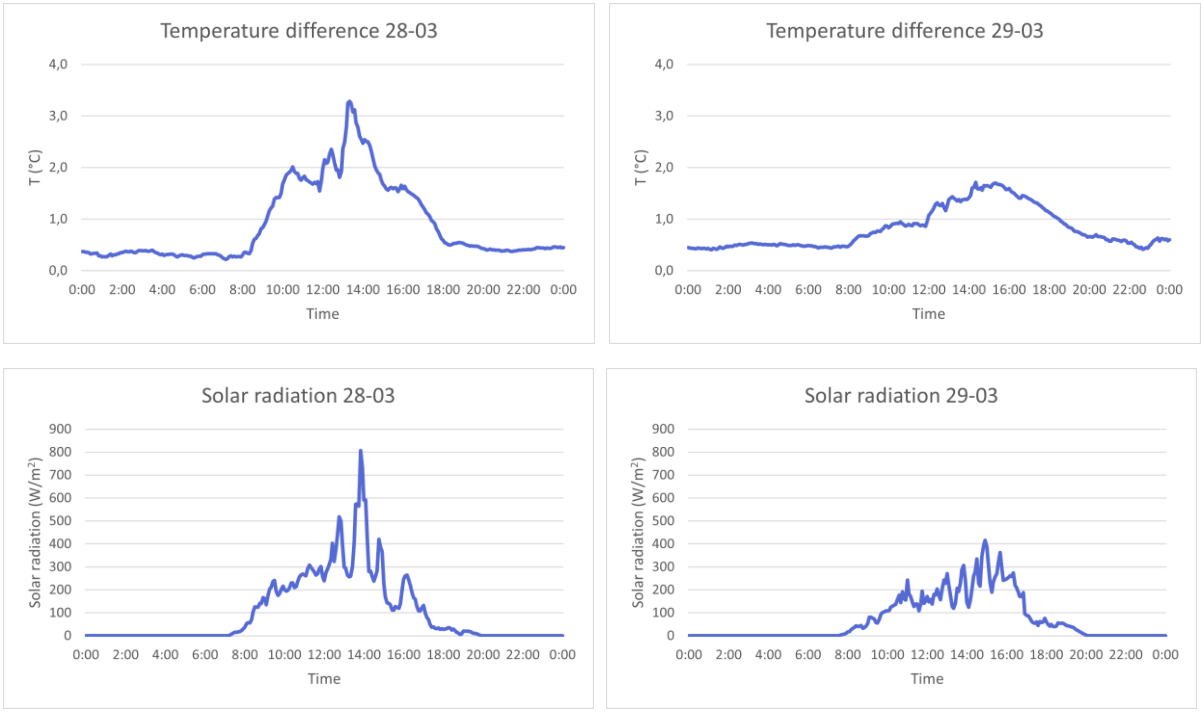

Figure 5.6: Temperature difference between panels and solar radiation on 28th and 29th of March

Another observation is that during the weekends, the temperature difference between the panels is also quite small. Even on warm and sunny days. This can be explained by the fact that panels are not watered during the weekends. A temperature difference might occur between the panels when they are wet because moss is capable of holding more water. As was seen in the literature (section 3.3.2 and section 3.3.3) and the lab experiments (section 4.3.1) mosses have a high capacity of taking up water. When water is available to the moss plants, they will retain more of it than the concrete. And when it evaporates, the moss has more water to evaporate resulting in a lower temperature for a longer time. For example, on the 18th of March. The temperature of the panels is higher than on the days before but the temperature of the moss panel at some point even exceeds that of the concrete panel. See Figure 5.5. Or on the 25th of March, the temperature of the panels exceeds 15°C but there is hardly a difference between the two panels. When we compare this to the 24th or 28th of March, the same temperatures of the panels are reached under almost the same weather conditions. But on these days, there is a temperature difference between the two panels. Figure 5.7 illustrates the differences between the 24th and 25th of March.

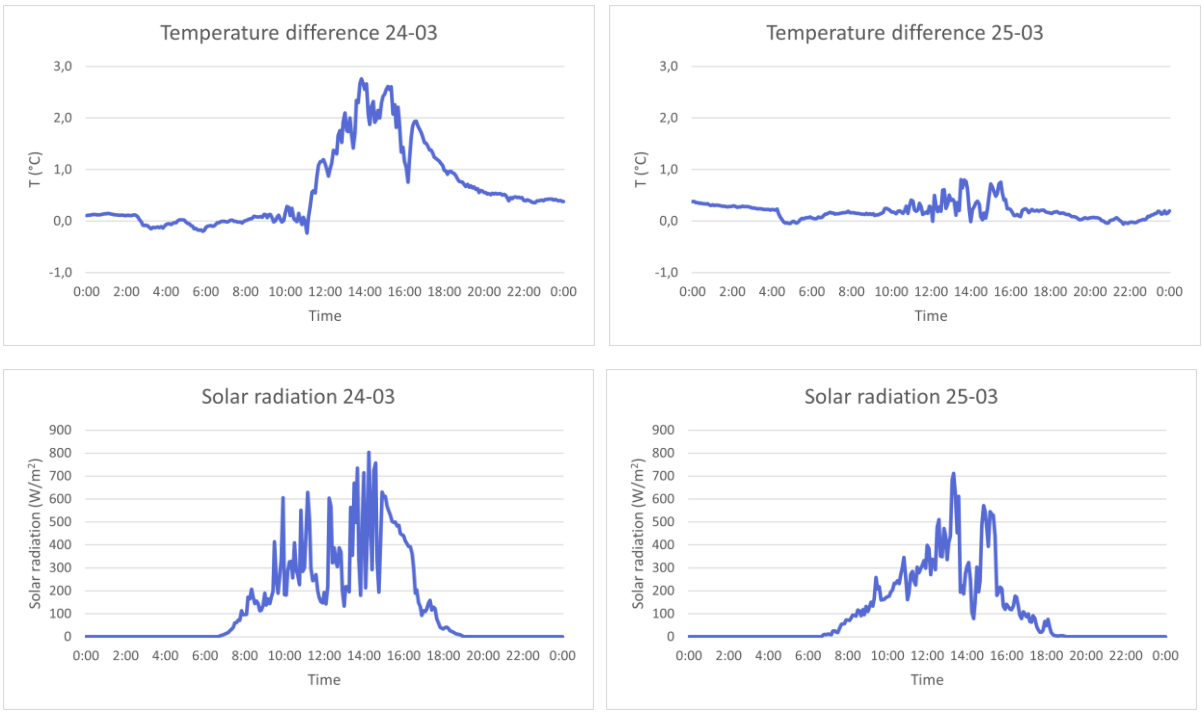

Figure 5.7: Temperature difference between panels and solar radiation on 24th and 25th of March

On rainy days, a temperature difference between the panels occurs depending on the duration of the rain event. For example, on the 23rd it rains during the night and morning. Afterwards, the sun breaks through, heats the panels, relative humidity drops and a temperature difference is noticeable due to a combination of albedo and evaporation of water. On the 31st of March, the rain continued throughout the day. On this day, both panels are soaked and take on the temperature of the rain. The relative humidity is also very high (90-100%) so evaporation is hard. The comparison between these days is shown in Figure 5.8.

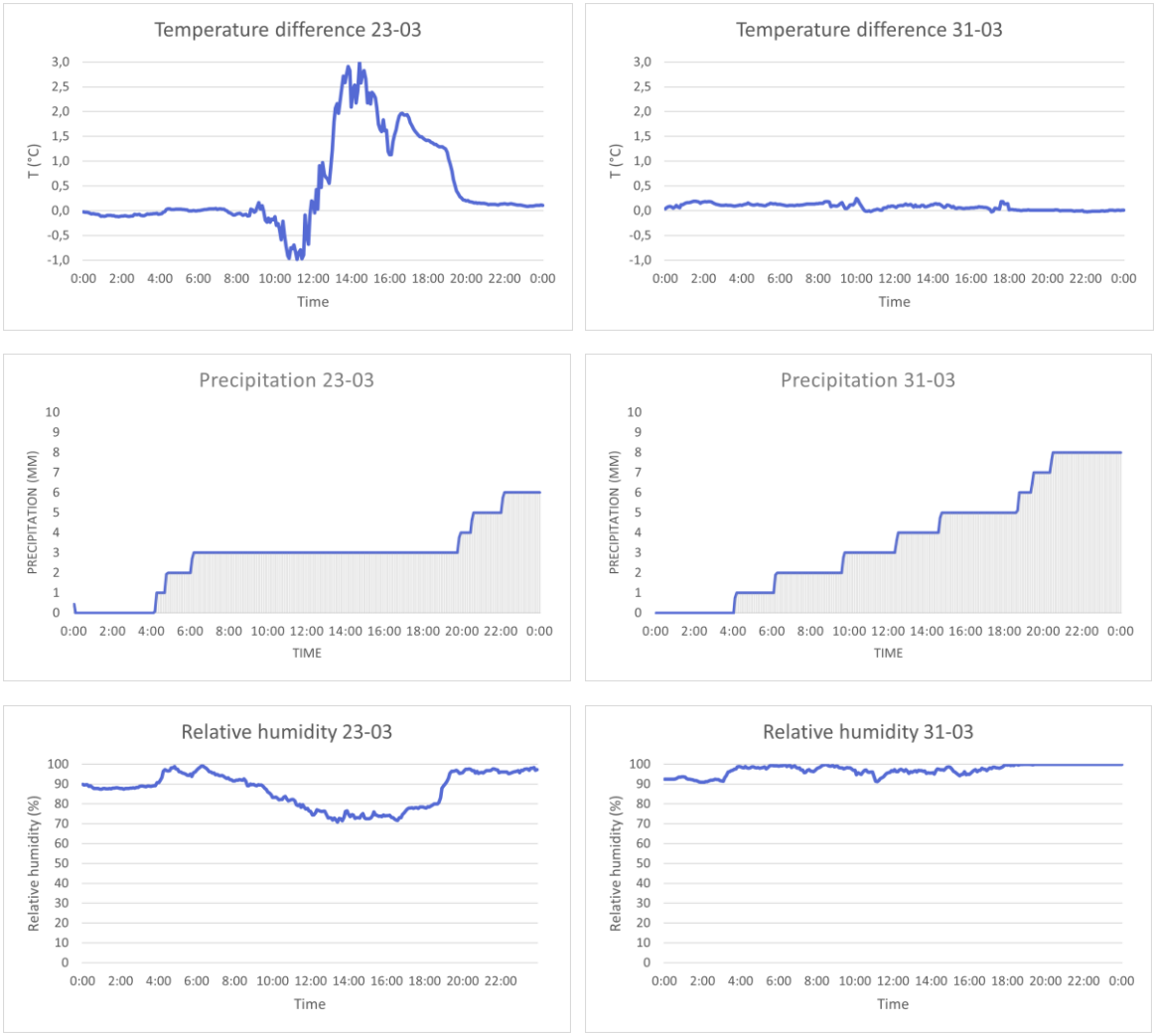

Figure 5.8: Temperature difference between panels and precipitation and relative humidity on 23rd and 31st of March

5.2.2 IR camera measurements

By performing measurements with an IR camera, the actual surface temperature of the façade was determined. On the 4th of April, measurements were done for about an hour. During this time, the panels were photographed when they were dry and after they were wetted.

At first, when the panels were dry, the values of the temperature sensors were lower than the values from the IR camera. Comparing the values obtained from the temperature sensors to the values of the IR camera measurement, a difference of 3,3 °C is seen for the moss panel and of 2,9 °C for the concrete panel when the panels are dry. When the panels were wet, this difference was very variable since the temperature of the surface changed rapidly and there is some delay in the temperature values of the sensors.

The photos taken with the IR camera show that moss temperatures are 2 to 3 °C higher than the concrete panel temperatures when dry. See Figure 5.9. This can be explained in two ways. First, the albedo of the moss is lower than that of the concrete as explained before in section 5.3.1. This same ability of the moss to act as an absorber of solar energy prevents it from reaching the surface beneath.

Secondly, the moss has air entrapment between its leaves. The level of hydration plays a significant role in temperature. Water changes its temperature more slowly than air. The air in the moss layer is more stagnant, it cannot be circulated away easily. So, when the air heats up, a warm layer of air is kept in place in front of the concrete. But the entrapped air could also have a lower temperature than the ambient air resulting in a cooler layer of air in front of the concrete. This stagnant air layer acts as an insulation layer (Glime, 2022).

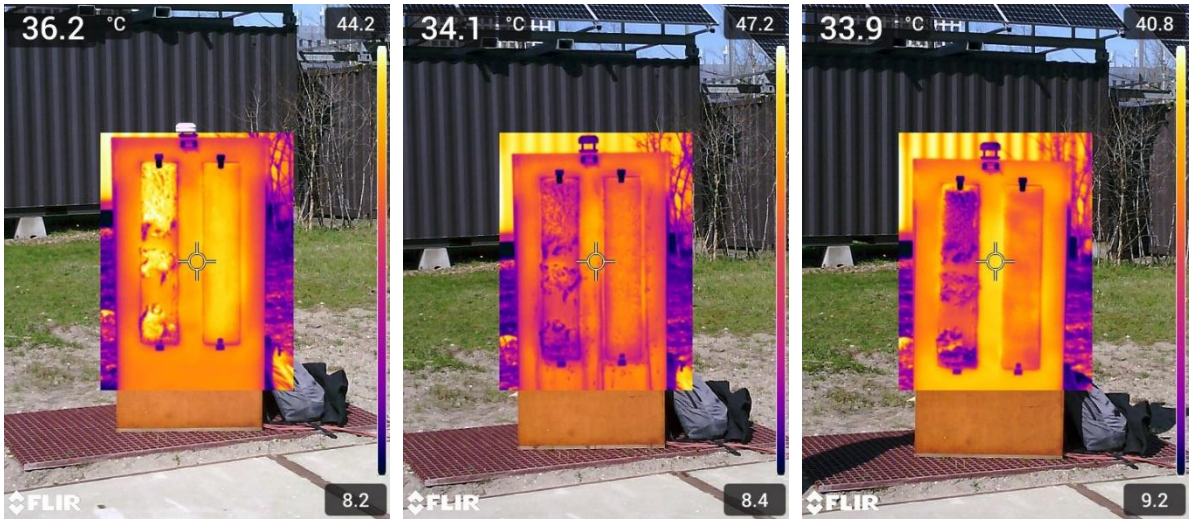

Figure 5.9: Photos taken with IR camera before, just after and half an hour after watering the panels

Both for the concrete and moss panels, the surface temperature dropped significantly (5°C to 10°C) when watering them. The initial drop in temperature is due to the water being cooler than the surface of the panels. Then temperatures stabilise and evaporation occurs. Both panels could be seen drying with the naked eye. Slowly temperatures start to rise again. The temperature of the moss panel is about 2°C to 5°C lower than the concrete panel when wet. Figure 5.10 shows the temperature course measured with the IR camera.

The moss can take advantage of water transfer from lower to upper parts of the moss plant. In the upper part, the water evaporates and cools the growing tips. Plants can reflect the sun by showing white, reflective surfaces to prevent the absorption of solar radiation. In bryophytes, this reflection may be achieved by hyaline (translucent) cells, white hair tips on leaves, or possibly even by the refractive nature of papillae (Glime, 2022).

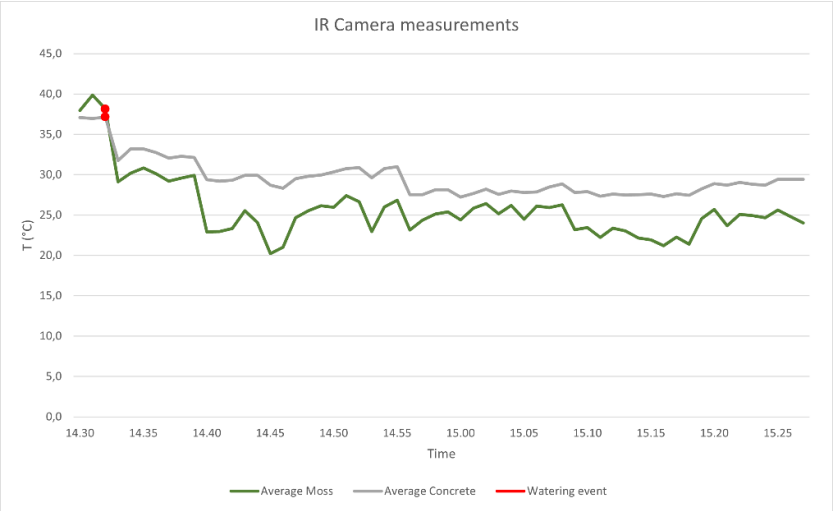

Figure 5.10: Average IR camera temperature measurements moss and concrete panel after watering event on 4th of April

In the temperature sensor measurements, the same trend of lowered temperature can be seen. Approximately two and a half hours later, the temperature is back at its 'old' or predicted level. See Figure 5.11.

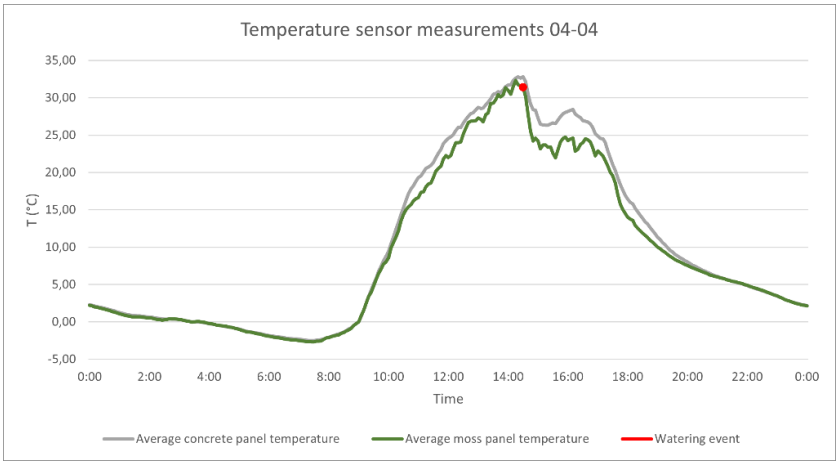

Figure 5.11: Average temperature sensor measurements moss and concrete panel 4th of April

The 17th of March shows the same trend. When watered the temperature of both the concrete and moss panel dropped by around 5 °C. On the 5th of April, the extent of cooling is in the same range of about 5°C for the moss panel. Here the concrete panel is not watered so the influence of watering becomes evident. With a duration of approximately 2 hours, the length of the cooling effect is also comparable. See Figures 5.12 and 5.13.

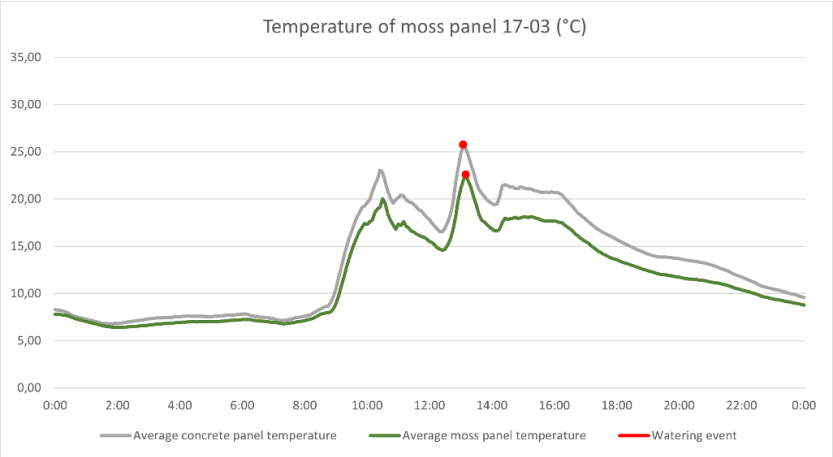

Figure 5.12: Average measured temperature moss and concrete panel with watering event on 17th of March

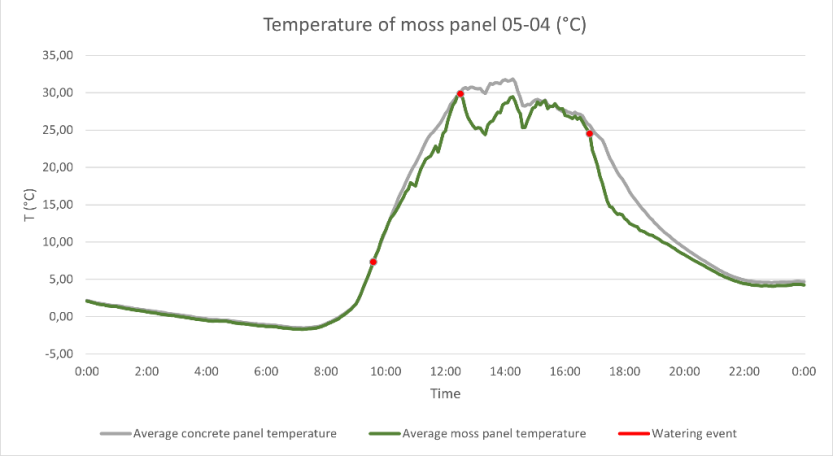

Figure 5.13: Average measured temperature moss and concrete panel with watering events on 5th of April

In conclusion, what can be seen from the temperature sensor and IR camera measurements is that temperature differences arise between the concrete and the moss panel. During sunny conditions, the temperature sensors behind the moss layer measure a lower temperature when the panels are dry because the moss takes up more solar radiation and acts as an insulation layer, trapping heat. Thus, the temperature sensors behind this layer stay cooler. After being wetted, the moss holds more water than the bare concrete resulting in more evaporation and a lower temperature for the moss panel again. Under rainy conditions, both panels have roughly the same temperature because there is no solar radiation and no evaporation of water.

The surface temperature measured with the IR camera is higher for the moss compared to the concrete when dry. The moss warms up more due to a lower albedo and entrapment of warm air. The surface temperature of the moss is lower compared to the concrete when wetted and stays lower for a longer time. This is due to the moss taking up more water, making it able to evaporate more water over an extended period.

5.3 Discussion

5.3.1 Reflection on testing

Working in an outside environment means that some variables are uncontrollable. A lot of different weather conditions happened during the period of testing but not necessarily the conditions in which the use of this façade is going to be highest. Namely, rainy days after sunny days or one very severe rain event on a very hot day. This test was performed in spring while the effect of cooling is especially useful in summer. For more accurate behaviour of the moss and concrete, this test should also be performed in the summertime.

Over the course of the experiment, the moss detached from the concrete panel and seemed dead in places. Therefore, the data gathered in the first few weeks is the most accurate. When the moss is dead it cannot hold water, so cooling will probably happen for a shorter amount of time. The moss detached from the bottom of the panel first. The temperature sensor located in this area started to take on the same values as the temperature sensors behind the bare concrete panel. Therefore, the data from week 5 of measurements and later is not used.

One of the temperature sensor cables was cut by a gardener during the experiment, resulting in a loss of data. This was one of the temperature sensors of the moss panel. So during the period in which this cable was out of use, the average temperature of the moss panel was taken over two, instead of three temperature sensor measurements. This makes the data of the moss panel from the 30th of March 08.40 AM till the 3rd of April 10.15 AM less reliable.

The concrete mix used was different for the concrete samples in the lab and the concrete used in the outside experiment. Respyre wants to keep their mix a secret since it is still a product in development. This affects the comparison between the lab and the outside experiment. The concrete might be able to absorb a different amount of water or evaporate it at a different rate.

5.3.2 Discussion of results

An observation that was made during the experiment was the increased temperature of the moss surface layer compared to the bare concrete surface when dry. This is partly explained due to the higher albedo of the concrete. As discussed in section 3.1.3, a higher albedo surface reflects more incoming solar radiation which is beneficial in countering the urban heat island effect when applied on roofs. However, in facades, a higher albedo means a lower temperature of the material but not necessarily a lower perceived temperature by a human on the street. If the reflected radiation is received by a pedestrian, this will increase their thermal discomfort (Erell et al., 2014; Schrijvers et al., 2016). Thus, the effect of decreased ambient air temperature as a result of higher façade albedo is cancelled by the received radiance. This means that the increased moss surface temperature is not necessarily a bad thing.

Another explanation for the increased temperature of the moss layer is the air entrapment in its leaves. This insulating property of the moss layer keeps the material behind it cooler. The implication of this extra insulation layer on the façade is yet to be investigated. By determining properties like the specific heat capacity and the heat conductivity of the moss layer, the amount of heat gain in winter and cooling gain in summer can be quantified. It is hypothesised that moss has a lower thermal mass than concrete. In the summertime, buildings often stay warm at night due to building materials with a high thermal mass. They hold the heat accumulated throughout the day. If moss has a lower thermal mass, it would lose its heat at night quicker. So if a moss layer can be used to prevent heating of the concrete behind it, buildings would stay cooler at night. This is when the urban heat island effect is more pronounced (Johnson et al., 1991; Koppe et al., 2004).

5.4 Conclusion

The concluding remarks for this chapter are given in answer to the sub-research question:

How is the relative temperature change for a bioreceptive concrete panel related to the weather conditions?

When panel temperatures rose above 15 to 20 °C, a difference between the concrete and moss panel was seen. This difference ranged from 0 to 5 °C. This temperature difference is caused by the presence of the moss. Because of higher solar radiation or watering of the panels, this effect is increased. On rainy or cloudy days, there is a small or no temperature difference between the panels.

With IR camera measurements, the actual surface temperature of the façade panels was determined. When dry, the moss surface temperature was about 2 to 3 °C higher than the concrete panel. This is explained by the difference in albedo between the two materials. The albedo of concrete is somewhere in the range of 0.10 - 0.40 whereas the albedo of moss is equal to 0.07 - 0.11. This means that the moss reflects less incoming shortwave radiation and absorbs more of it. Secondly, the moss has air entrapped between its leaves. The air in the moss layer is more stagnant, it cannot be circulated away easily. So when the air heats up, a warm layer of air is kept in place in front of the concrete. But the entrapped air could also have a lower temperature than the ambient air resulting in a cooler layer of air in front of the concrete. This stagnant air layer acts as an insulation layer.

When applying water to the panels, the surface temperature dropped significantly (5 °C to 10 °C) for both panels. The temperature of the moss panel is about 2 to 5 °C lower than the concrete panel when wet. The moss can take advantage of water transfer from lower to upper parts of the moss plant. In the upper part, the water evaporates and cools the growing tips. Bryophytes reflect solar radiation by hyaline cells, white hair tips on leaves, or possibly even by the refractive nature of papillae. For a watering event of 40 ml for each panel, the temperature decrease lasts for about two to two and a half hours for concrete and moss respectively.

The increased temperature of the moss layer as a result of a lower albedo compared to the concrete surface is not necessarily bad for thermal comfort. While a higher albedo surface is beneficial on roofs to counter the urban heat island effect, it can increase thermal discomfort for pedestrians on the street when applied in a facade.

The insulating property of the moss layer keeps the material behind it cooler. In further research, the specific heat capacity and heat conductivity can be investigated to quantify the insulating property of the material. Moss is hypothesised to have a lower thermal mass than concrete, which could keep buildings cooler at night when the urban heat island effect is more pronounced.

6

Programming

6.1 Model set-up

To simulate the cooling behaviour of a bioreceptive concrete façade panel, a model is made in Excel. This model is based on the test set-up on the Green Village and validated using the data gathered there. Using this model, simulations can be run for conditions which have not been measured yet. It is also possible to alter variables to test which characteristics are best suited to maximize the evaporative cooling effect.

6.1.1 Energy balance

The model is based on an energy balance for the situation as tested at the Green Village. This allows validation of the model. Figure 6.1 shows this energy balance.

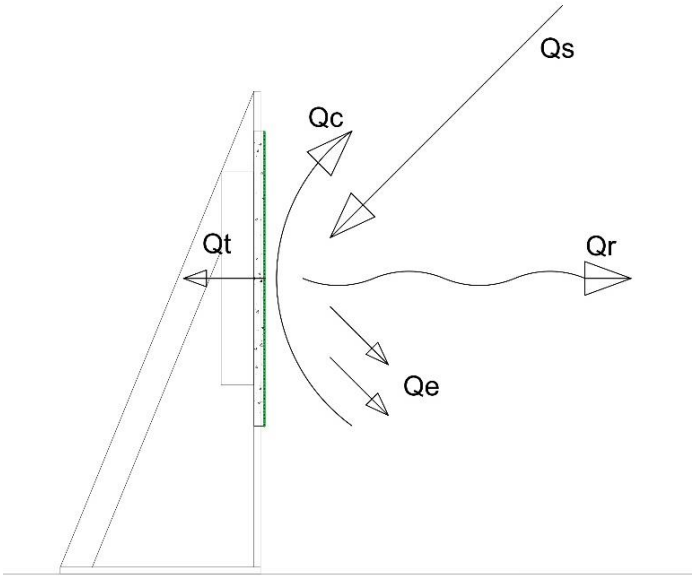

Figure 6.1: Energy balance of the test set-up at the Green Village

The energy balance describes the different heat fluxes in the system. It is based on the energy balance equation (Jóhannesson, 2006; van der Spoel, 2017):

$$\Sigma Q = \rho c V \frac{\partial T}{\partial t}$$

$$Q_s + Q_r + Q_c + Q_t + Q_e = \rho c V \frac{\partial T}{\partial t}$$

$$\alpha I + h_r\left(T_{sky} - T_{surf}\right) + h_c\left(T_{air} - T_{surf}\right) + U\left(T_i - T_{surf}\right) + Lg = \rho c V \frac{\partial T}{\partial t} \quad (6.1)$$

In which each term on the left-hand side of equation 6.1 represents a heat flux:

Q_s : Solar radiation [W/m^2]

Q_r : Radiative exchange with the sky [W/m^2]

Q_c : Convective heat transfer [W/m^2]

Q_t : Conduction into the wall [W/m^2]

Q_e : Evaporation [W/m^2]

And the right-hand side represents the thermal capacity of the control volume with:

ρ: mass density [kg/m^3]

c: specific heat capacity [J/kgK]

V: volume [m^3]

To solve this equation for each time step, data is needed on the solar radiation, the air temperature, the temperature of the panel, the wind speed along the wall, and the evaporation of water from the system. Each term of the energy balance is discussed in more detail below.

Solar radiation

Incoming solar radiation can be split into three components: direct, diffuse and reflected solar radiation. This radiation can be absorbed, reflected or transmitted. The absorbed radiation affects the heat budget of the surface according to equation 6.2:

$$Q_s = \alpha I \quad (6.2)$$

In this equation, α is the absorptance of the material and I is the incoming solar radiation. In the case of opaque materials, the absorptance is equal to 1 minus albedo.

Radiative exchange

Thermal radiative exchange is the transfer of heat energy through electromagnetic radiation. All objects emit radiation based on their temperature and emissivity. And there is always an exchange between an object and its surroundings.

Radiative exchange in this model is based on a configuration where a roof is exposed solely to the sky. That is not correct for the situation modelled in this research. The panel is exposed for a large amount to the sky. However, it is difficult to correctly model all the different surfaces that can be seen by the panels in the test set-up. Therefore a simplification is made.

Long wave radiation exchange with the sky can be calculated using:

$$Q_r = h_r(T_{sky} - T_{surf}) \tag{6.3}$$

$$h_r = \frac{\varepsilon\, \sigma\, (T_{sky}^4 - T_{surf}^4)}{T_{sky} - T_{surf}} \tag{6.4}$$

The temperature of the sky is assumed to be 20 °C colder than the air temperature at any given moment.

Convective heat transfer

Convection is the process of heat transfer between a solid surface and a fluid in motion. In this case, the (moss covered) concrete façade with the wind. Surface convective heat transfer can be calculated as follows:

$$Q_c = h_c(T_{air} - T_{surf}) \tag{6.5}$$

The airflow along the surface is generated by an external force and not by temperature differences between the surface and the medium. Therefore this is forced convection. The surface convective heat transfer coefficient, h_c can then be calculated using the Nusselt number:

$$h_c = \frac{Nu\lambda}{L} \tag{6.6}$$

$$Nu = f(Re, \mathrm{Pr}) \tag{6.7}$$

The criteria for turbulent flow along a flat surface are as follows:

$$Nu = \frac{0.037 * Re^{0.8} Pr}{1 + 2.443 * Re^{-0.1}(Pr^{\frac{2}{3}} - 1)} \tag{6.8}$$

$$Re = \frac{u\, L}{v} \tag{6.9}$$

$$Pr = \frac{v\, \rho\, c}{\lambda} \tag{6.10}$$

To calculate the Reynolds number, the flow velocity of air, *u* (m/s) is needed. Both Reynolds and Prandtl number are calculated using properties of air shown in Table 6.1 (Jóhannesson, 2006).

Table 6.1: Properties of dry air at atmospheric pressure for different temperatures

ϑ (°C)	-20	0	20	40
ρ (kg/m^3)	1.395	1.293	1.205	1.127
β (K^{-1})	-	0.00367	0.00343	0.00320
c (J/kgK)	1006	1006	1007	1008
λ (W/mK)	-	0.0243	0.0257	0.0271
ν (m^2/s)	-	13.3E-6	15.11E-6	16.97E-6

Conduction

The wall heat flux is determined by the amount of storage and conduction of heat into the wall. Conduction happens according to Fourier's law under the simplification that this is a steady state, one-dimensional situation.

$$Q_t = -\lambda \frac{dT}{dx} = U(T_i - T_{surf}) \tag{6.11}$$

The 'internal' temperature is assumed to be equal to the air temperature since the panel is standing outside. *U* is the thermal transmittance which can be calculated by dividing over the thermal resistance of the different layers of the construction. The thermal resistance of a construction layer is based on its thickness and thermal conductivity.

$$U = \Sigma \frac{1}{R} \tag{6.12}$$

$$R = \frac{d}{\lambda} \tag{6.13}$$

Evaporation

Moisture will play a role in the heat balance when it evaporates from the surface of the wall. The exchange of vapour between the wall surface and the air is related to convective heat transfer. Lewis law gives the coefficient of surface moisture transfer β and the surface moisture resistance *Z*. This is related to the convective heat transfer coefficient h_c as:

$$\beta = 6.2 * 10^{-9} * (0.8)^{n-1} * h_c \tag{6.14}$$

For outside conditions *n=1* for turbulent flow.

The vapour flux from the wall surface g is given by:

$$g = \beta(p_{air} - p_{surf}) = \frac{(p_{air} - p_{surf})}{Z_{p,air}} \quad (6.15)$$

The amount of vapour flux is influenced by the temperature and relative humidity through p_{air} and p_{surf}. The saturation vapour pressure of the air is calculated based on the temperature of the air. The higher the temperature of the air, the higher the saturation vapour pressure. The relative humidity of the air is then used to calculate the actual vapour pressure in the air.

When moisture from the concrete or moss evaporates changing from fluid to liquid state, the heat flux that belongs to phase-changing elements in the system is given by:

$$Q_e = L * g \quad (6.16)$$

In this equation, *L* is the latent heat of vaporization and *g* is the vapour flux from the wall surface.

Rain events

Based on the amount of moisture that was taken up and the volume of the concrete during the lab tests, the volumetric water content was determined. The porous concrete can take up around 200 kg of water per m^3 of concrete.

To calculate the amount of rain that hits a façade, the following formula can be used (Jóhannesson, 2006):

$$S = N * \frac{u}{u_v} \quad (6.17)$$

With S: the quantity of driving rain [kg/m^2]

N: the precipitation [kg/m^2]

u: wind velocity [m/s]

u_v: the vertical component of the velocity of raindrops [m/s]

During extreme rain events, amounts of 25 mm of rain per hour can hit the façade at a speed of 2 m/s. For average-sized raindrops (3-4 mm diameter), the speed at which they fall is approximately 8-9 m/s (Van Boxel, 1998). If the wind and rain hit the façade head-on, the amount of rain that hits the façade is then equal to 6.25 kg/m^2. Which for the concrete test panel of thickness 0.03 m is equal to 208 kg/m^3. This would saturate the panel completely.

As a reference, the 40 ml of water added to the panels during testing at the Green Village is approximately equal to a rain event of 1 mm which hits the façade with a wind speed of 2 m/s.

6.1.2 Discretisation

The energy balance is non-stationary and calculates a single node on the surface of the panel. It is discretized using the explicit method. The temperature of the next time step is calculated using weather data input for this time step, the temperature at this time step, the time step itself and some material properties. All values are normalized for 1 m^2 surface area. The balance is one-dimensional, which means that only heat flow in the x-direction is assumed (van der Spoel, 2017).

$$\rho c V \frac{\Delta T}{\Delta t} = Q_s + Q_r + Q_c + Q_t + Q_e \tag{6.18}$$

$$\rho c V \frac{T_{n+1} - T_n}{\Delta t} = Q_s + Q_r + Q_c + Q_t + Q_e \tag{6.19}$$

Solving for T_{n+1} gives:

$$T_{n+1} = \frac{\Delta t}{\rho c V}(Q_s + Q_r + Q_c + Q_t + Q_e) + T_n \tag{6.20}$$

$$T_{n+1} = \frac{\Delta t}{\rho c V}\left(\alpha I + h_r\left(T_{sky} - T_n\right) + h_c(T_{air} - T_n) + U(T_i - T_n) + Lg\right) + T_n \tag{6.21}$$

6.2 Validation

The energy balance is a method to approximate the temperature of the façade panels. By adding more components to the energy balance, it becomes more accurate. The model is validated using the data measured at the Green Village. A few characteristic days have been selected to show how the model approximates the measured data under different weather conditions. Also, the evaporation of moisture from the façade panels is modelled and discussed.

6.2.1 Temperature modelling

The surface temperature of the moss panel is higher than the temperature sensors measured, as was seen in the IR camera measurement. Therefore, the model is validated using the data from the concrete panel. Once the model is calibrated, it is altered to simulate the moss panel temperature. In Appendix D, all input values of the model are shown.

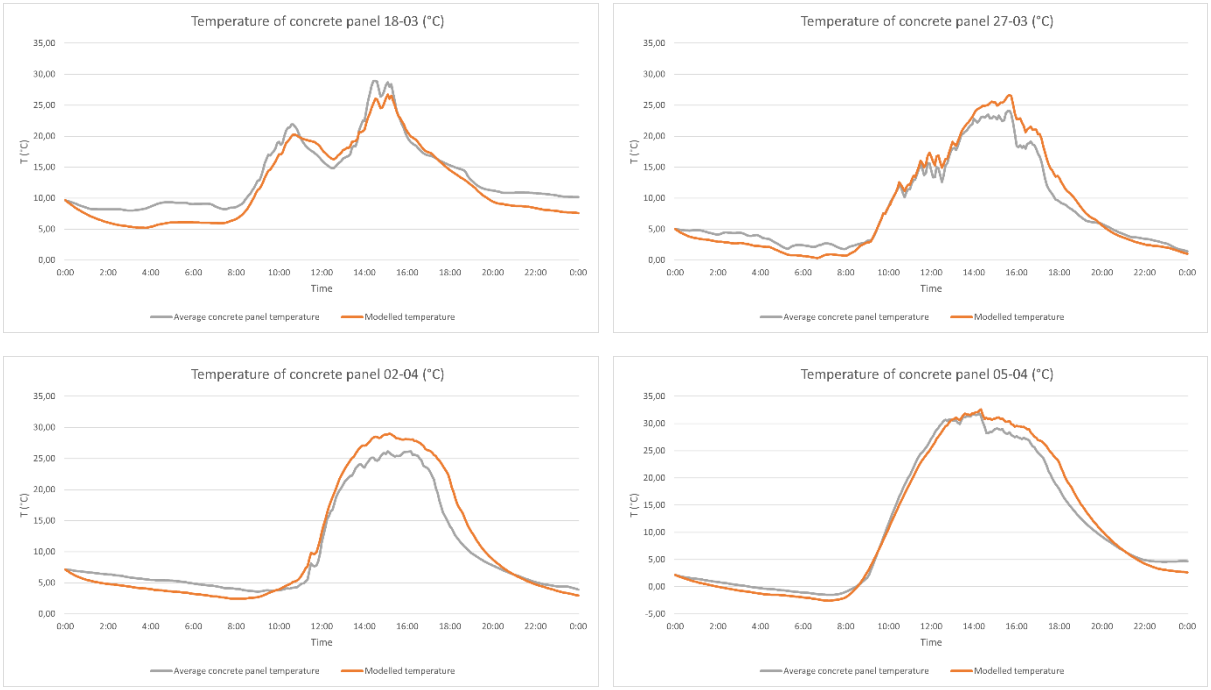

Figure 6.2: Model approximations on sunny days, 18th and 27th of March, 2nd and 5th of April

On sunny days, the approximation of the model is quite good as can be seen in Figure 6.2. Deviation from the measured data could occur because of measurement errors. Or through less accurate estimates of input variables. Some degree of deviation will always be present because a model is an approximation of the reality.

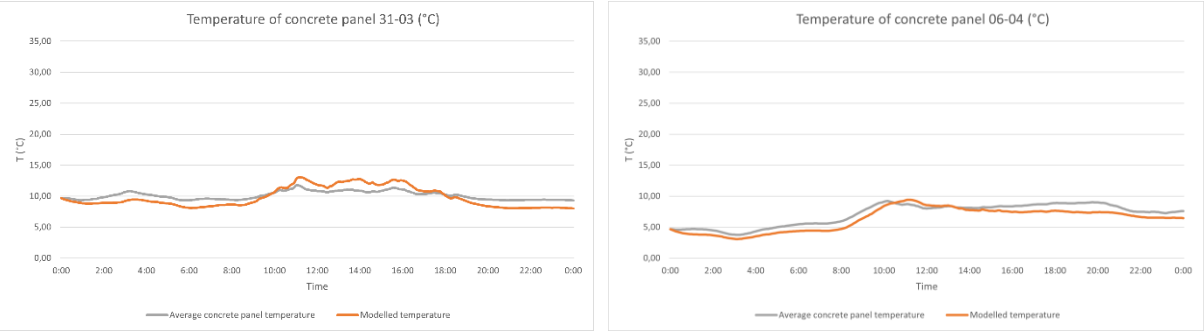

Figure 6.3: Model approximations on rainy days, 31st of March and 6th of April

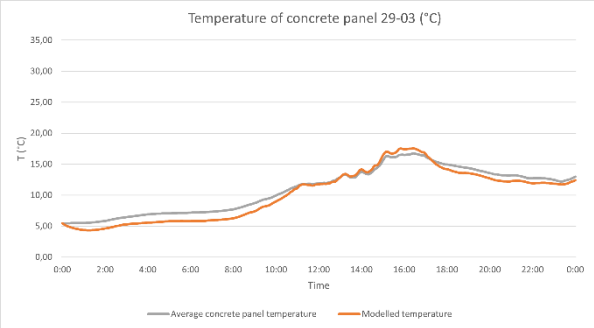

Figure 6.4: Model approximation on cloudy day, 29th of March

On rainy or cloudy days, when there is no solar radiation, the approximation is also quite good as seen in Figures 6.3 and 6.4. Evaporation is not yet a part of the modelling since if the rain persists throughout the day, no evaporation will take place. This will happen when the sun starts shining after a rain event.

6.2.2 Evaporation modelling

Now, the evaporation of moisture from the concrete panel is modelled. After a rain event, when the sun shines, the model becomes less accurate because it overestimates the temperature. This happens because the model does not account for the evaporation of water from the panel yet. When the evaporation is modelled, the model is more accurate. This is under the assumption that the panel is capable of evaporating water the entire time and that the relative humidity in the concrete is equal to the relative humidity in the air.

During the rain event on the 23rd of March, there was 3 mm of precipitation. The wind speed was approximately 2 m/s during the whole day. If the rain falls at a speed of 6 m/s, the amount of rain that hits the façade is then equal to 1 kg/m^2. That means that the façade has approximately 33 kg/m^3 of water to evaporate. The amount of water which evaporates here according to the model is approximately equal to this 33 kg/m^3. Therefore, the calibration of the evaporation modelling also seems quite accurate. However, the speed at which the rain falls is an estimate. If the rain falls with a speed of 9 m/s for example, the amount of rain that hits the façade would be 22 kg/m^3. Discrete water events showed clearly in the measured data, especially on hot days. Figure 6.5 shows the model approximation for this day.

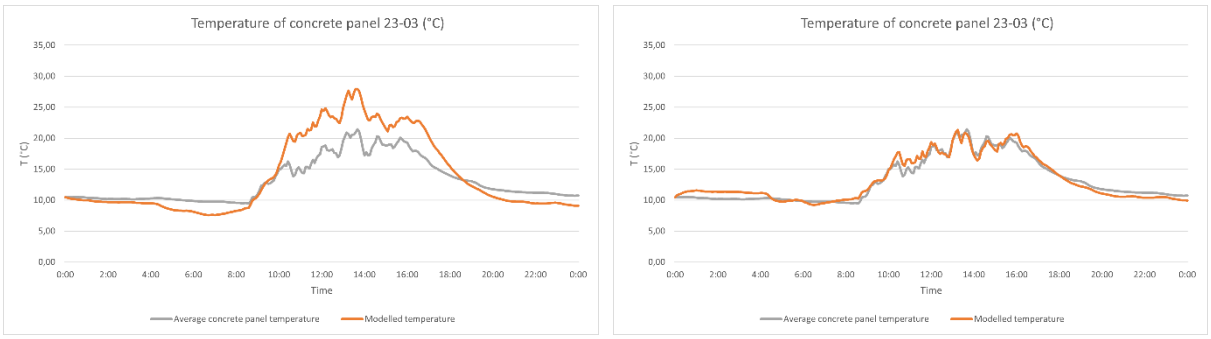

Figure 6.5: Model approximation on rainy day, 23rd of March, with and without evaporation modelling

On the 4th of April, 40 ml of water was added to the wall surface. Evaporation is turned on in the model at the time of the watering event. When 40 ml of water has evaporated, the evaporation stops. The resulting graph can be seen in Figure 6.6 In this case, the modelled data matches the measured data well.

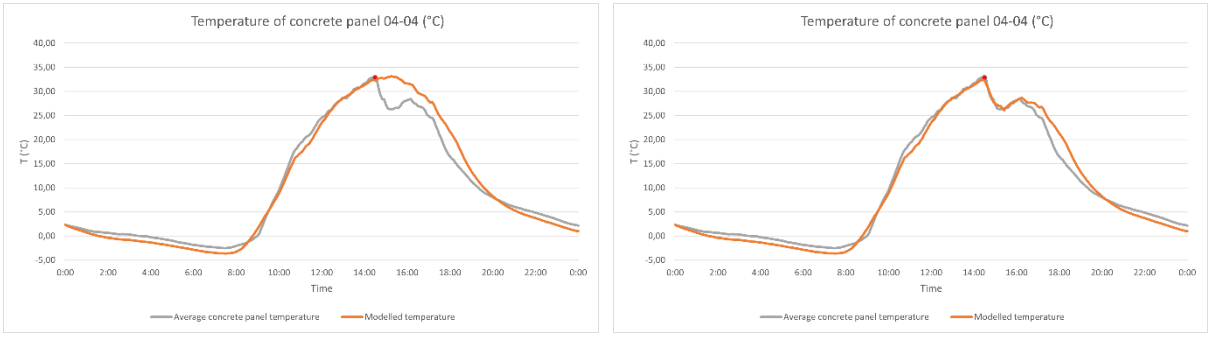

Figure 6.6: Model approximations on sunny day, 4th of April, with and without evaporation modelling

For other data sets it is not that accurate. The evaporation in the watering event in Figure 6.7 is first estimated based on the assumption that the relative humidity is the same in the concrete as in the surrounding air. The amount of moisture that evaporates is 30 ml according to the model. This is too little and the temperature does not drop to the level of the measured data. When increasing the relative humidity of the concrete manually by 10% for each time step, the surface vapour pressure increases resulting in a bigger vapour flux. Through this increase in evaporation, the figure on the right-hand side is obtained which is more accurate. In this case, 40 ml of water has evaporated and the temperature does drop to the level of the measured data.

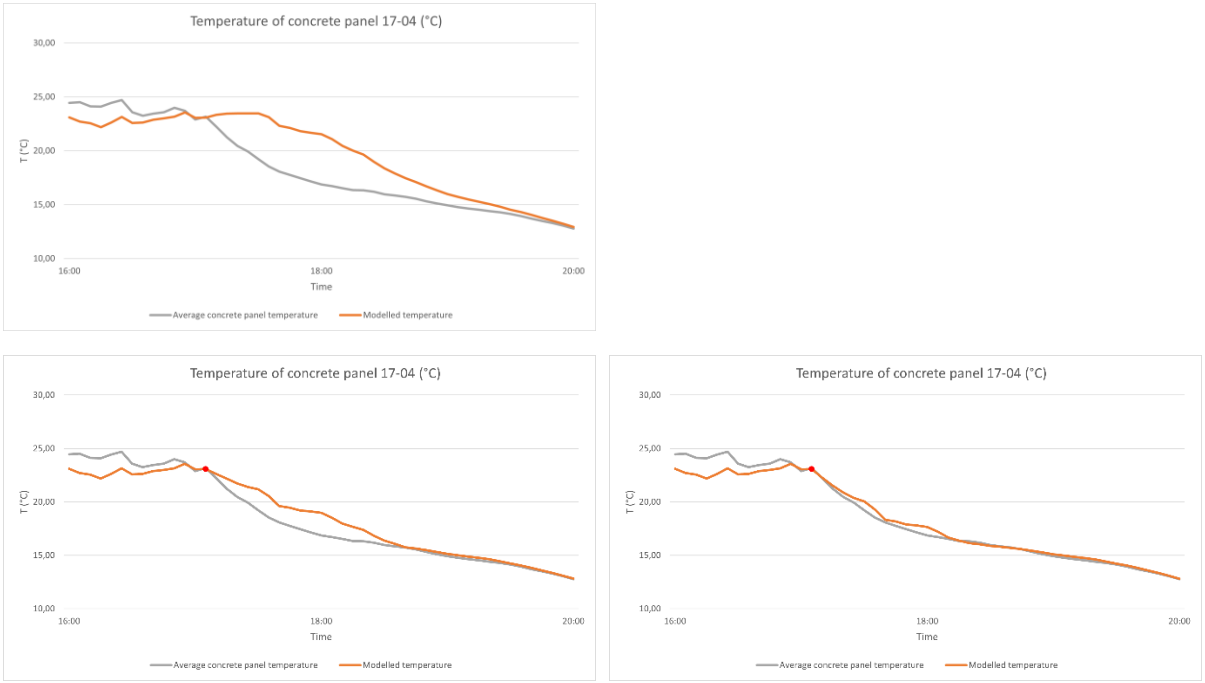

Figure 6.7: Model approximations on 17th of April, with and without evaporation modelling, and with improvement on the model

This exposes the disadvantage of the evaporation modelling. There is no water balance of the system in place in the model. A water event is manually added at a specific time. Modelling a water balance would be quite difficult. Data would be needed for example on the amount of moisture present in the system or the relative humidity of the air in the concrete to be able to properly calibrate it. These variables are hard to measure.

For the moss panel, it is harder to check if the results are correct because of the temperature difference between the measured and modelled data. For example, on the 5th of April, the evaporation from the moss is modelled. See Figure 6.8. For each of the three watering events, 40 ml of water evaporates. This seems to be an accurate estimation of the temperature graph looking at the steepness of the curve after evaporation but it is hard to validate.

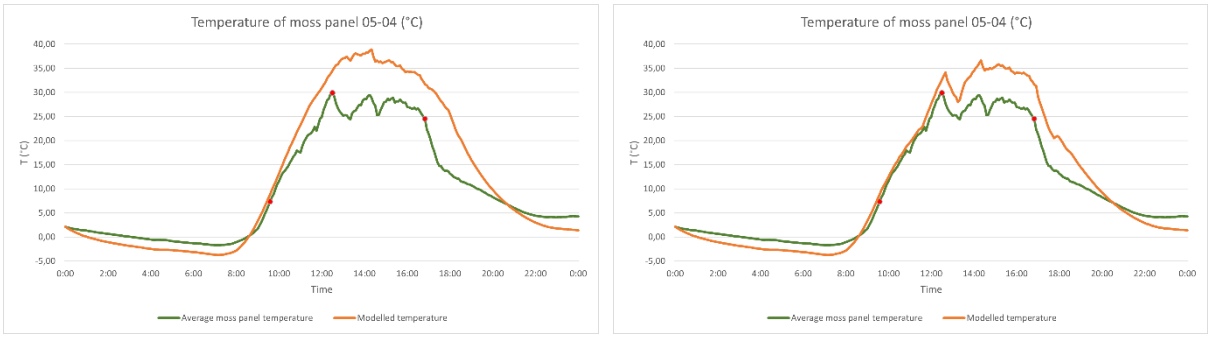

Figure 6.8: Model approximations on 5th of April, with and without evaporation modelling

Overall, the model is quite accurate in modelling the course of the temperature of a façade panel over time. However, when moisture comes into play, more data is needed to accurately calibrate the model. This is because the amount of evaporation in the model is determined among other things by the relative humidity in the air, the relative humidity in the concrete and the wind speed. If one of these approximations is slightly off, differences may arise between the measured and modelled values. The amount of added water is also not accurate because it was applied with a plant sprayer. And the temperature of the water can also play a role. But under some assumptions, the model does give an indication of the extent of cooling.

6.2.3 Comparison to lab measurements

In the lab experiments, Bryum capillare was the moss species with the highest water uptake. For a surface area of 83 x 83 mm, the moss was capable of taking up 32.4 g of water. Per square meter, this would equal 4703 g of water. For a thickness of the moss layer of 10 mm, the volumetric weight would be equal to 470 kg/m^3. For the pleurocarpous mosses, which were used in field testing, this number was in the range of 27 to 27.4 g of water. Which is equivalent to 3919 to 3977 g of water per square meter or 392 to 398 kg/m^3. The concrete took up 21.1 g of water which is equal to 3063 g of water per square meter or 204 kg/m^3 since the sample tested was 15 mm thick. For the concrete façade used in testing which measures 900 x 180 x 30 mm with a moss layer of 10 mm on top, the total reservoir would be 1.63 kg of water. Which is the equivalent of a 45 mm precipitation event where the rain falls at a speed of 9 m/s hitting the façade with a speed of 2 m/s. If horizontal wind speeds are 5 m/s, a precipitation event of 18 mm would completely saturate the façade. This is calculated using equation .. However, a different concrete mixture and different moss species were used and this is under the assumption that the façade absorbs all the rain that hits it so, in reality, this result could differ. The total reservoir could be increased to 1,75 kg of water for this façade panel by using Bryum capillare which takes up more water.

For the 4th of April, the evaporation rate of the water evaporating from the concrete or moss surface is calculated based on the modelled drop in surface temperature. So through reverse engineering, these values are obtained. The conditions during field testing are similar to the lab conditions in terms of relative humidity, which was around 45% RH. But the temperature was somewhere in the range of 15°C to 35°C since the ambient temperature is 12°C and the panel temperatures are approximately 37-38°C at the start of the watering event. Table 6.2 shows the evaporation rates at the start of the watering event for the surface area of the samples used in the lab.

Table 6.2: Evaporation rates concrete and moss panel at the start of watering event on 4th of April

Field testing	12 ~ 38 °C, 45% RH
Concrete	3.20 g/h
Moss	10.10 g/h

Table 6.3: Evaporation rates concrete and pleurocarpous mosses during lab testing at 50% RH

Lab testing	25°C, 50% RH	15°C, 50% RH
Concrete	3.02 g/h (SD 0.2)	1.40 g/h (SD 0.3)
Rhynchostegium confertum	7.48 g/h (SD 3.6)	2.81 g/h (SD 1.6)
Eurhynchium striatum	10.79 g/h (SD 1.1)	4.98 g/h (SD 1.4)

Table 6.3 shows the evaporation rates for the concrete and the pleurocarpous mosses for different temperatures and 50% RH. Comparing these numbers to the results of the field measurements, for both the concrete and the moss panel, the evaporation rates are in the same range as the lab results at 25°C and 50% RH. But, the differences between the lab and the field testing have to be taken into account. These are the wind speed, a different concrete mixture, solar radiation, and a difference in the moss species used.

6.3 Results

By inputting found results of outdoor testing in the model it is possible to alter and test variables. This will provide information on how to design moss-covered concrete facade panels to maximize the evaporative cooling effect.

6.3.1. Modelling a heat wave

In the Netherlands, a heatwave happened in the summer of 2022. On the 17th of August, a rain event took place in which 16 mm of rain fell within one hour. In total, 28 mm fell that day as measured by the weather station of the Green Village. This rain event ended that heat wave. By using the data on relative humidity increase, wind speed increase and ambient temperature decrease leading up to that rain event, similar rain events can be simulated on other tropic days. By varying the amount of precipitation during these simulations, the extent of cooling can be investigated. Also, insight will be provided on the difference between a regular concrete façade and one grown with moss in terms of its cooling.

The day that was chosen for the heat wave simulation, is the 14th of August 2022. Temperatures reached over 32 °C with low wind speeds, high values for solar radiation, and a high UV index. This day was a typical day in which heat stress could occur. According to the PET thermal comfort index, for these conditions, the perceived temperature reaches 47,9 °C in the sun and 35,6 °C in the shade at the hottest time of day. By using the validated model with the input data from the Green Village for this day, the temperature profile for a bare concrete façade and a moss-covered concrete façade is found.

Moss water evaporation is based on a factor retrieved from the measured data. This accounts for the extra water retention of the moss surface. The extra surface roughness of the moss is accounted for by using a different formula for convective heat transfer. It has a forced and natural convection component (U.S. Department of Energy, 2022).

$$h_c = h_f + h_n \tag{6.22}$$

$$h_f = 2.537 W_f R_f \left(\frac{P u_z}{A}\right)^{1/2} \tag{6.23}$$

$$h_n = 1.31 |\Delta T|^{1/3} \tag{6.24}$$

With:

W_f: wind direction modifier, for windward surfaces equal to 1.0

R_f: roughness factor equal to 2.17 for very rough surfaces

P: perimeter of the surface [m]

u_z: wind speed [m/s]

A: surface area [m^2]

ΔT: temperature difference between surface and air

Both the duration and the intensity of cooling have been accounted for in this way.

6.3.2 Simulation results

Three different intensities of rain have been simulated as can be seen in Figures 6.9 and 6.10. Evaporation is based on the amount of rain which falls during one of these events and then evaporates from the façade. In reality, the temperature of the façade will probably drop earlier because of the clouds blocking the sun and the decrease in ambient temperature. Also, the temperature drop could be overestimated because evaporation happens based on the conditions of a very dry, hot day. When in reality, if a rain event occurs, these conditions change. This simulation is realistic when a sudden release of water from a reservoir happens. Which could be a strategy in mitigating the urban heat island effect on hot days in summer.

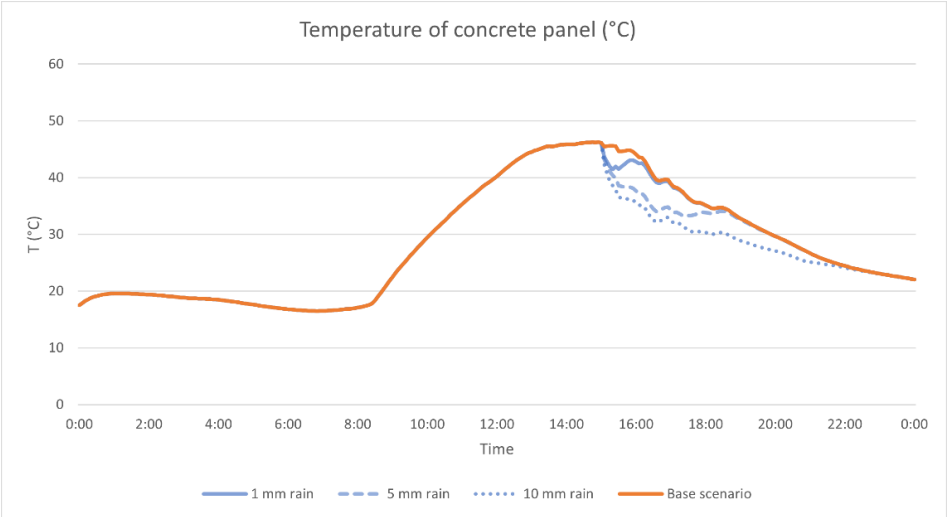

Figure 6.9: Simulation of concrete façade temperature on 14th of August with rain scenarios of different intensity

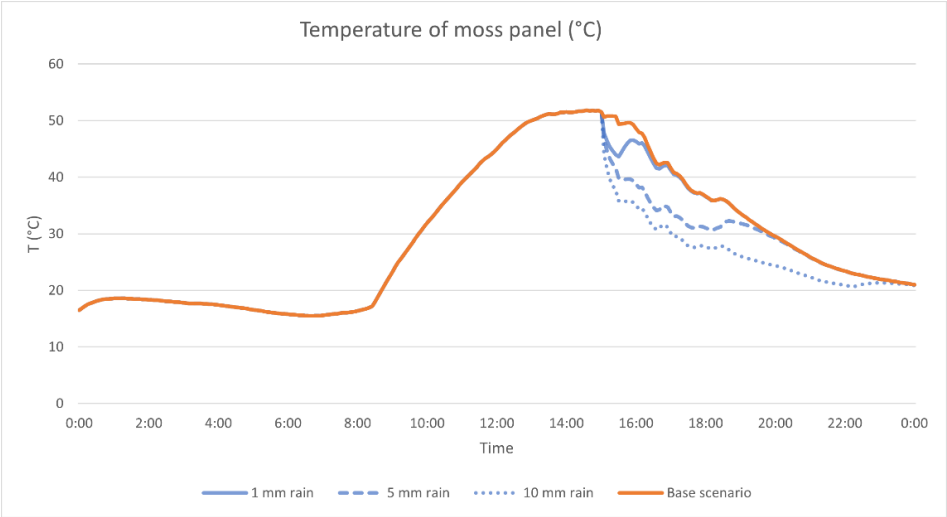

Figure 6.10: Simulation of moss façade temperature on 14th of August with rain scenarios of different intensity

From these figures, it becomes evident that evaporative cooling can have a significant effect on the temperature of the façade. The cooling effect is higher for the moss façade, but the initial temperature of the moss façade is also higher because of the higher albedo. When the façade temperature is quite high, the impact of cooling is exacerbated because it is also calculated based on the saturation vapour pressures of the air and the material which are based on their respective temperatures. A 1 mm rain event decreases the surface temperature of the façade by a few degrees. But the effect does not hold for a very long time. When enough moisture is added to the system, cooling can hold for quite some time. A 10 mm rain event decreases concrete surface temperature up to 10 °C initially, and the effect lasts for a few hours. The length and intensity of cooling can be extended through the application of moss on a façade. Then, for a 10 mm rain event, the initial temperature reduction is equal to 15 °C, and the effect lasts for 6 hours. So the application of moss improves the ability of a façade to be cooled by rain.

An assumption that is made in this model is that the total amount of driving rain that hits the facade is taken up by the panels. In reality, part of it runs or splashes off. And the same goes for the evaporation from the panels. All water that hits the facade is assumed to be able to evaporate. Maybe some water is bound in the concrete pores. The consequence is that the amount of cooling is overestimated. If a water balance was to be implemented, the amount of water available for evaporation would be a more accurate estimate. The temperature drop that can be seen in both Figures 6.9 and 6.10 would be less sudden because the water reservoir would fill up over some time. Irrigation, precipitation, evaporation, throughflow and runoff create a dynamic balance of water in the system. These factors will depend on formulas with variables like the relative humidity of air and material, precipitation amount and speed, ambient and material temperature, vapour pressure of air and material, wind speed etc. In the current model, most of these variables do not affect each other. For example, the relative humidity of the panel does not decrease with increasing wind speeds which would probably happen in reality. In a dynamic water balance, this would happen and all these variables would therefore be more accurate. The relations between these variables require a theoretical background that would have to be checked with results from measurements. Eventually, this would result in a more accurate evaporation and temperature profile.

Overall, the results of the current model suggest that this might be a good measure to lower building material temperatures which in turn affect thermal comfort. Quantifying the amount of thermal comfort increase, however, proves to be difficult. This will be illustrated with the following example based on a calculation from Westhoff. (Westhoff, 2020)

In the sunlit PET equation, the ambient temperature is one variable.

$$PET_{sun} = -13.26 + 1.25T_a + 0.011Q_s - 3.37\ln(u_{1.2}) + 0.078T_w + 0.0055Q_s\ln(u_{1.2}) + 5.56\sin(\varphi) - 0.0103Q_s\ln(u_{1.2})\sin(\varphi) + 0.0546B_b + 1.94S_{vf}$$

For hot summer conditions, the ambient temperature has to drop around 5 °C to move down one scale in thermal perception as described in Table 3.1. The energy needed to cool down 1 m^3 of air, 5 °C is calculated using the following formula:

$$P = m * c * \Delta T \tag{6.25}$$

In which:

P: energy needed for temperature decrease of air mass m [J]

m: weight of the air that is cooled [kg]

c: specific heat capacity of air [J/kgK]

ΔT: temperature decrease of air [K]

The weight of the air that is cooled is calculated through:

$$m = \rho * V \tag{6.26}$$

With:

m: weight of the air that is cooled [kg]

ρ: density of air [kg/m^3]

V: volume of air [m^3]

The amount of water in kg needed to reach this temperature drop is calculated using:

$$W = \frac{P}{L} \tag{6.27}$$

With:

W: water that needs to evaporate [kg]

P: energy needed for temperature decrease of air mass m [J]

L: latent heat of vaporization [J/kg]

To cool down an air volume of 1 m^3, with properties of air at 20 °C (density of 1,205 kg/m^3, specific heat capacity of 1007 J/kgK) in front of a bioreceptive concrete façade with 5 °C, the amount of water that needs to evaporate is equal to 0,0024 kg or 2,4 ml. This would mean that the air would be cooled with 88 °C when 40 ml of water evaporates which is unrealistic. This method is too simple and overestimates the cooling through evaporation. Part of the evaporation cools the façade surface and not the air, the air in front of the façade is not stagnant and the displacement of the air is large. To accurately predict the effect of the cooling of the façade surface on the thermal comfort of people, a CFD simulation must be performed. Then the temperature gain can be simulated by including a lot of intricate variables like the temperature of the air, the flow of air along the wall surface, the relative humidity, and evaporation from the surface.

6.3.3 Improving the design

To improve the cooling qualities of the bioreceptive façade, a few measures could be applied. This can be done by altering the concrete or the moss. Cooling is increased when there is more moisture available for evaporation. So the moisture reservoir of the system should be increased. For concrete, the water reservoir can be enlarged by increasing the open pore space. However, by increasing the open pore space, the strength properties of the material will decrease. Even though this concrete is a façade material and not structural in nature, it should not be too brittle. Otherwise, the façade might take damage. And if the pores become too big, the water will not be held anymore because capillary action is absent.

To improve the moisture capacity of the moss layer, a different moss species can be chosen. The currently applied species on the moss panel in the field testing were pleurocarpous. From the lab experiments, it can be seen that acrocarpous mosses which grow in cushions, take up more water and take longer to evaporate it. This is also corroborated by literature as can be read in section 3.3.2.

To be able to apply the façade in different conditions and different orientations, desiccation tolerance is important. Desiccation tolerance is the ability of the moss plant to survive dry tissues and restart photosynthesis upon rewetting. Three factors are of importance for a moss to be drought tolerant (Glime, 2022):

1. Limiting the damage to tissue during desiccation to a reparable level
2. Maintaining the physiological integrity in a dry state so that metabolism can resume quickly after rehydration
3. Putting repair mechanisms into effect after rehydration. Especially to retain or regain the integrity of the membrane and membrane-bound organelles.

A way to improve the performance of mosses might be to harden them in the lab. Hardening is the process of increasing the resistance to stress factors in a moss. Essentially training them to perform better in harsh circumstances. This can be done by slow drying the mosses, exposing them to drought. First, they are exposed to very high relative humidity of around 98%, then to desiccating conditions. This increases their drought tolerance. Another option is abscisic acid (ABA) application. ABA is a plant hormone used to induce specific responses in plant development. By applying ABA, transpirational water loss in moss plants can be reduced. Thus, delaying desiccation and increasing drought tolerance.

When applied on a non-northern facing façade, UV light can be harmful to mosses. When mosses grow on rocks they often have a lot of sun exposure. Some moss species have measures in place to protect themselves from UV light. Hyaline tips and awns can protect moss against UV light during dry spells. The leaves of mosses often twist when dry, and have infolded margins, thickened cell walls, small cells and papillae to protect themselves from UV light damage (Glime, 2022). Using a moss species which has these measures, the moss-covered concrete can be improved resulting in an even higher evaporative cooling effect of a façade.

6.4 Discussion

The model and data used from the weather station of the Green Village have some limitations and improvements can be made. These are discussed per term of the energy balance.

Solar radiation

Two sets of solar radiation data were given by the data platform of the Green Village. One was measured by the weather station, the other was measured by a pyranometer. The data from the pyranometer was more accurate but included a lot of missing data points. Therefore the less accurate data from the weather station was used. This might result in modelled data that is a bit less accurate. It could explain deviation from the measured data on sunny days.

Radiative exchange with the sky

Radiative exchange happens between all objects and their surroundings based on their temperature and emissivity. In the model, the simplification is made that the panels only have radiative exchange with the sky. In reality, the panels 'see' a lot more than just the sky. By adding view factors, more surfaces could be included in the radiative exchange. Another simplification that is made is the temperature of the sky. This is assumed to always be 20 °C lower than that of the ambient air. In reality, this might be more constant than the ambient air temperature and the difference between the two might be higher or lower than 20 °C. These simplifications could explain deviation from measured data at night. The ambient temperature is then closer to the temperature of the sky. This results in a lower radiative loss of heat. Especially on clear nights, the modelled temperature is often lower than the measured temperature.

Convective heat transfer

The formula used for convective heat transfer is one of many that is mentioned in literature. It depends on many different variables like the roughness of the surface, the wind speed, wind direction and incident angle, turbulent or natural convection, temperature, thermal conductivity and other properties of the air. There is no consensus on which formula is best, one formula is not necessarily better than the other. Therefore, for certain situations, a certain formula could give more accurate results.

Wind speed is used in the convective heat transfer and evaporation calculation. The used data was measured very locally. Wind speeds can differ a lot for different locations, so when using this model on a façade at a different location than the Green Village, data is needed on local wind speeds.

Conduction

Conduction is calculated in the model as in a regular façade calculation. However, the panels in the measurement are located outside. Therefore the 'internal' temperature is equal to the air temperature because both the front and the back of the construction have the same ambient conditions. The resistance of heat conduction for the surface R_e is therefore used twice and there is not much conduction of heat through the construction.

The insulation on the back of the panels was a Styrofoam board. It was not applied completely airtight against the backside of the panels because the surface was not completely flat. Therefore, the actual amount of thermal conductivity from this layer might be higher than modelled resulting in a higher thermal transmittance. But since the share of conduction in the energy balance is already quite low, this difference is negligible.

Evaporation

Another improvement is the addition of a water mass balance. It makes it less time-consuming to use the model since only input data is needed. In the current model, the evaporation part has to be modelled by hand in the case of a rain event. By adding a water mass balance, the model also will be more accurate. The amount of moisture available is more accurate. However, to model this part, data is needed on moisture in the system, the porosity of the concrete and the relative humidity of the air in the pores. This would allow for accurate calibration of the model but these variables are difficult to measure.

The temperature of rain could also be added since this also affects the temperature of the surface. In current models sometimes a simplification is made during rain events where the convection coefficient is set to a high number and the surface temperature used is the wet-bulb temperature (U.S. Department of Energy, 2022).

The moss evaporation is now modelled by a factor which covers the difference in properties between the moss and the concrete surface. There is no formula or relation yet that accurately describes the evaporation from a moss surface taking into account the biological properties of the moss. This would improve the model even further. The convective heat transfer formula is adapted for the moss surface based on literature. A very rough surface is assumed which increases evaporation.

Dynamic model

The heat balance used is one-dimensional, heat flow only occurs in the x-direction. To improve the model, this could be expanded with heat flow in the y and z direction as well. And this would also make it possible to add more nodes. A multi-nodal model could give an image of the temperature distribution over the entire surface or volume. However, this kind of modelling would not be possible in Excel because of the heavy computations.

The model could be improved by computing and minimizing the error between measured and modelled data. By doing this across several different data sets, input variables could be optimized. However, this could mean that to fit the data as best as possible, the input variable would take up an unreasonable value which is not in line with reality. So constraints would have to be put in place.

The IR camera shows that the measured data of the moss panel is not accurate for surface temperature. So the model is validated mostly on concrete data and altered for the moss. By taking measurements with the IR camera, instead of measurements with temperature sensors, a more realistic surface temperature is measured. This would allow for better validation of the moss part of the model.

6.5 Conclusion

The concluding remarks for this chapter are given in answer to the sub-research questions:

How can the cooling behaviour of a bioreceptive concrete façade be modelled?

What are the ideal characteristics of a bioreceptive concrete façade panel for decreasing the temperature of the urban environment?

A model is made based on the energy balance of the façade system as applied in the field testing. This allowed for the calibration of the model based on the data measured during the field testing. The non-stationary model, calculating temperatures of a single node on the surface of the panel, is discretized using the explicit method. This provides accurate temperature profiles of the façade panels.

Water events were used to calibrate the evaporation part of the model. The amount of water that evaporates is based on the amount of water that falls during a rain event. By adding it to the energy balance, the temperature decreases. The disadvantage of the evaporation modelling is the lack of a water balance. Water events are added manually at a specific time. Modelling a water balance requires more data to properly calibrate it.

After calibration, the model is used to simulate a heat wave in the Netherlands. It uses data from the summer of 2022 when a heat wave struck. The effect of rain events with different intensities is shown. A 10 mm rain event can decrease the concrete surface temperature by up to 10°C initially, and the effect lasts for a few hours. Applying moss on a façade can extend the length and intensity of cooling, resulting in an initial temperature reduction of 15°C after a 10 mm rain event. Also, the length of the cooling duration is extended. Therefore, moss application improves the cooling ability of a façade surface after rain. However, to accurately predict the effect of the cooling of the façade surface on the thermal comfort of people, a CFD simulation has to be performed.

The cooling effect can be enlarged by improving the design. A measure that can be implemented is the increase of the pore volume of the concrete, creating a bigger reservoir of water. By choosing a moss species with different characteristics, the performance of the façade can be improved even more. It should be able to grow on concrete, preferably in cushion form and be desiccation tolerant. This is achieved in mosses by limiting the tissue damage, resuming metabolism after rehydration quickly and putting repair mechanisms into effect after rehydration. The drought tolerance can be enhanced by hardening the moss by slow drying them, exposing them to drought or ABA application.

7

Discussion

The evaporative cooling effect of a moss-covered concrete façade is found through experimental research and a modelling study. The water uptake and release of four moss species and bioreceptive concrete are found through lab research. Not much literature was found on the evaporation of water from mosses. By quantifying the amount of water uptake and creating a profile of water release over time, an indication is given for water behaviour in mosses. These findings were explained through literature on moss morphology. The results were in line with information found in literature and can help in deciding on the use of moss species for application in a bioreceptive façade.

Testing could be improved by drying the moss samples once before the actual experiment to remove the excess weight of sand. Secondly, samples were placed horizontally in the climate chamber and therefore data on evaporation is less accurate. Evaporation is more efficient on vertical surfaces, which results in higher total heat transfer rates and evaporation time is up to 10% shorter when moss is applied vertically in a façade (Qi et al., 2019). Another influence that was not accounted for in the climate chamber was air circulation. It is assumed that air circulation was quite low, but it might affect the evaporation of the samples. By monitoring wind speeds inside the climate chamber, these effects can be taken into account.

Because testing was done on a biological material, which is not uniform, the weight or surface area can differ from sample to sample. By using multiple samples per moss species, the effect of these differences is reduced. Water uptake was not very constant for all the moss species. The standard deviation of measurements was quite high compared to the concrete. By increasing the sample size, the results become more accurate. Because the moss is alive, experiments might also influence its properties. Drying and rewetting for example might damage the cell structure of the moss. Especially if it happens quickly (Glime, 2022). This might influence the performance of taking up water or holding it. However, a decrease in the performance of the mosses was not seen over the course of the experiment.

The surface temperature decrease that happens through the evaporation of water from a bare concrete façade panel and from a moss-covered concrete façade panel was measured in an outdoor test set-up. The results can be used as standalone information and as input for the calibration of the model that was made.

By testing in an outdoor environment, the behaviour of a façade can be seen in an actual application. This provides insight into the use of the material, potential drawbacks and aspects that still need to be improved. A drawback of testing outside is the lack of desired weather conditions in which the test is performed. By repeating the test in a different season, namely summer, the effect of cooling under hot conditions can be examined. By performing tests on a façade with a higher surface area the cooling effect could increase. The effect of cooling on the environment might be measurable. Also, only one façade orientation was used. The test could have very different outcomes when the façade is facing in another direction. This information is needed before applying it in practice. The moss, a biological

material, died over the course of testing. Therefore, to obtain more representative and accurate data on the behaviour of this façade material, the product still needs to be improved. If the moss survives all year round, tests can be performed which monitor the long-term behaviour of the façade.

There are also improvements to be made in the test setup. The temperature sensors measured the temperature just below the concrete surface of the panels. This does not provide the most accurate data on the surface temperature of the façade panels. With an IR camera, the actual surface temperature of the facade is measured. By testing with an IR camera continuously, accurate data can be retrieved for a longer time. To be able to compare the data from the outside measurements to the results from the lab experiments, the same materials have to be used. The bioreceptive concrete mixture and the moss species cultivated on the bioreceptive concrete, have to be the same for both tests. And by weighing the samples outside as well, the amount of water in the system can be monitored.

By using the data measured, a model is constructed based on the energy balance equation. This model is capable of finding the surface temperature of a façade based on weather data input. The model is made in Excel, and it is based on several different formulas. All of these formulas have their limitations and assumptions. These have to be taken into account when processing and interpreting the results.

The model requires a lot of data which is measured very locally. Therefore, it is hard to use the model for a façade in a different location. This also means that there are a lot of input values that have to be altered. The model can be improved by creating an interface which allows for easy alteration of these input variables. Although a lot of data is required, the model is not heavy computationally. This is beneficial for calculation times. It does, however, require some manual work for loading the data sets. Another advantage of the model is that it is easy to add components. For example, a different heat flux which affects the energy balance can be added easily.

One component that can be improved in the model is the evaporation part. Through the addition of a water mass balance, it will be less time-consuming to use the model since only input data is needed. In the current model, the evaporation part is modelled by hand. By adding a water balance, the amount of moisture available is more accurate. However, to model this part, data is needed on moisture in the system, the porosity of the concrete and the relative humidity of the air in the pores. This would allow for calibration of the model but these variables are difficult to measure. The evaporation from the moss surface is now modelled by a factor which covers the difference in properties between the moss and the concrete surface. There is no formula or relation yet that accurately describes the evaporation from a moss surface taking into account the biological properties of the moss. Nevertheless, based on the formulas for evaporation from a surface, the model follows the trend line of the measurements. Therefore, it is accurate to some degree but this can be improved by measuring more rain events in the field.

By replacing materials that accumulate and radiate a lot of heat, the urban heat island effect is countered. But, the link between the surface temperature of the façade to the thermal comfort of a pedestrian on the street is yet to be made. This can be done by quantifying the amount of cooling of the ambient air in front of the façade. To accurately predict this value, a CFD simulation must be performed. Then the temperature gain can be simulated by including a lot of intricate variables.

8

Conclusions

The goal of this thesis was to quantify the evaporative cooling effect that a bioreceptive concrete façade might have on the urban environment. Therefore, the objective of this research was to quantify the amount of temperature change through the evapotranspiration of moss by measuring and modelling the amount of water uptake and release and the temperature decrease of the panel which it induces. An answer is formulated to the research question:

What is the evaporative cooling effect of moss-covered concrete facades on the urban environment?

The evaporative cooling effect was examined for multiple moss species in a laboratory environment. Under set ambient conditions, the amount of evaporation was measured. Bryum capillare was the moss species with the highest water uptake, water retention and drying time. For a surface area of 83 x 83 mm, the moss was capable of taking up 32.4 g of water. Per square meter, this would equal 4703 g of water. For a thickness of the moss layer of 10 mm, the volumetric weight would be equal to 470 kg/m^3. For the pleurocarpous mosses, this number was in the range of 27 to 27.4 g of water. Which is equivalent to 3919 to 3977 g of water per square meter or 392 to 398 kg/m^3. The concrete took up 21.1 g of water which is equal to 3063 g of water per square meter or 204 kg/m^3 since the sample tested was 15 mm thick.

It was seen that evaporation happens faster directly after a watering event. There is also a high degree of variability in the evaporation rates between the different species directly after a watering event. However, after a certain amount of time passes, most mosses evaporate water at approximately the same speed. The exception to this rule is Bryum capillare, which maintains a consistently higher evaporation rate. Mosses are more desiccation tolerant when they grow in cushion form, reducing the surface-to-volume ratio and creating additional capillary spaces which hold water. Under conditions of high temperature (25°C) and low relative humidity (50% RH), all moss species demonstrate the highest levels of evaporation.

In field testing, the temperature of two bioreceptive concrete panels was monitored. One was grown with moss, and the other was completely bare. When panel temperatures rose above 15 to 20 °C, the moss panel became 0 to 5 °C cooler than the concrete panel. This is due to higher solar radiation which the moss absorbs, preventing it from reaching the surface beneath. And due to watering of the panels because the moss would keep hold of the water longer, resulting in a cool layer of air trapped lowering the temperature measured. There was little to no temperature difference between the panels on rainy or cloudy days.

IR camera measurements showed the actual surface temperature of both panels on a hot, sunny day. The dry moss surface temperature was about 2 to 3 °C warmer than the concrete panel surface due to the lower albedo of moss, which absorbs more shortwave radiation. The increased temperature of the moss surface compared to the concrete surface is not necessarily bad for thermal comfort. While a

higher albedo surface is beneficial on roofs to counter the urban heat island effect, it can increase thermal discomfort for pedestrians on the street when applied in a facade. Another explanation for the increased temperature of the moss layer is the air entrapment in its leaves. This insulating property of the moss layer keeps the material behind it cooler as measured in field testing. The implication of this extra insulation layer on the façade is yet to be investigated. By determining properties like the specific heat capacity and the heat conductivity of the moss layer, the amount of heat gain in winter and cooling gain in summer can be quantified. It is hypothesised that moss has a lower thermal mass than concrete. If this is true, it would lose its heat at night quicker. So if a moss layer can be used to prevent heating of the concrete behind it, buildings would stay cooler at night when the urban heat island effect is more pronounced.

Watering the panels significantly lowers the surface temperature (5 °C to 10 °C), with the moss panel being about 2 to 5 °C cooler than the concrete panel when wet. The moss takes up more water and holds it longer than the porous concrete. Therefore, more evaporation can take place resulting in lower temperatures for the moss panel. The cooling effect lasts for about two to two and a half hours for the concrete and moss panels respectively after a 40 ml watering event. Which is roughly equal to a 1 mm rain event at low wind speeds. This shows that applying moss on a concrete façade works in cooling down the façade surface temperature more than a bare concrete façade would.

A model based on the energy balance of the façade system was calibrated using the field testing data. The non-stationary model uses the explicit method to calculate the temperatures of a single node on the panel surface, providing accurate temperature profiles of different weather conditions. Evaporation modelling was calibrated using water events but lacks a water balance which requires more data to calibrate. Irrigation, precipitation, evaporation, throughflow and runoff create a dynamic balance of water in the system. These factors will each depend on formulas with variables like the relative humidity of air and material, precipitation amount and speed, ambient and material temperature, vapour pressure of air and material, wind speed etc. All these variables will be more accurate when they are related to each other through these formulas which they do not in the current model. Eventually, this would result in a more accurate evaporation and temperature profile.

The model is then used to simulate a heat wave and the thermal behaviour of the façade. The effect of rain events with different intensities is calculated. A 10 mm rain event, equal to filling up the reservoir of the façade with 185 kg/m^3 for a horizontal wind speed of 5 m/s, decreases surface temperatures up to 15 °C and the effect lasts for a few hours. To increase this effect, the pore volume of the concrete can be increased. This will only work up to a certain extent because with bigger pores, capillary action and strength properties will decrease. Furthermore, a moss species should be chosen which grows on concrete, in cushion form and is desiccation tolerant. This could increase the water retention of the façade by 70 kg/m^3 if we base it on the results of the lab testing.

Applying bioreceptive concrete on facades does keep them cooler for a longer time after a rain event. In that way, it mitigates the urban heat island effect because materials that accumulate and radiate a lot of heat are replaced. To accurately quantify the effect of applying bioreceptive concrete as a mitigation strategy against the urban heat island effect, a CFD model could help to predict the decrease of ambient temperature in front of a bioreceptive facade.

9

Recommendations

The product of bioreceptive concrete is relatively new. Therefore, before being able to use it in practice, more information is needed on its properties and applicability. Recommendations for further research are given to make the most of the ecosystem services that this material provides.

Field testing

First of all, this product should be tested outside more. By monitoring and evaluating the long-term performance of bioreceptive concrete facades, the durability and maintenance requirements will become clearer. Also, the performance under all the different environmental conditions that happen throughout the year can be mapped. The façade might also behave differently in different climates. Its use should be tested in those climates to check the difference in performance which might be better or worse. And through testing different façade orientations, the applicability of the façade on different sides of a building and in certain parts of the city is explored. This is needed before urban planners and architects can start including this product in their designs.

The façade area tested should be higher. By testing these facades on a larger scale, it might be possible to measure air temperature change. And with a more extensive set of equipment, more variables could be measured which are influenced by the evaporation from the façade surface. For example, the relative humidity in the air in front of the façade could be interesting to monitor.

In the current test set-up, the samples outside were not weighed. This would make the outside testing resemble the lab testing more. It would provide data on the water content in the system. This would make way for an easier comparison, putting the results from the lab testing in more perspective.

Improving the design

To maximize the evaporative cooling effect, the design of moss-covered concrete facades can be improved further. In terms of the concrete, the potential of increasing the pore volume of concrete to enhance the cooling effect further should be explored. The balance between pore size, capillary action, and strength properties should be taken into account when doing so.

In terms of the moss, the first improvement to the design should be to improve the adhesion of mosses to the concrete surface. This is a boundary condition for the product to work. Then, ways of improving moss water uptake can be investigated. Ecologists and scientists might be able to alter the genetic, biological or chemical properties of the moss to increase water uptake.

For designers, a recommendation is to try to design different ways of adding water to the façade. Waiting for rain might not be the most effective way of cooling through evaporation. Because the moment of cooling cannot be chosen. Maybe supplying water from a reservoir of water from a green

roof to the façade would be a useful way to start the evaporation process. This would make it possible to have some more regulation of the water release on the façade but the moss would still provide cooling for a longer time than when spraying that same amount of water into the air.

Modelling

To improve the modelling of the evaporation behaviour of moss-covered facades, some recommendations are given. By finding the characteristic values for the parameters of this new building material, they can be used as a basis for a simulation in a program like ENVI-met. These parameters include the leaf area index, emissivity, specific heat capacity, thermal conductivity and density. But, the evaporation from the façade is not a function yet in these programs so that behaviour is more difficult to model. If this problem is solved, it would show the use in cooling of this material on a bigger scale like an urban canyon, a neighbourhood or a city.

By adding a water balance to the model, the amount of moisture available for evaporation is more accurate. By computing the irrigation, precipitation, evaporation, throughflow and runoff in a dynamic balance, the evaporation and temperature profiles would become more accurate. These factors will depend on formulas with variables like the relative humidity of air and material, precipitation amount and speed, ambient and material temperature, vapour pressure of air and material, wind speed etc. These should be monitored during outside testing to calibrate the model. Extra components can be added like irrigation.

To link façade surface temperature to thermal comfort, a CFD simulation should be performed. This shows how air moves in front of and against the façade. Properties of the façade surface like the roughness, relative humidity at the surface, temperature of the surface and evaporation from the facade are needed to accurately predict the wind movement and temperature. Actual cooling of ambient air can then be computed and this would provide the missing link between façade surface temperature and thermal comfort.

Other potential benefits

The research done in this thesis shows that moss has an insulating property. It keeps the material behind the moss layer cooler. Other implications of this extra insulation layer in a façade composition remain to be investigated. Where this thesis mainly focussed on the effect of this material on the outside environment, it might also affect the indoor climate of buildings. By determining properties like the specific heat capacity and the heat conductivity of the moss layer, the amount of heat gain in winter and cooling gain in summer can be quantified.

Other potential benefits of the use of bioreceptive concrete are also being researched. There are a lot of ecosystem services that this product might positively affect like the increase of biodiversity, the water retention capacity to relieve pressure on the sewage system, purifying the air by capturing particulate matter, sound absorption and capturing CO2 or nitrogen. Different types of mosses might provide specific benefits for these different goals. Research is needed to further quantify the effect that these moss species have on the different ecosystem services. A precondition is that it should be possible to cultivate them on bioreceptive concrete which is not possible for all moss species. The behaviour of these different moss species should then also be tested in an actual outdoor situation. Architects, urban planners and designers can then purposely apply them in the built environment.

10

References

Akbari, H., & Matthews, H. D. (2012). Global cooling updates: Reflective roofs and pavements. *Energy and Buildings*, *55*, 2–6. https://doi.org/10.1016/j.enbuild.2012.02.055

Albers, R., Cornet, C., van Hulten, M., de Moor, W., Ottelé, M., Sarabèr, A., Speelman, N., Swinkels, M., Vermeulen, E., de Vree, R., van der Wegen, G., & Zwijnenberg, J. (2017). Biologische aangroei op beton. *STUTECH Rapport*, *35*.

Amado, C. (2022). Unravelling the Urban Heat Island Phenomenon in the Netherlands; A Multicity Spatial Analysis on the Distributive component of Environmental Justice, analysing the Urban Green Infrastructure, and the Urban Heat Island Effect. *Leiden University*. https://ssrn.com/abstract=4049664

Anderson, G. B., & Bell, M. L. (2011). Heat waves in the United States: Mortality risk during heat waves and effect modification by heat wave characteristics in 43 U.S. communities. *Environmental Health Perspectives*, *119*(2), 210–218. https://doi.org/10.1289/ehp.1002313

Anderson, M., Lambrinos, J., & Schroll, E. (2010). The potential value of mosses for stormwater management in urban environments. *Urban Ecosystems*, *13*(3), 319–332. https://doi.org/10.1007/S11252-010-0121-Z

Blok, D., Heijmans, M. M. P. D., Schaepman-Strub, G., van Ruijven, J., Parmentier, F. J. W., Maximov, T. C., & Berendse, F. (2011). The Cooling Capacity of Mosses: Controls on Water and Energy Fluxes in a Siberian Tundra Site. *Ecosystems*, *14*(7), 1055–1065. https://doi.org/10.1007/S10021-011-9463-5

Buch, H., Evans, A. W., & Verdoorn, F. (1938). A preliminary check list of the Hepaticae of Europe and America (North of Mexico). *Ann. Bryol.*, *10*.

de Wit, M. H. (2009). *Heat, Air and Moisture in Building Envelopes* (W. H. van der Spoel, Ed.). Technische Universiteit Eindhoven.

Deilami, K., Kamruzzaman, M., & Liu, Y. (2018). Urban heat island effect: A systematic review of spatio-temporal factors, data, methods, and mitigation measures. *International Journal of Applied Earth Observation and Geoinformation*, *67*, 30–42. https://doi.org/10.1016/j.jag.2017.12.009

D'Ippoliti, D., Michelozzi, P., Marino, C., de'Donato, F., Menne, B., Katsouyanni, K., Kirchmayer, U., Analitis, A., Medina-Ramón, M., Paldy, A., Atkinson, R., Kovats, S., Bisanti, L., Schneider, A., Lefranc, A., Iñiguez, C., & Perucci, C. A. (2010). The impact of heat waves on mortality in 9 European cities: results from the EuroHEAT project. *Environmental Health*, *9*(37). http://www.ehjournal.net/content/9/1/37

Erell, E., Pearlmutter, D., Boneh, D., & Kutiel, P. B. (2014). Effect of high-albedo materials on pedestrian heat stress in urban street canyons. *Urban Climate*, *10*, 367–386. https://doi.org/http://dx.doi.org/10.1016/j.uclim.2013.10.005

Fischer, E. M., & Schär, C. (2010). Consistent geographical patterns of changes in high-impact European heatwaves. *Nature Geoscience*, *3*, 398–403. https://doi.org/10.1038/NGEO866

Gago, E. J., Roldan, J., Pacheco-Torres, R., & Ordóñez, J. (2013). The city and urban heat islands: A review of strategies to mitigate adverse effects. *Renewable and Sustainable Energy Reviews*, *25*, 749–758. https://doi.org/10.1016/j.rser.2013.05.057

Gasparrini, A., Guo, Y., Sera, F., Vicedo-Cabrera, A. M., Huber, V., Tong, S., de Sousa Zanotti Stagliorio Coelho, M., Hilario Nascimento Saldiva, P., Lavigne, E., Matus Correa, P., Valdes Ortega, N., Kan, H., Osorio, S., Kyselý, J., Urban, A., Jaakkola, J. J. K., Ryti, N. R. I., Pascal, M., Goodman, P. G., … Armstrong, B. (2017). Projections of temperature-related excess mortality under climate change scenarios. *The Lancet Planetary Health*, *1*(9), e360–e367. https://doi.org/10.1016/S2542-5196(17)30156-0

George, R. P., Ramya, S., Ramachandran, D., & Kamachi Mudali, U. (2013). Studies on Biodegradation of normal concrete surfaces by fungus Fusarium sp. *Cement and Concrete Research*, *47*, 8–13. https://doi.org/10.1016/j.cemconres.2013.01.010

Glime, J. M. (2022). *Bryophyte Ecology*. Michigan Technological University. https://digitalcommons.mtu.edu/bryophyte-ecology/

Guillitte, O. (1995). Bioreceptivity: a new concept for building ecology studies. *Science of the Total Environment*, *167*(1–3), 215–220. https://doi.org/https://doi. org/10.1016/0048-9697(95)04582-l

Hagentoft, C. E. (2007). *HAMSTAD WP2 Modelling: Determination of liquid water transfer properties of porous building materials and development of numerical assessment methods*.

Hamerlynck, E. P., Tuba, Z., Csintalan, Z., Nagy, Z., Henebry, G., & Goodin, D. (2000). Diurnal variation in photochemical dynamics and surface reflectance of the desiccation-tolerant moss, Tortula ruralis. *Plant Ecology*, *151*(1), 55–63. https://doi.org/10.1023/A:1026594623578

Heaviside, C., Macintyre, H., & Vardoulakis, S. (2017). The Urban Heat Island: Implications for Health in a Changing Environment. *Current Environmental Health Reports*, *4*, 296–305. https://doi.org/10.1007/s40572-017-0150-3

Heijmans, M. M. P. D., Arp, W. J., & Berendse, F. (2001). Effects of elevated CO2 on vascular plants on evapotranspiration in bog vegetation. *Global Change Biology*, *7*, 817–827. https://doi.org/10.1046/J.1354-1013.2001.00440.X

Jóhannesson, G. (2006). *Lectures on Building Physics; Heat and Moisture Transfer*.

Johnson, G. T., Oke, T. R., Lyons, T. J., Steyn, D. G., Watson, I. D., & Voogt, J. A. (1991). Simulation of surface urban heat islands under “ideal” conditions at night. *Boundary-Layer Meteorology*, *56*, 275–294.

Jones, V. A. S., & Dolan, L. (2012). The evolution of root hairs and rhizoids. *Annals of Botany*, *110*, 205–212. https://doi.org/10.1093/aob/mcs136

Kanare, H. M. (2007). Moisture in Concrete. In *Concrete Floors and Moisture*.

Kleerekoper, L., Van Esch, M., & Salcedo, T. B. (2012). How to make a city climate-proof, addressing the urban heat island effect. *Resources, Conservation and Recycling*, *64*, 30–38. https://doi.org/10.1016/J.RESCONREC.2011.06.004

Klein, M. (2020). Bioreceptive facade design. *TU Delft*. http://resolver.tudelft.nl/uuid:893288a9-2ad9-4471-aca1-90929a7eca86

Koch, K., Ysebaert, T., Denys, S., & Samson, R. (2020). Urban heat stress mitigation potential of green walls: A review. *Urban Forestry & Urban Greening*, *55*. https://doi.org/10.1016/J.UFUG.2020.126843

Koopmans, S., Heusinkveld, B. G., & Steeneveld, G. J. (2020). A standardized Physical Equivalent Temperature urban heat map at 1-m spatial resolution to facilitate climate stress tests in the Netherlands. *Building and Environment*, *181*. https://doi.org/10.1016/J.BUILDENV.2020.106984

Koppe, C., Kovats, S., Jendritzky, G., Menne, B., Baumüller, J., Bitan, A., Díaz Jiménez, J., Ebi, K. L., Havenith, G., Santiago, C. L., Michelozzi, P., Nicol, F., Matzarakis, A., McGregor, G., Nogueira, P. J., Sheridan, S., & Wolf, T. (2004). Heat-waves: risks and responses. *World Health Organization*.

Kosanović, S., Klein, T., Konstantinou, T., Radivojević, A., & Hildebrand, L. (2018). Sustainable and resilient building design: approaches, methods and tools. In *sustainable and resilient building design approaches, methods and tools* (Vol. 5). TU Delft Open. https://books.bk.tudelft.nl/index.php/press/catalog/book/isbn.9789463660327

Koster, K. L., Balsamo, R. A., Espinoza, C., & Oliver, M. J. (2010). Desiccation sensitivity and tolerance in the moss Physcomitrella patens: Assessing limits and damage. *Plant Growth Regulation*, *62*(3), 293–302. https://doi.org/10.1007/S10725-010-9490-9

Kovats, R. S., & Hajat, S. (2008). Heat Stress and Public Health: A Critical Review. *Annual Review of Public Health*, *29*, 41–55. https://doi.org/10.1146/annurev.publhealth.29.020907.090843

Krupa, J. (1977). The interdependence between transpiration intensity and the anatomical structure of moss leaves. *Acta Societatis Botanicorum Poloniae*, *46*(1), 57–68. https://doi.org/https://doi.org/10.5586/asbp.1977.005

Kuijpers-Van Gaalen, I. M., Zeegers, A., Erdtsieck, P., van der Linden, A. C., & Selten, T. A. J. (2006). *Bouwfysica* (A. C. van der Linden, Ed.; 4th ed.). ThiemeMeulenhoff.

Kurth, J. C. (2008). Mitigating biofilm growth through the modificiation of concrete design and practice. *Georgia Institute of Technology*.

Lamke, L. 0, & Wedin, B. (1971). Water Evaporation from Normal Skin under Different Environmental Conditions. *Acta Dermato-Venereologica*, *51*, 111–119.

Li, R. (2021). Quay walls Greening with Mosses. *TU Delft*. http://resolver.tudelft.nl/uuid:c64760c9-16db-4656-96ef-9dd842b1641e

Manso, S., De Muynck, W., Segura, I., Aguado, A., Steppe, K., Boon, N., & De Belie, N. (2014). Bioreceptivity evaluation of cementitious materials designed to stimulate biological growth. *Science of The Total Environment*, *481*(1), 232–241. https://doi.org/http://dx.doi.org/10.1016/j.scitotenv.2014.02.059

Matzarakis, A., Mayer, H., & Iziomon, M. G. (1999). Applications of a universal thermal index: Physiological equivalent temperature. *International Journal of Biometeorology*, *43*(2), 76–84. https://doi.org/10.1007/S004840050119

Medina-Ramón, M., & Schwartz, J. (2007). Temperature, temperature extremes, and mortality: a study of acclimatisation and effect modification in 50 US cities. *Occupational and Environmental Medicine*, *64*, 827–833. https://doi.org/10.1136/oem.2007.033175

Mir, M. A. (2011). Green façades and building structures. *TU Delft*. http://resolver.tudelft.nl/uuid:f262c218-8801-4425-818f-08726dde5a6c

Mustafa, K. F., Prieto, A., & Ottele, M. (2021). The Role of Geometry on a Self-Sustaining Bio-Receptive Concrete Panel for Facade Application. *Sustainability*, *13*. https://doi.org/https://doi.org/10.3390/su13137453

Nilsson, A. L. (1987). Blood Flow, Temperature, and Heat Loss of Skin Exposed to Local Radiative and Convective Cooling. *Journal of Investigative Dermatology*, *88*(5), 586–593.

Norton, B., Bosomworth, K., Coutts, A., Williams, N., Livesley, S., Trundle, A., Harris, R., & Mcevoy, D. (2013). Planning for a Cooler Future: Green Infrastructure to Reduce Urban Heat. *Climate Adaptation for Decision-Makers*.

Oke, T. R. (1982). The energetic basis of the urban heat island. *Quarterly Journal of the Royal Meteorological Society*, *108*(455), 1–24. https://doi.org/10.1002/QJ.49710845502

Pogačar, T., Casanueva, A., Kozjek, K., Ciuha, U., Mekjavić, I. B., Bogataj, L. K., & Črepinšek, Z. (2018). The effect of hot days on occupational heat stress in the manufacturing industry: implications for workers' well-being and productivity. *International Journal of Biometeorology*, *62*, 1251–1264. https://doi.org/https://doi.org/10.1007/s00484-018-1530-6

Prieto, B., & Silva, B. (2005). Estimation of the potential bioreceptivity of granitic rocks from their intrinsic properties. *International Biodeterioration and Biodegradation*, *56*(4), 206–215. https://doi.org/10.1016/J.IBIOD.2005.08.001

Priyadarsini, R., Hien, W. N., & David, C. K. W. (2008). Microclimatic modeling of the urban thermal environment of Singapore to mitigate urban heat island. *Solar Energy*, *82*, 727–745. https://doi.org/10.1016/j.solener.2008.02.008

Proctor, M. C. F. (2000a). Mosses and alternative adaptation to life on land. *New Phytologist*, *148*(1), 1–6. https://doi.org/10.1111/J.1469-8137.2000.00751.X

Proctor, M. C. F. (2000b). The bryophyte paradox: tolerance of desiccation, evasion of drought. *Plant Ecology*, *151*(1), 41–49. https://doi.org/10.1023/A:1026517920852

Qi, W., Li, J., & Weisensee, P. B. (2019). Evaporation of Sessile Water Droplets on Horizontal and Vertical Biphobic Patterned Surfaces. *Langmuir*, *35*(52), 17185–17192. https://doi.org/10.1021/acs.langmuir.9b02853

Quincot, G., Azenha, M., Barros, J., & Faria, R. (2011). State of the art – Methods to measure moisture in concrete. *Universidade Do Minho*.

Rajagopalan, P., Lim, K. C., & Jamei, E. (2014). Urban heat island and wind flow characteristics of a tropical city. *Solar Energy*, *107*, 159–170. https://doi.org/http://dx.doi.org/10.1016/j.solener.2014.05.042

Ross, P., Edwards, S., Genney, D., Godfrey, M., Moore, O., Pilkington, S., & Wright, J. (2022). Interactive key to British Mosses and Liverworts. *British Bryological Society*. https://www.britishbryologicalsociety.org.uk/wp-content/uploads/2022/11/Field-Guide-key-digital-Paul-Ross.pdf

Santamouris, M. (2020). Recent progress on urban overheating and heat island research. Integrated assessment of the energy, environmental, vulnerability and health impact. Synergies with the global climate change. *Energy and Buildings*, *207*. https://doi.org/https://doi.org/10.1016/j.enbuild.2019.109482

Santamouris, M., Ding, L., & Osmond, P. (2019). Urban Heat Island Mitigation. *Decarbonising the Built Environment*, 337–355. https://doi.org/https://doi.org/10.1007/978-981-13-7940-6_18

Scheirer, D. C. (1980). Differentiation of Bryophyte Conducting Tissues: Structure and Histochemistry. *Bulletin of the Torrey Botanical Club*, *107*(3), 298–307. https://doi.org/https://doi.org/10.2307/2484153

Schmidt, M. (2009). Rainwater Harvesting for Mitigating Local and Global Warming. *Fifth Urban Research Symposium*. http://www.gebaeudekuehlung.de/URS2009Marseille.pdf

Schrijvers, P. J. C., Jonker, H. J. J., De Roode, S. R., & Kenjereš, S. (2016). The effect of using a high-albedo material on the Universal Temperature Climate Index within a street canyon. *Urban Climate*, *17*, 284–303. https://doi.org/http://dx.doi.org/10.1016/j.uclim.2016.02.005

Semenza, J. C., Rubin, C. H., Falter, K. H., Selanikio, J. D., Flanders, D. W., Howe, H. L., & Wilhelm, J. L. (1996). Heat-Related Deaths during the July 1995 Heat Wave in Chicago. *The New England Journal of Medicine*, *335*(2), 84–90. https://doi.org/https://doi.org/10.1056/NEJM199607113350203

Smoyer, K. E., Rainham, D. G. C., & Hewko, J. N. (2000). Heat-stress-related mortality in five cities in Southern Ontario: 1980–1996. *International Journal of Biometeorology*, *44*(4), 190–197. https://doi.org/https://doi.org/10.1007/s004840000070

Sparrius, L. (2016). Biofilms, mossen en korstmossen op beton. *Bryologische En Lichenologische Werkgroep*, *3*.

Stache, E. (Eva), Schilperoort, B. (Bart), Ottelé, M. (Marc), & Jonkers, H. M. (Henk). (2022). Comparative analysis in thermal behaviour of common urban building materials and vegetation and consequences for urban heat island effect. *Building and Environment*, *213*. https://doi.org/https://doi.org/10.1016/j.buildenv.2021.108489

Taha, H. (1997). Urban climates and heat islands: Albedo, evapotranspiration, and anthropogenic heat. *Energy and Buildings*, *25*(2), 99–103. https://doi.org/https://doi.org/10.1016/S0378-7788(96)00999-1

Takebayashi, H., & Moriyama, M. (2007). Surface heat budget on green roof and high reflection roof for mitigation of urban heat island. *Building and Environment*, *42*(8), 2971–2979. https://doi.org/10.1016/j.buildenv.2006.06.017

The World Bank. (2023, April 3). *Urban Development Overview*. https://www.worldbank.org/en/topic/urbandevelopment/overview

Ulpiani, G., Di Giuseppe, E., Di Perna, C., D'Orazio, M., & Zinzi, M. (2019). Design optimization of mist cooling for Urban Heat Island mitigation: experimental study on the role of injection density. *IOP*

Conference Series: Earth and Environmental Science, *296*. https://doi.org/10.1088/1755-1315/296/1/012025

Ulpiani, G., di Perna, C., & Zinzi, M. (2020). Mist cooling in urban spaces: Understanding the key factors behind the mitigation potential. *Applied Thermal Engineering*, *178*. https://doi.org/https://doi.org/10.1016/j.applthermaleng.2020.115644

U.S. Department of Energy. (2022). EnergyPlus Documentation Engineering Reference. *EnergyPLUS*.

Van Boxel, J. (1998). Numerical model for the fall speed of raindrops in a rainfall simulator. *I.C.E. Special Report*, *1*, 77–85. https://dare.uva.nl/search?identifier=f900db81-bbe8-43eb-b266-676dbfb7ba6d

van der Spoel, W. H. (2017). Playing with heat balances; an introduction to numerical modelling of heat transfer problems. *TU Delft*.

Veeger, M., Ottelé, M., & Prieto, A. (2021). Making bioreceptive concrete: Formulation and testing of bioreceptive concrete mixtures. *Journal of Building Engineering*, *44*. https://doi.org/https://doi.org/10.1016/j.jobe.2021.102545

Vitt, D. H., Crandall-Stotler, B., & Wood, A. (2014). Bryophytes: Survival in a dry world through tolerance and avoidance. *Plant Ecology and Evolution in Harsh Environments*, 267–295. https://www.researchgate.net/publication/297363188_Bryophytes_Survival_in_a_dry_world_through_tolerance_and_avoidance

Westhoff, L. L. (2020). Spontaneous moss growth on concrete. *TU Delft*. http://resolver.tudelft.nl/uuid:28be3a5c-a011-4b54-b2ea-190b05e23fdc

Wong, S. F., Wee, T. H., Swaddiwudhipong, S., & Lee, S. L. (2001). Study of water movement in concrete. *Magazine of Concrete Research*, *53*(3), 205–220. https://doi.org/10.1680/MACR.2001.53.3.205

Yin, C., Yuan, M., Lu, Y., Huang, Y., & Liu, Y. (2018). Effects of urban form on the urban heat island effect based on spatial regression model. *Science of the Total Environment*, *634*, 696–704. https://doi.org/https://doi.org/10.1016/j.scitotenv.2018.03.350

Zamski, E., & Trachtenberg, S. (1976). Water movement through hydroids of a moss gametophyte. *Israel Journal of Botany*, *25*, 168–173.

11

Appendices

Appendix A: moss sampling

This appendix shows the method of sampling the mosses that were used in the lab testing. The different collected moss species are shown with information to categorize them.

Sampling is done using the following scheme:

1. Taking pictures

Overview picture of the location.

Detailed picture of the moss.

2. Taking samples

Sampling is done when the moss meets the following requirements:

It grows directly on the stony substrate.

The sample is of the right size or tufts can be collected together to reach a big enough sample (10x10 cm)

With a putty knife, the moss can be detached from its growth surface. The putty knife is 10cm wide so it is easy to collect samples of the right size. The moss sample is then put into a tray for transportation to the lab where the second part of this research can be conducted.

3. Determine species and categorise

With a picture of the moss, apps like PictureThis and Plantnet can help to get a first idea of which species of moss it is. With the help of reference images on the internet, the family to which the moss belongs should be traceable. Then the moss is investigated further with a microscope to establish its specific species. With a tool created by Paul Ross, the species was established (Ross et al., 2022).

Categorizing of mosses

Based on earlier research into this topic and sampling by other people several locations in Delft have been selected to visit. If moss is found in these locations, they will then be categorised based on some site conditions which are derived from the thesis of Roberto Li (Li, 2021).

Moss 1: *Rhynchostegium confertum*

Location: *Jaffalaan*

The material of the substrate layer: *Natural stone*

Surface orientation: *[horizontal~~/vertical/sloped~~] [~~north/east/south/west~~]*

Living/moisture condition: *[dry~~/moist air/wet~~]*

Daylight conditions: *[partial shade]*

Figure A.1: Finding location of moss Rhynchostegium confertum

Figure A.2: Microscope photos of moss Rhynchostegium confertum

Moss 2: N/A 1

Location: *Jaffalaan*

The material of the substrate layer: *Natural stone*

Surface orientation: *[horizontal~~/vertical/sloped~~] [~~north/east/south/west~~]*

Living/moisture condition: *[dry~~/moist air/wet~~]*

Daylight conditions: *[]*

Figure 11.3: Finding location of unidentified moss species 1

Figure 11.4: Microscope photos of unidentified moss species 1

Moss 3: *Plagiomnium affine*

Location: *Jaffalaan*

The material of the substrate layer: *Natural stone*

Surface orientation: *[horizontal~~/vertical/sloped~~] [~~north/east/south/west~~]*

Living/moisture condition: *[dry~~/moist air/wet~~]*

Daylight conditions: *[Shaded by trees]*

Figure 11.5: Finding location of moss Plagiomnium affine

Figure 11.6: Microscope photos of moss Plagiomnium affine

Moss 4: *Anomodon viticulosus*

Location: *Arboretum-Heempark*

The material of the substrate layer: *Brick*

Surface orientation: *[~~horizontal/~~vertical~~/sloped~~] [north~~/east/south/west~~]*

Living/moisture condition: *[~~dry/moist air/~~wet]*

Daylight conditions: *[]*

Figure 11.7: Finding location of moss Anomodon viticulosus

Figure 11.8: Microscope photos of moss Anomodon viticulosus

Moss 5: *Eurhynchium striatum*

Location: *Bieslandse bos*

The material of the substrate layer: *Brick*

Surface orientation: *[~~horizontal~~/vertical~~/sloped~~] [north/east/~~south/west~~]*

Living/moisture condition: *[dry~~/moist air/wet~~]*

Daylight conditions: *[]*

Figure 11.9: Finding location of moss Eurhynchium striatum

Figure 11.10: Microscope photos of moss Eurhynchium striatum

Moss 6: N/A 2

Location: *Aart van der Leeuwlaan 332*

The material of the substrate layer: *Cementitious brick*

Surface orientation: *[~~horizontal/vertical/~~sloped] [~~north/east~~/south/west]*

Living/moisture condition: *[dry~~/moist air/wet~~]*

Daylight conditions: *[Shaded by building]*

Figure 11.11: Finding location of unidentified moss species 2

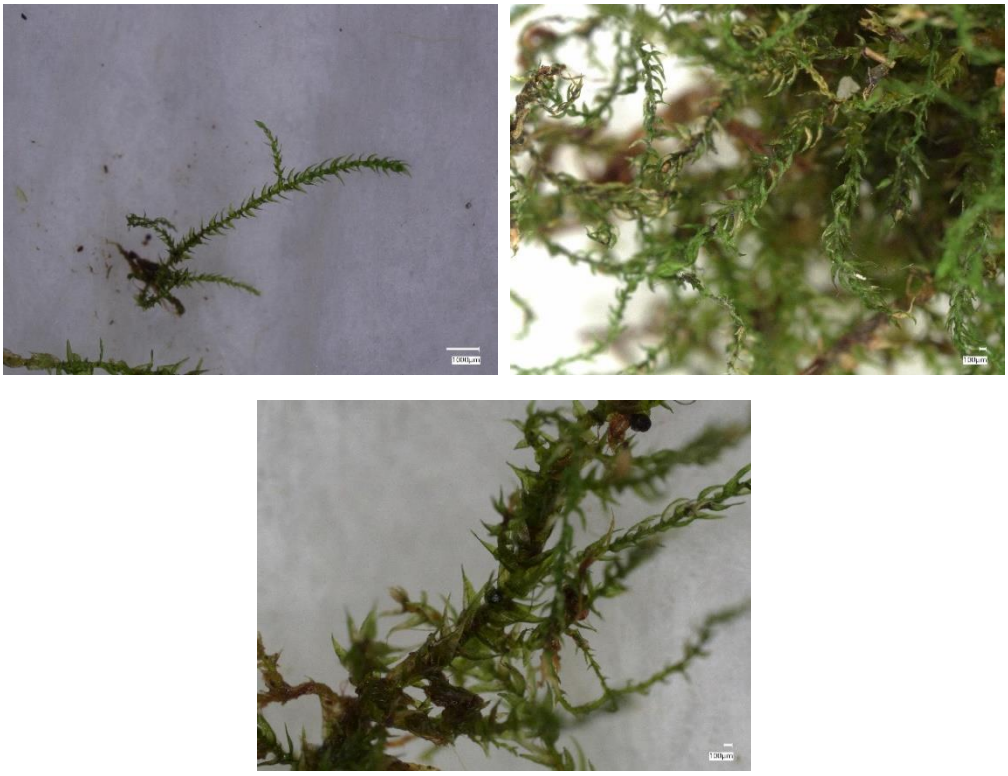

Figure 11.12: Microscope photos of unidentified moss species 2

Moss 7: *Bryum capillare & Didymodon rigidulus*

Location: *Kandelaarbrug*

The material of the substrate layer: *Concrete/asphalt*

Surface orientation: *[~~horizontal/vertical/~~sloped] [north/east~~/south/west~~]*

Living/moisture condition: *[dry~~/moist air/wet~~]*

Daylight conditions: *[Shaded by trees]*

Figure 11.13: Finding location of moss *Bryum capillare & Didymodon rigidulus*

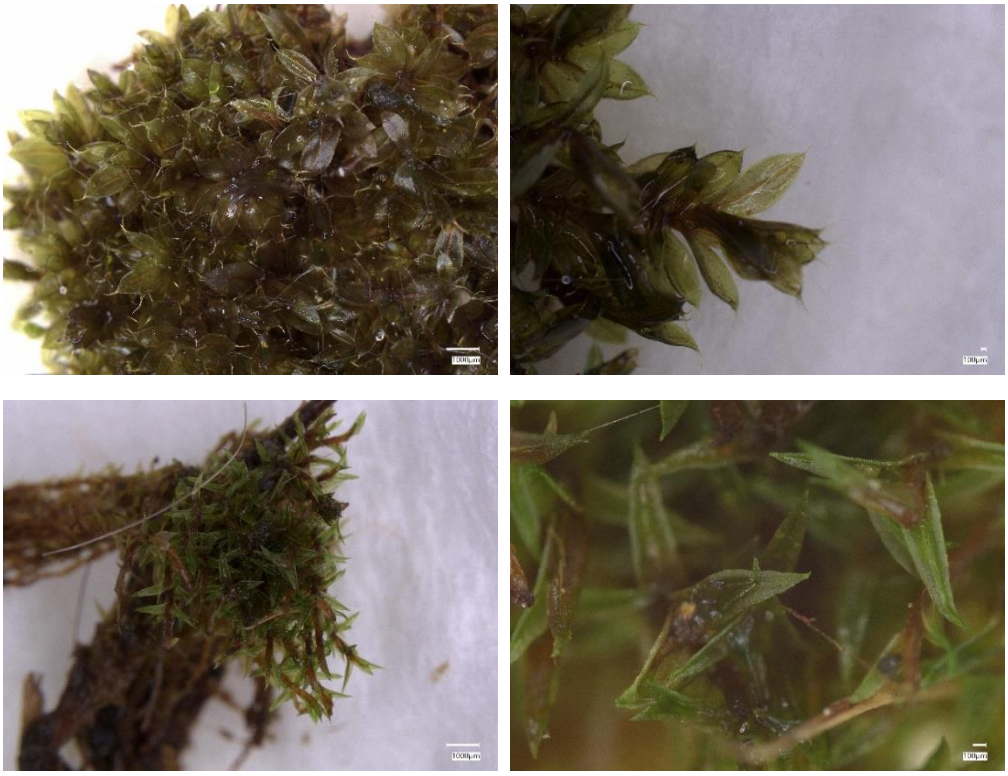

Figure 11.14: Microscope photos of moss *Bryum capillare & Didymodon rigidulus*

Moss 8: *Syntrichia ruralis*

Location: *Ackerdijkse plassen*

The material of the substrate layer: *Concrete*

Surface orientation: *[horizontal~~/vertical/sloped~~] [~~north/east/south/west~~]*

Living/moisture condition: *[dry~~/moist air/wet~~]*

Daylight conditions: *[Exposed to sun]*

Figure 11.15: Finding location of moss Syntrichia ruralis

Figure 11.16: Microscope photos of moss Syntrichia ruralis

Appendix B: procedure of lab testing

In Appendix B, the procedure of lab testing is discussed and divided into three subsections: determining the evaporation of water from the moss species, determining the evaporation of water from the concrete samples, and determining the evaporation of water from the concrete + moss samples together.

Determining evaporation of water from moss

1. Wetting of moss

Submerge moss in water and allow it to absorb water. Then take it out and remove excess water by dabbing it with paper tissue.

2. Drying and weighing

First, the moss is weighed to determine its initial weight. Then, the moss is allowed to dry at a certain temperature and relative humidity. It is weighed every hour between 08.00 am and 17.00 pm. This results in 10 measurement points during one day. The samples are weighed again the next day to see if they completely dried out the day before or not. If this is not the case the measurements can continue hourly. Missing data points overnight can be found from the trend line when the data points are plotted against time. The experiment stops when the weight does not change anymore in three consecutive data points.

Determining evaporation of water from concrete

1. Wetting of concrete

Submerge concrete in water and allow it to absorb water. When there is no perceptible change in the weight of the wet material upon resubmerging, the capillary moisture content is reached. Then take it out and remove excess water by dabbing it with paper tissue.

2. Shield the sides of the concrete

Wrap the sides and back of the concrete in plastic foil. This allows moisture only to evaporate from the top surface just like it would in a façade.

3. Drying and weighing

First, the concrete is weighed to determine its initial weight. Then, the concrete is allowed to dry at a certain temperature and relative humidity. It is weighed every hour between 08.00 am and 17.00 pm. This results in 10 measurement points during one day. The samples are weighed again the next day to see if they completely dried out the day before or not. If this is not the case the measurements can continue hourly. Missing data points overnight can be found from the trend line when the data points are plotted against time. The experiment stops when the weight does not change anymore in three consecutive data points.

Determining evaporation of water from concrete + moss

1. Wetting of concrete + moss

Submerge concrete in water and allow it to absorb water. When there is no perceptible change in the weight of the wet material upon resubmerging, the capillary moisture content is reached. Simultaneously submerge moss in water and allow it to absorb water. Then take them both out and remove excess water by dabbing it with paper tissue.

2. Shield the sides of the concrete

Wrap the sides and back of the concrete in plastic foil. This allows moisture only to evaporate from the top surface just like it would in a façade.

3. Place the moss on top of the concrete sample

The mosses and concrete samples were linked to each other at the start of the experiment. The moss is placed on top of the concrete sample covering the surface from which evaporation takes place.

4. Drying and weighing

First, the combined sample is weighed to determine its initial weight. Then, the sample is allowed to dry at a certain temperature and relative humidity. It is weighed every hour between 08.00 am and 17.00 pm. This results in 10 measurement points during one day. The samples are weighed again the next day to see if they completely dried out the day before or not. If this is not the case the measurements can continue hourly. Missing data points overnight can be found from the trend line when the data points are plotted against time. The experiment stops when the weight does not change anymore in three consecutive data points.

Appendix C: extensive results lab testing

Appendix C shows the results for the decrease in weight and evaporation rates under different conditions for moss and concrete samples. Results are shown in graphs over the duration of the testing period, 5 days.

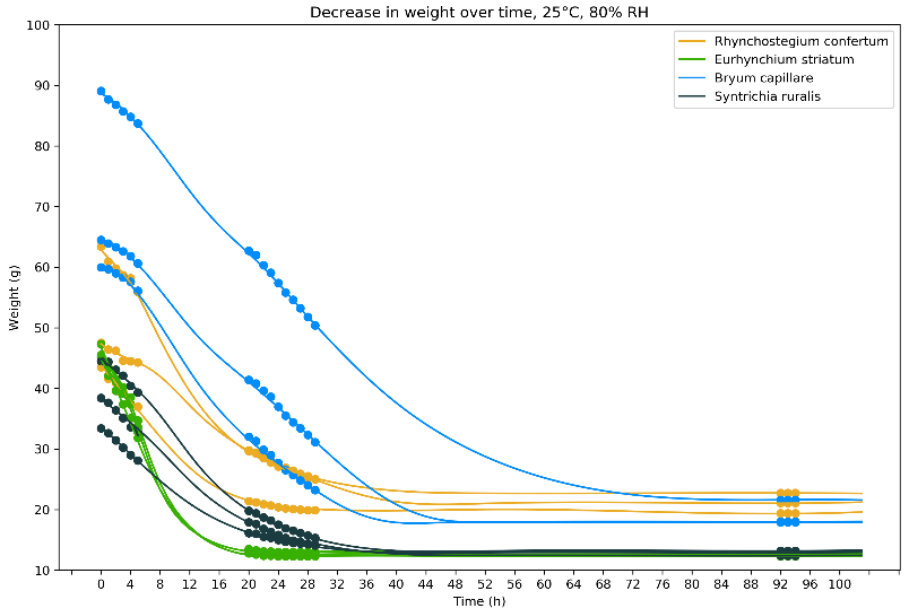

Figure 11.17: Decrease in weight (g) over time (h) for different moss species at 25°C, 80% RH

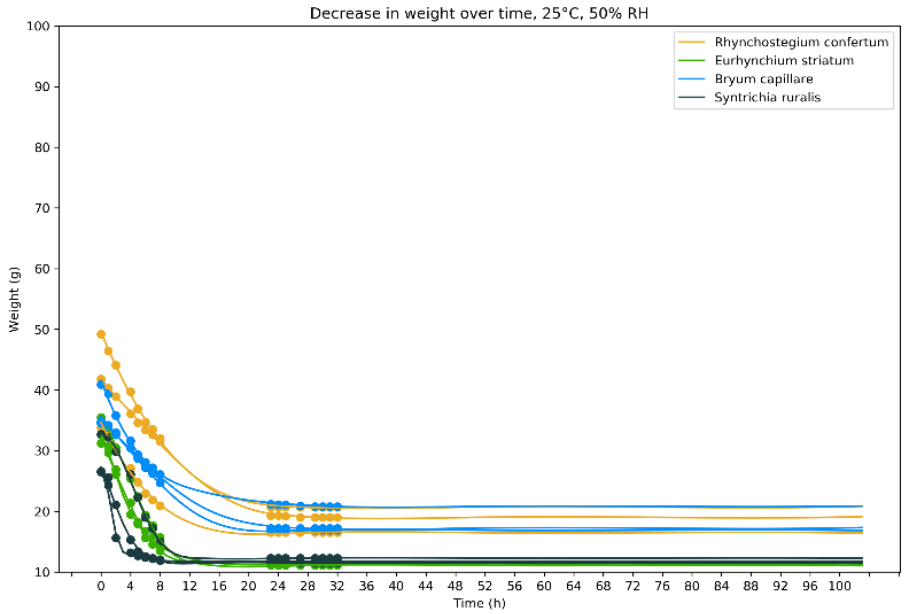

Figure 11.18: Decrease in weight (g) over time (h) for different moss species at 25°C, 50% RH

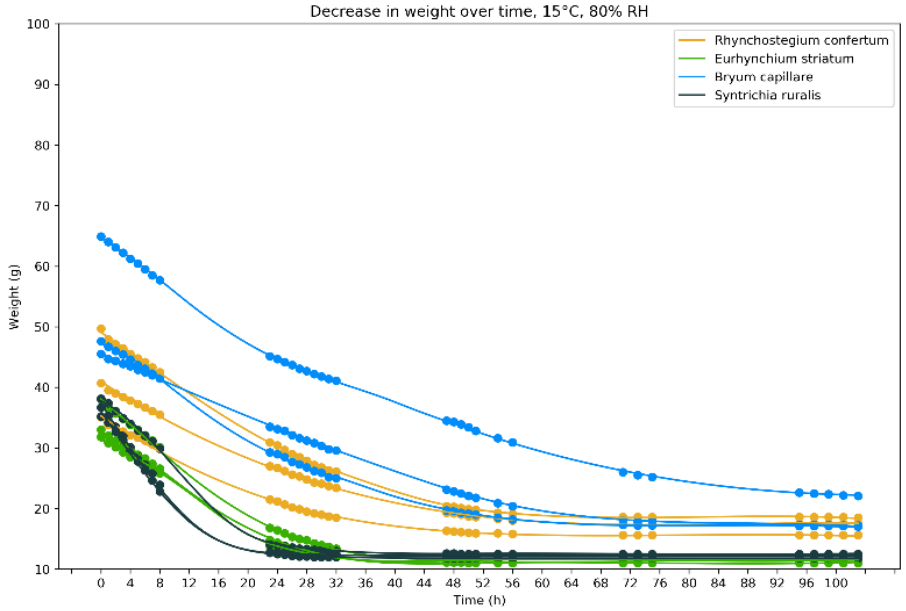

Figure 11.19: Decrease in weight (g) over time (h) for different moss species at 15°C, 80% RH

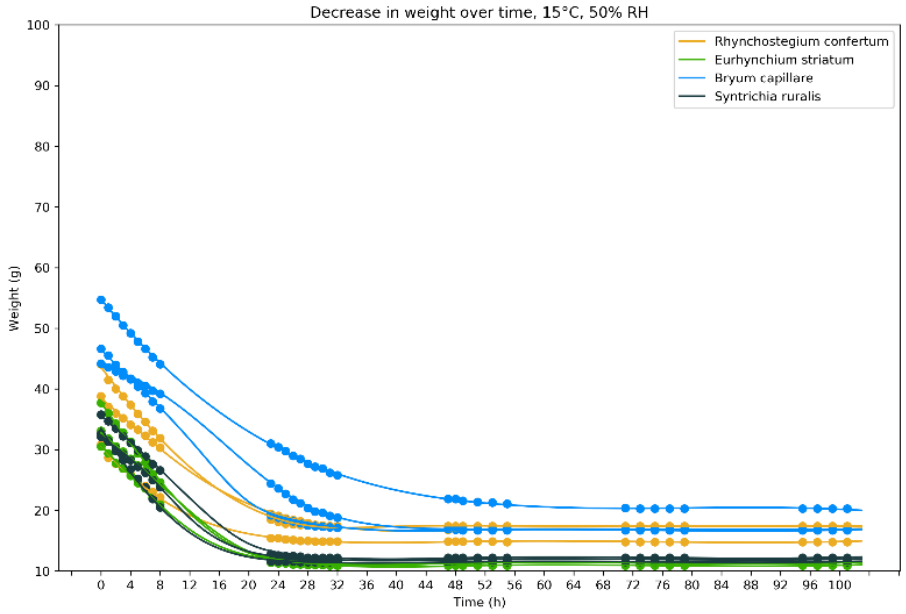

Figure 11.20: Decrease in weight (g) over time (h) for different moss species at 15°C, 50% RH

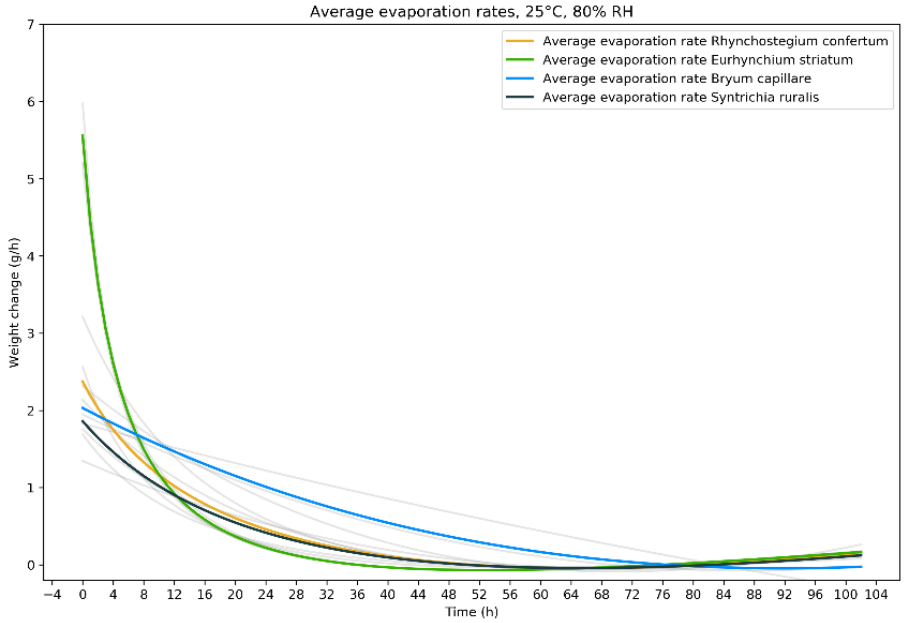

Figure 11.21: Average evaporation rate moss samples 25°C, 80% RH

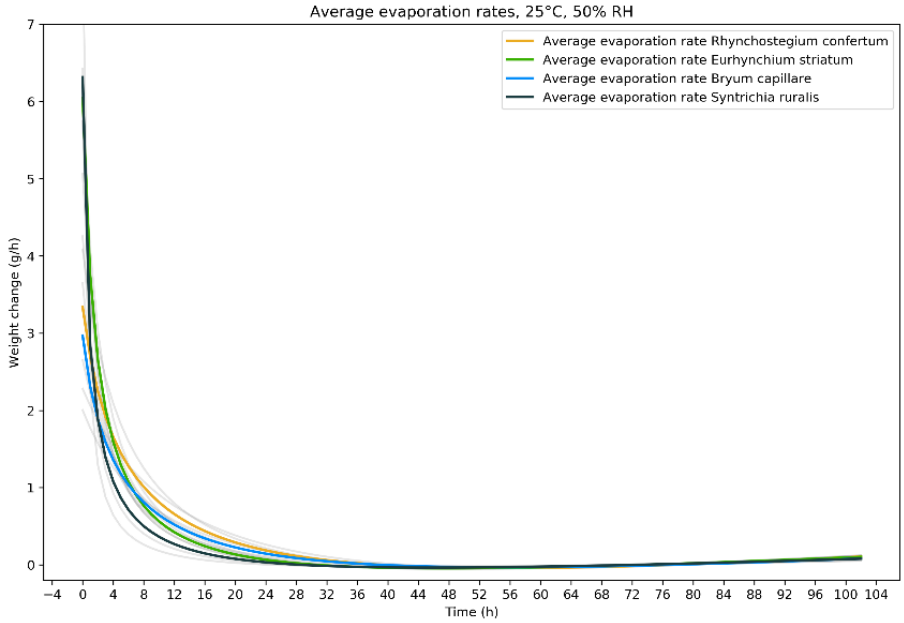

Figure 11.22: Average evaporation rate moss samples 25°C, 50% RH

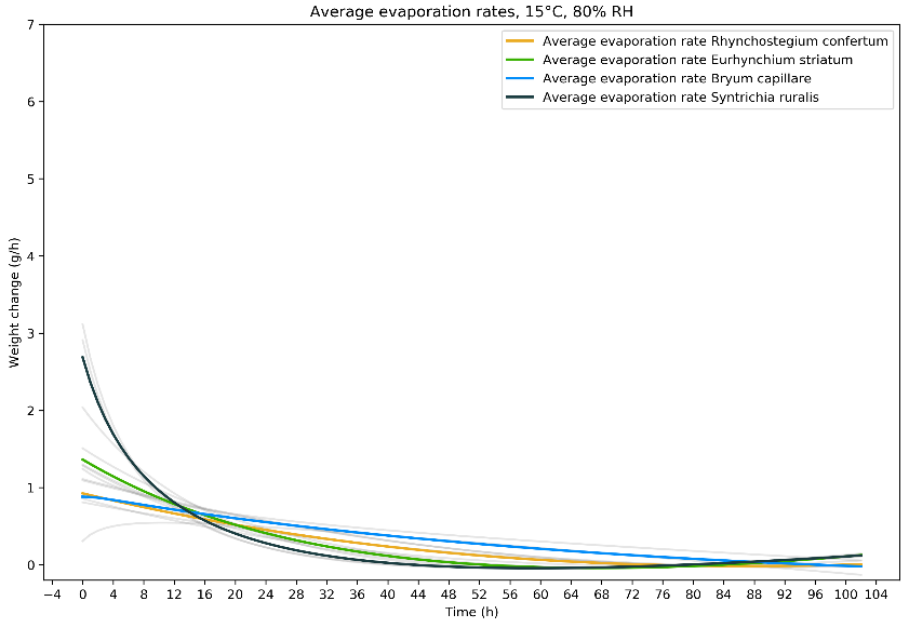

Figure 11.23: Average evaporation rate moss samples 15°C, 80% RH

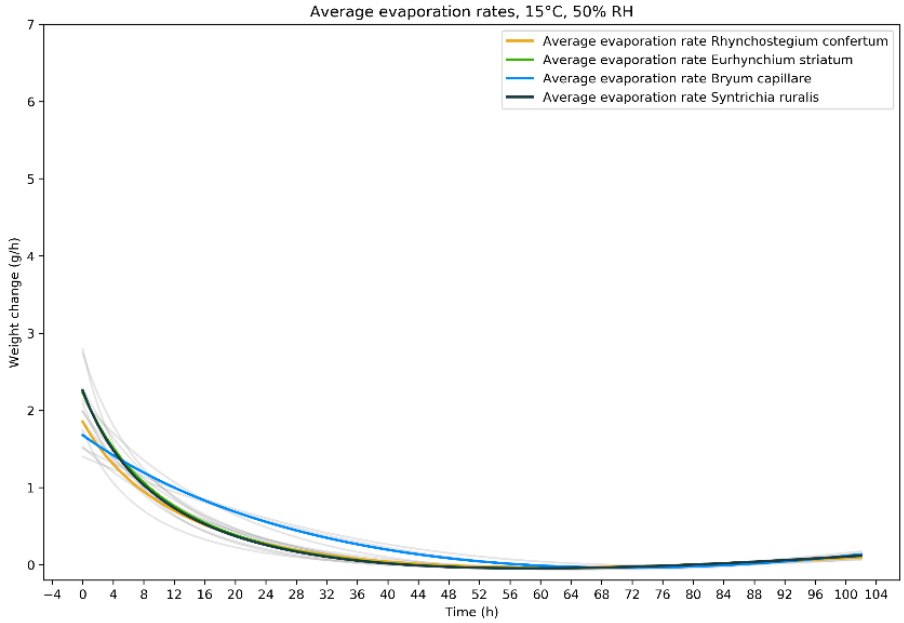

Figure 11.24: Average evaporation rate moss samples 15°C, 50% RH

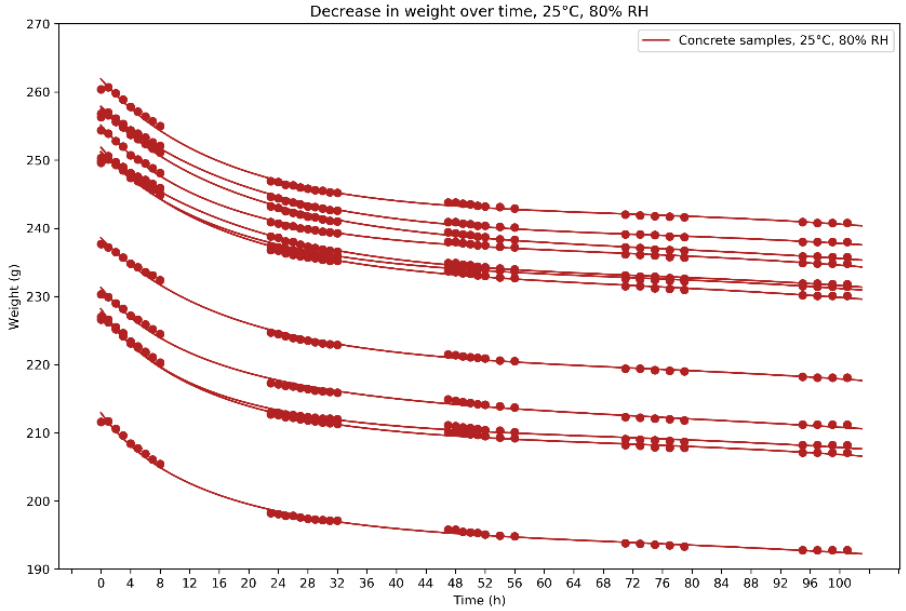

Figure 11.25: Decrease in weight (g) over time (h) for concrete samples 25°C, 80% RH

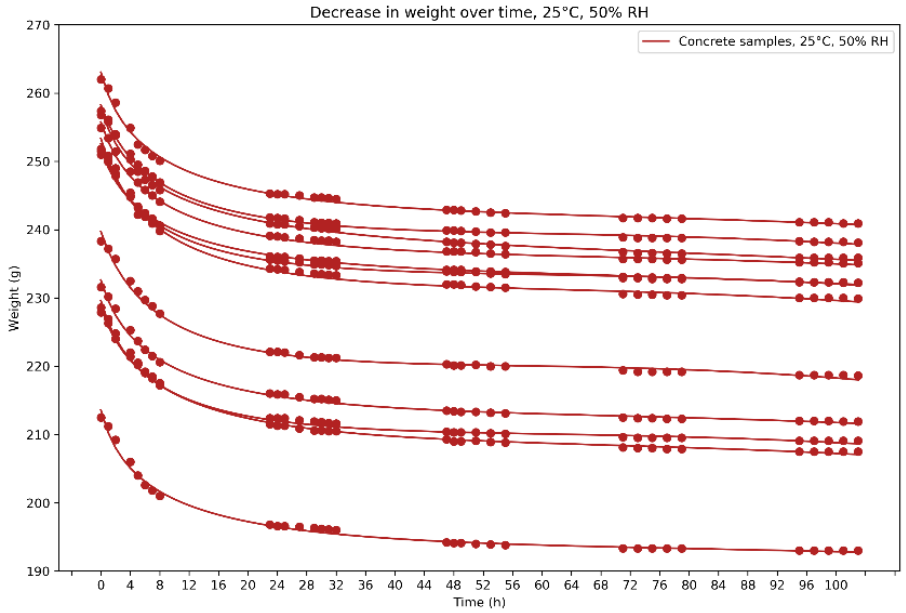

Figure 11.26: Decrease in weight (g) over time (h) for concrete samples 25°C, 50% RH

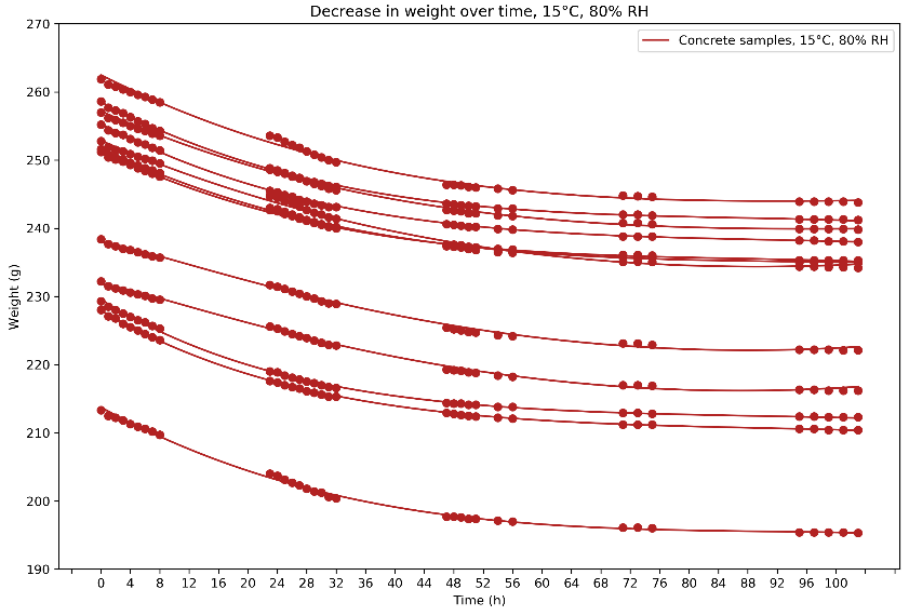

Figure 11.27: Decrease in weight (g) over time (h) for concrete samples 15°C, 80% RH

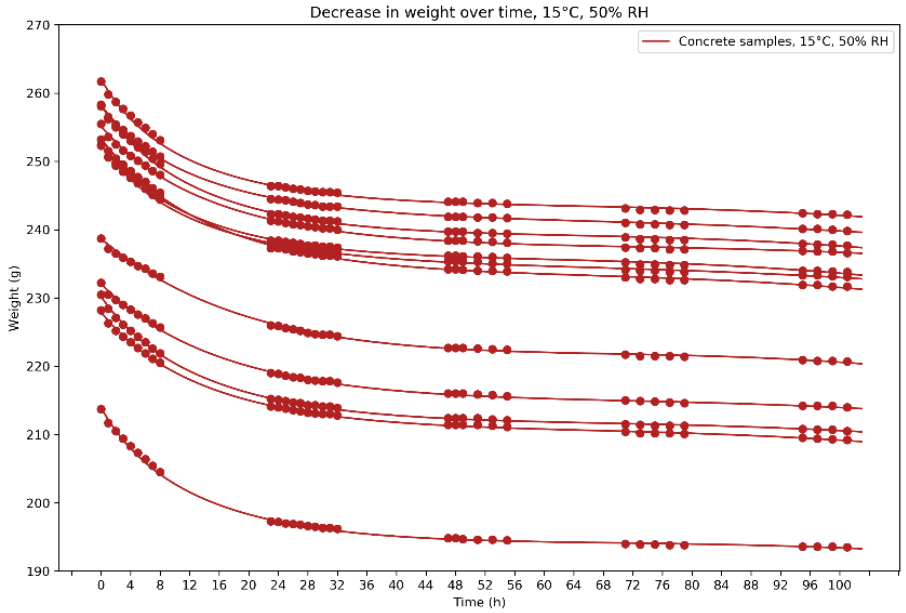

Figure 11.28: Decrease in weight (g) over time (h) for concrete samples 15°C, 50% RH

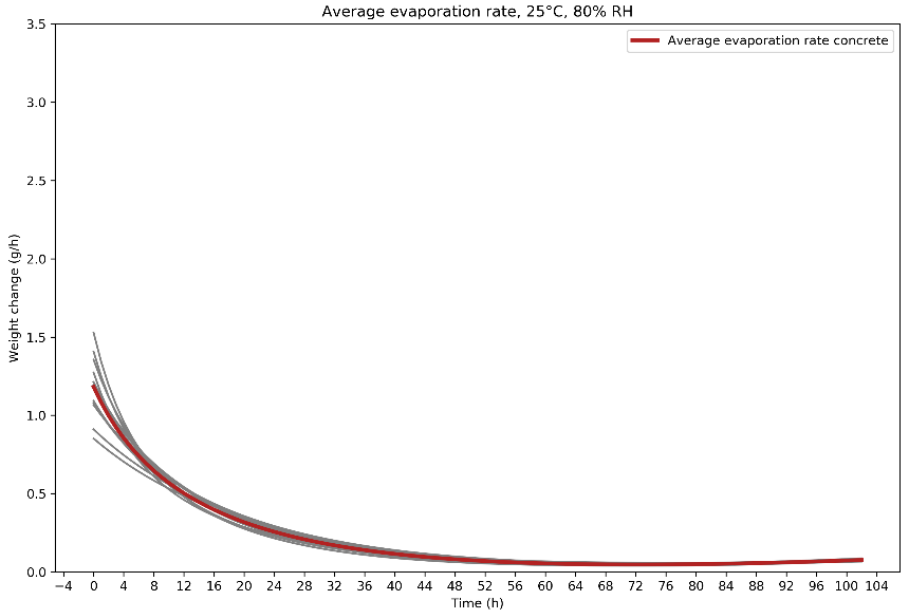

Figure 11.29: Average evaporation rate concrete samples 25°C, 80% RH

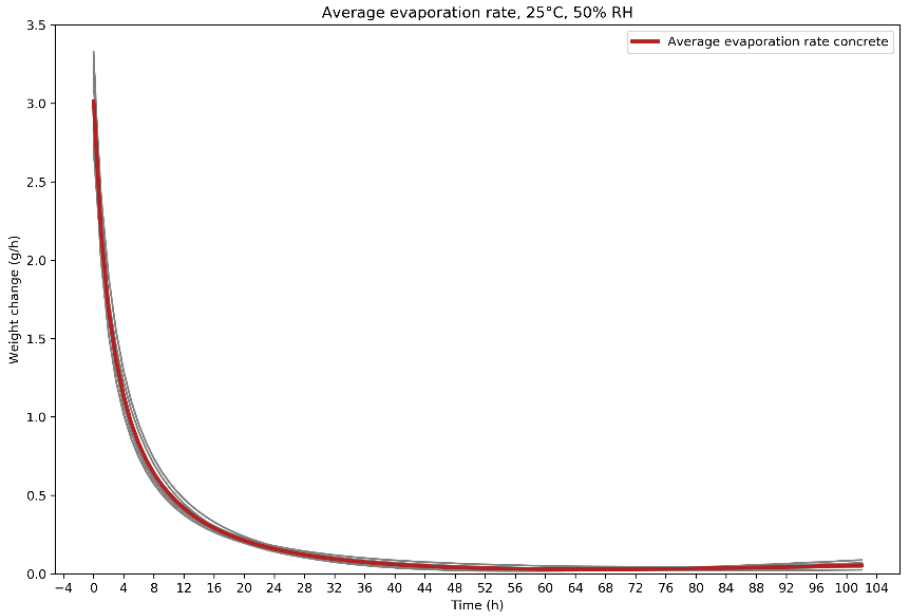

Figure 11.30: Average evaporation rate concrete samples 25°C, 50% RH

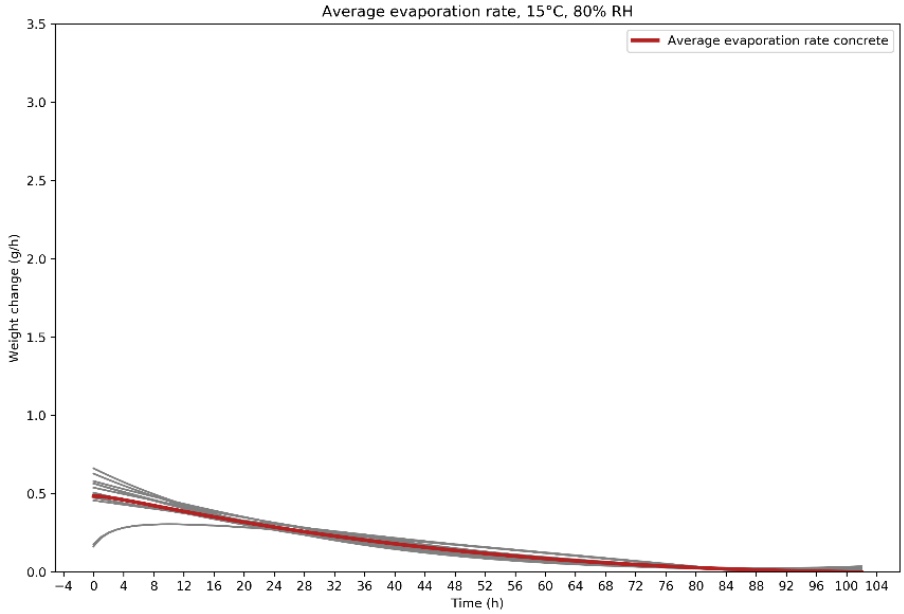

Figure 11.31: Average evaporation rate concrete samples 15°C, 80% RH

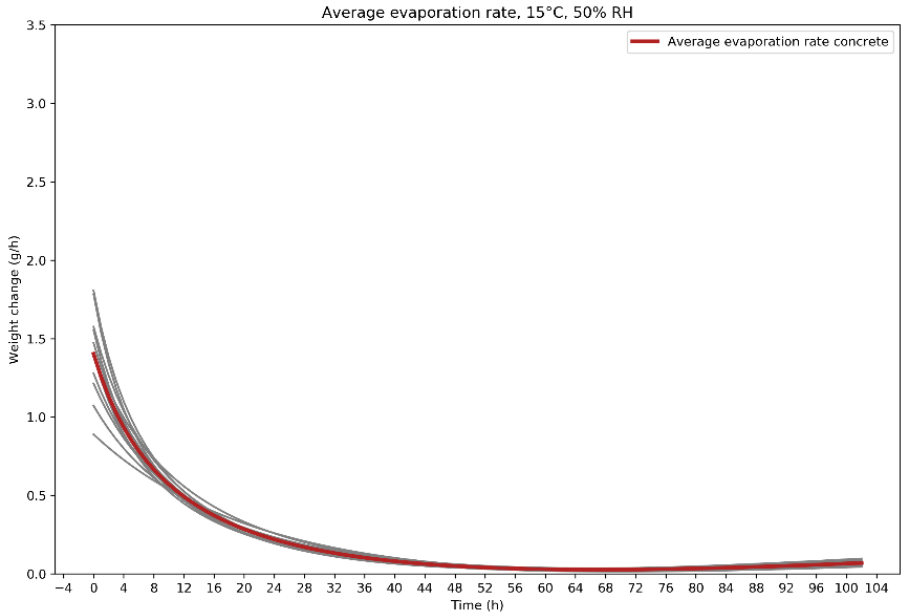

Figure 11.32: Average evaporation rate concrete samples 15°C, 50% RH

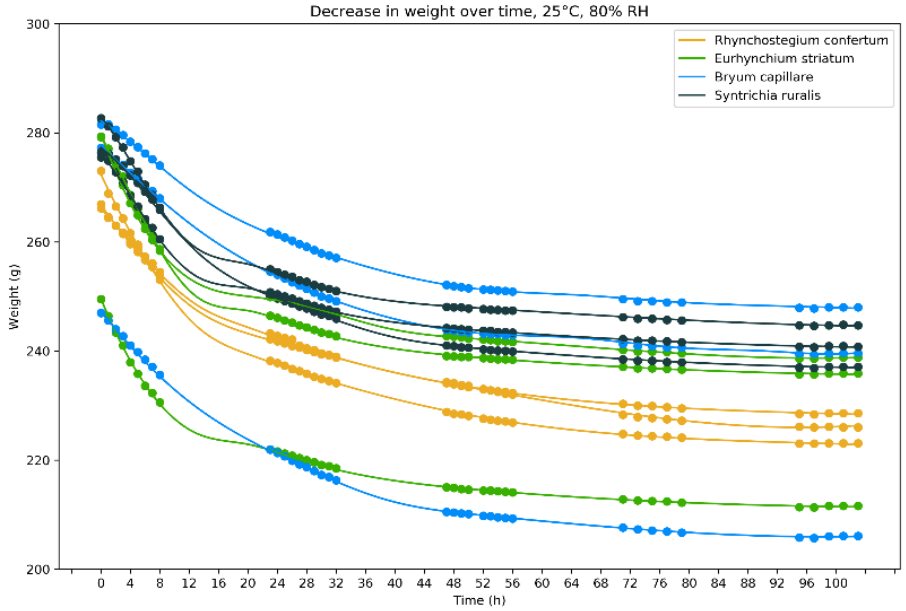

Figure 11.33: Decrease in weight (g) over time (h) for concrete with different moss species at 25°C, 80% RH

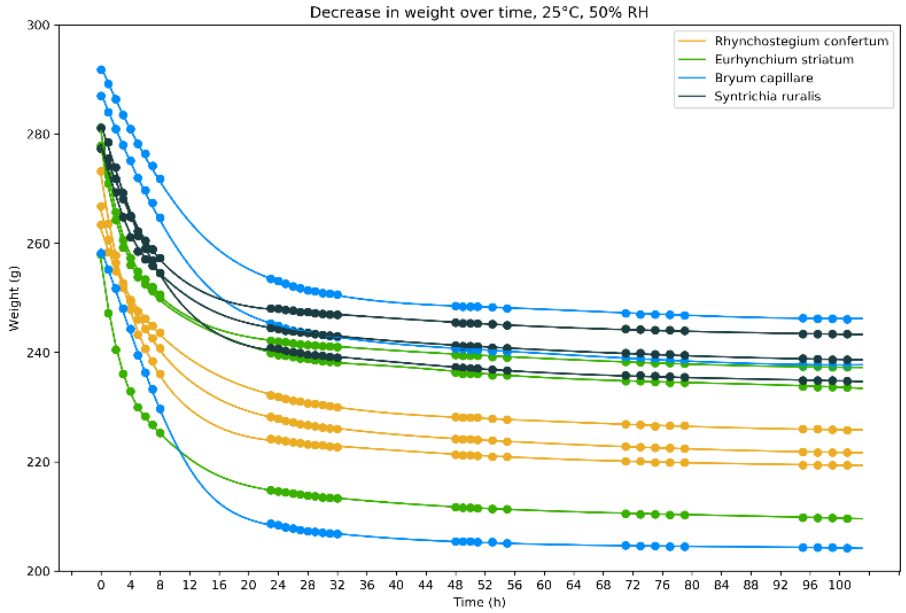

Figure 11.34: Decrease in weight (g) over time (h) for concrete with different moss species at 25°C, 50% RH

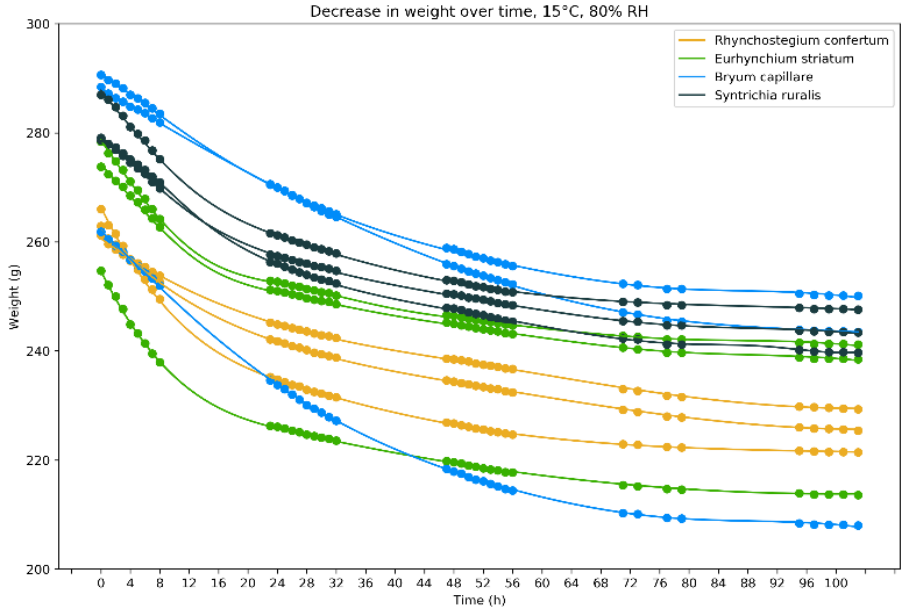

Figure 11.35: Decrease in weight (g) over time (h) for concrete with different moss species at 15°C, 80% RH

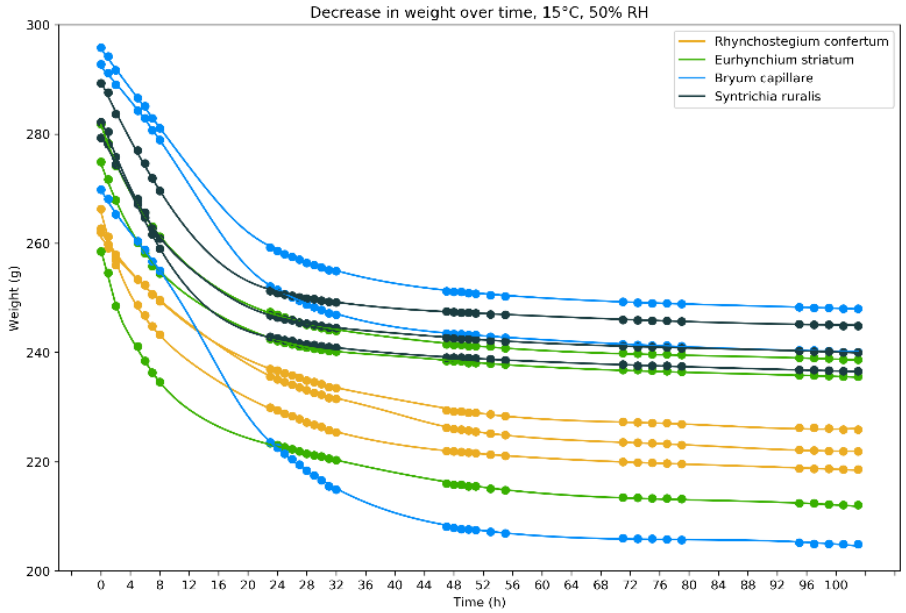

Figure 11.36: Decrease in weight (g) over time (h) for concrete with different moss species at 15°C, 50% RH

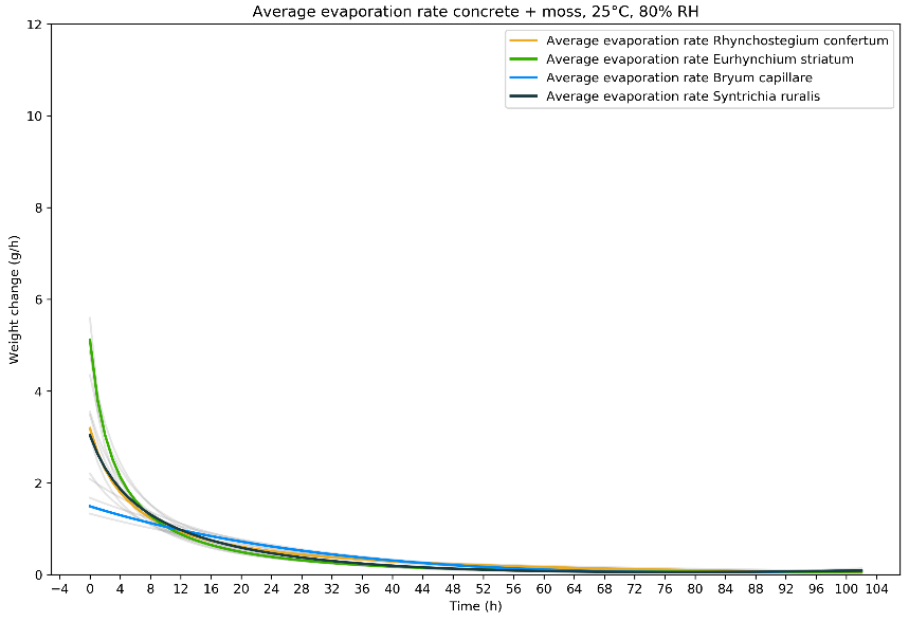

Figure 11.37: Average evaporation rate concrete + moss samples 25°C, 80% RH

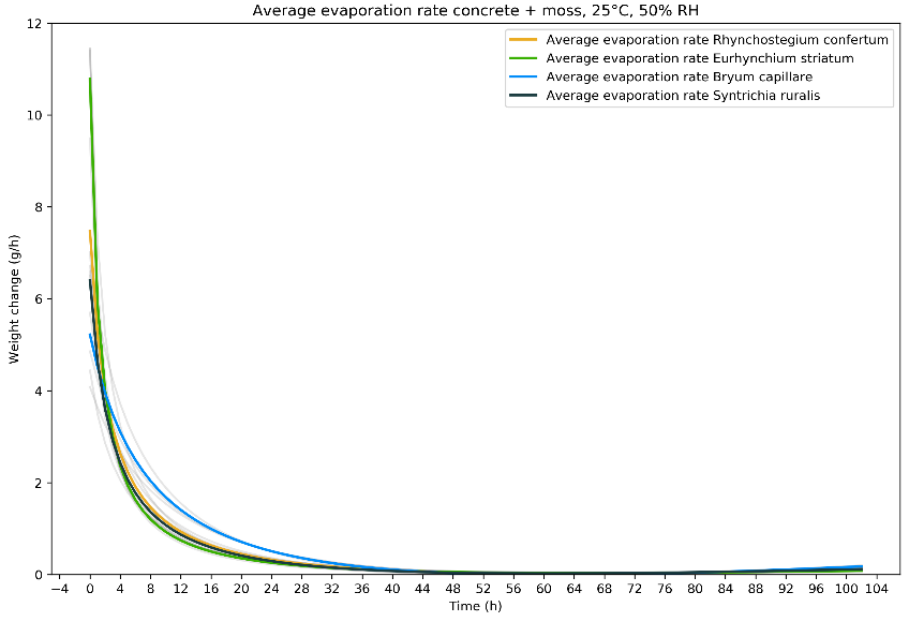

Figure 11.38: Average evaporation rate concrete + moss samples 25°C, 50% RH

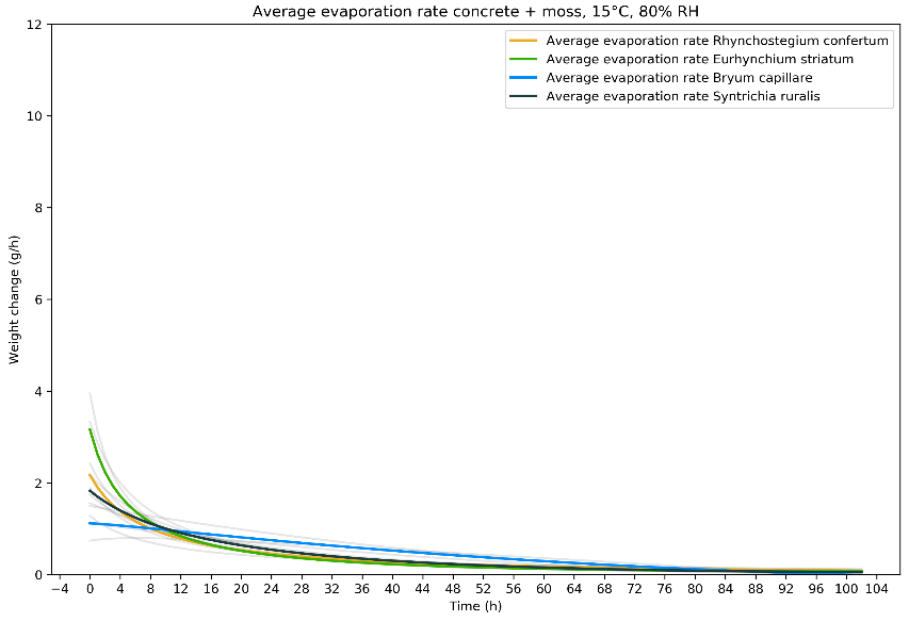

Figure 11.39: Average evaporation rate concrete + moss samples 15°C, 80% RH

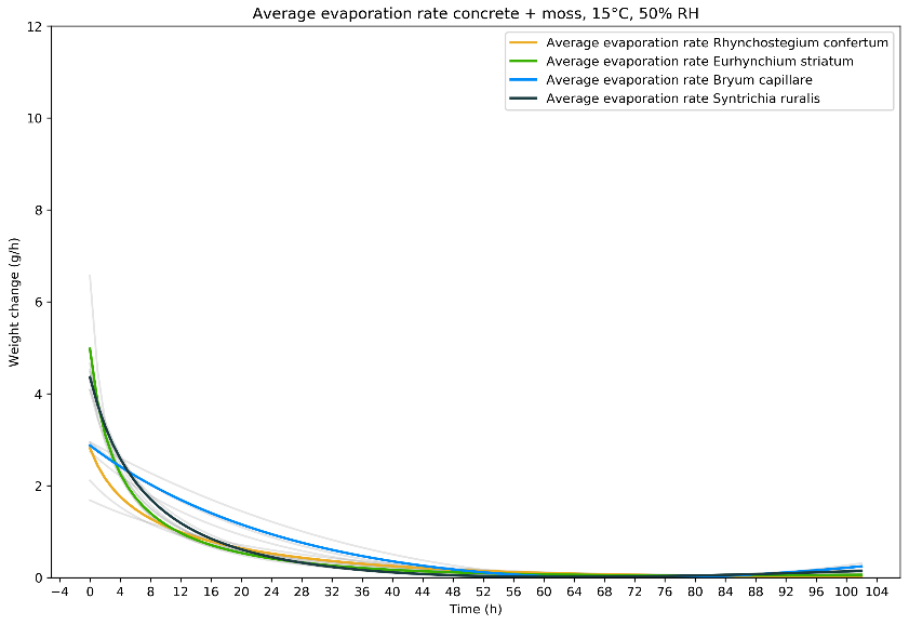

Figure 11.40: Average evaporation rate concrete + moss samples 15°C, 50% RH

Appendix D: input values of dynamic model

Appendix D contains the input values for different parts of the dynamic model. The values are categorised per component of the energy balance.

Solar radiation

	Absorptance (-)	Albedo (-)
Concrete	0.60	0.40
Moss	0.85	0.15

Radiative exchange sky

	σ (W/m^2K^4)
Stefan-Boltzmann constant	5.67E-08

Convective heat transfer

Temperature ϑ (°C)	-20	0	20	40
Density ρ (kg/m^3)	1.395	1.293	1.205	1.127
Bowen ratio β (K^{-1})	-	0.00367	0.00343	0.00320
Specific heat capacity c (J/kgK)	1006	1006	1007	1008
Thermal conductivity λ (W/mK)	-	0.0243	0.0257	0.0271
Kinematic viscosity v (m^2/s)	-	13.3E-6	15.11E-6	16.97E-6

Conduction

	Thickness panel (m)	Thermal conductivity (W/mK)
Styrofoam	0.1	0.028
Concrete	0.03	2.4
Moss	0.005	0.5

Evaporation

	L (J/kg)
Latent heat of vaporization	2.50E06

	W_f (-)
Wind direction modifier	1.0

	R_f (-)
Roughness factor	2.17

Dynamic model

	ρ (kg/m^3)
Density	2300

	c (J/kgK)
Specific heat capacity	840

	V (m^3/m^2)
Volume per surface area	0.03

	Δt (s)
Time step	300